PLIO-PLEISTOCENE LANDSCAPE EVOLUTION ON THE HIGH PLAINS
OF SOUTHWESTERN KANSAS

By

Anthony L. Layzell

Submitted to the graduate degree program in Geography and the Graduate Faculty of the University of Kansas in partial fulfillment of the requirements for the degree of Doctor of Philosophy.

________________________________

Chairperson Dr. Rolfe Mandel

________________________________

Dr. Johannes Feddema

________________________________

Dr. Stephen Hasiotis

________________________________

Dr. Daniel Hirmas

________________________________

Dr. Gregory Ludvigson

Date Defended: 2 March 2015

The Dissertation Committee for Anthony L. Layzell

certifies that this is the approved version of the following dissertation:

PLIO-PLEISTOCENE LANDSCAPE EVOLUTION ON THE HIGH PLAINS OF SOUTHWESTERN KANSAS

Chairperson Rolfe Mandel

Date approved: 23 March 2015

# ABSTRACT

This dissertation investigates patterns and forcing mechanisms of Plio-Pleistocene landscape evolution in the Cimarron River valley, southwestern Kansas. Particular attention was given to the geomorphic history of the Cimarron River and the response to environmental forcing. During the Pliocene, the ancestral Cimarron River deposited the alluvial sediments of the Ogallala Formation. The Pliocene age is inferred from $\delta^{13}C$ values that indicate >50% $C_4$ biomass – a Pliocene phenomenon in the Great Plains. In order to provide better age constraints, a new technique to date volcanogenic zircons preserved in paleosols was utilized. A concordia age of 64.2±3.9 Ma was obtained but appears to represent detrital populations.

Evidence of late-Pleistocene alluviation occurs in the form of distinct valley fills beneath two terrace surfaces (T-1 and T-2). During Marine Isotope Stages (MIS) 5–4, the Cimarron River rapidly aggraded. Paleoenvironmental data from alluvial fills suggest a cool and likely wet environment between ~77–58 ka. Paleoenvironmental data from eolian sediments, however, indicate multiple climatic shifts between ~84–54 ka that resulted in episodic eolian deposition and soil formation on the High Plains surface. During MIS 3, the paleoenvironmental record from both alluvial (~52–28 ka) and eolian (~52–29 ka) deposits indicates a shift to warmer, drier conditions. This shift resulted in slower rates of alluviation and cumulic soil formation in the T-2 fill. Rates of eolian deposition on the uplands also slowed at this time, resulting in the formation of a soil that represents the Gilman Canyon Formation pedocomplex.

Chronostratigraphic data indicate that the Cimarron River incised over 25 m before ~28 ka likely due to local base level lowering from the dissolution of Permian evaporite beds during the late Pleistocene. The bulk of the T-1 fill aggraded between ~28–13 ka in response to cooler, wetter climatic conditions. Around 13 ka, sedimentation rates declined due to warmer and probably drier conditions, forming a cumulic soil in the T-1 fill. Overall, this dissertation fills an important gap in our understanding of landscape evolution on the High Plains by shedding light on chronostratigraphic relationships and paleoclimatic change during the period of record.

## ACKNOWLEDGEMENTS

This dissertation represents the culmination of several years of research and would not have been possible without the help and support of numerous people and institutions. First and foremost, I am indebted to my advisor, Rolfe Mandel, and Greg Ludvigson who have been strong proponents of this research, always been very gracious with their time, and have offered me their unwavering support during my graduate career. I also thank the other members of my committee for their service, advocacy, and guidance.

I extend my gratitude to Roy Brown and Andi Curtiss of Cattle Empire, Gary Headrick (USDA), Bill Miller (Haskell County Road Department), Thelma Collison, and Sally Black for permitting and facilitating access to study sites. Bridget Sanderson, Kevin Fenyak and Greg Cane are thanked for their assistance with particle size and isotopic analyses and Brian Sitek for zircon processing. I am also grateful to Tammy Rittenour for her collaboration as well as to the broader Quaternary science community for encouragement and insight over the years.

The Geological Society of America, the Kansas Academy of Science, the Society for Sedimentary Geology (SEPM), the National Science Foundation (NSF EAR-1023285 and the Integrative Graduate Education and Research Traineeship program) and the US Geological Survey (STATEMAP program) provided funding for this research.

Finally, I thank my family, especially my wife Lindsey, for their love, support, patience and encouragement. They have waited a long time for this.

TABLE OF CONTENTS

# CHAPTER 1

# INTRODUCTION

## 1.1. Introduction

Studies of landscape evolution seek to describe the interactions between form and process that result in observable landscape changes over a range of spatial and temporal scales. The integration of such studies is important for understanding long-term earth surface processes as well as for projecting future environmental change. This study examines Plio-Pleistocene landscape evolution in the Cimarron River valley, located on the High Plains of southwestern Kansas (Fig. 1.1). In the study area, the High Plains surface is predominantly underlain by the Miocene and early Pliocene-aged sediments of the Ogallala Formation. Pleistocene sediments primarily comprise alluvial fills in the Cimarron River valley and eolian deposits on uplands. These various deposits contain valuable archives that are used in this dissertation to reconstruct past landscape and paleoenvironmental change during the Plio-Pleistocene.

## 1.2. Goals

The overarching goal of this research was to investigate patterns and forcing mechanisms of Plio-Pleistocene landscape evolution in the Cimarron River valley. There are four specific research objectives: 1) Determine the characteristics and stratigraphic relationships of alluvial and eolian deposits, together with associated buried soils, in the Cimarron River valley; 2) Establish a numerical chronology for the deposition of Plio-

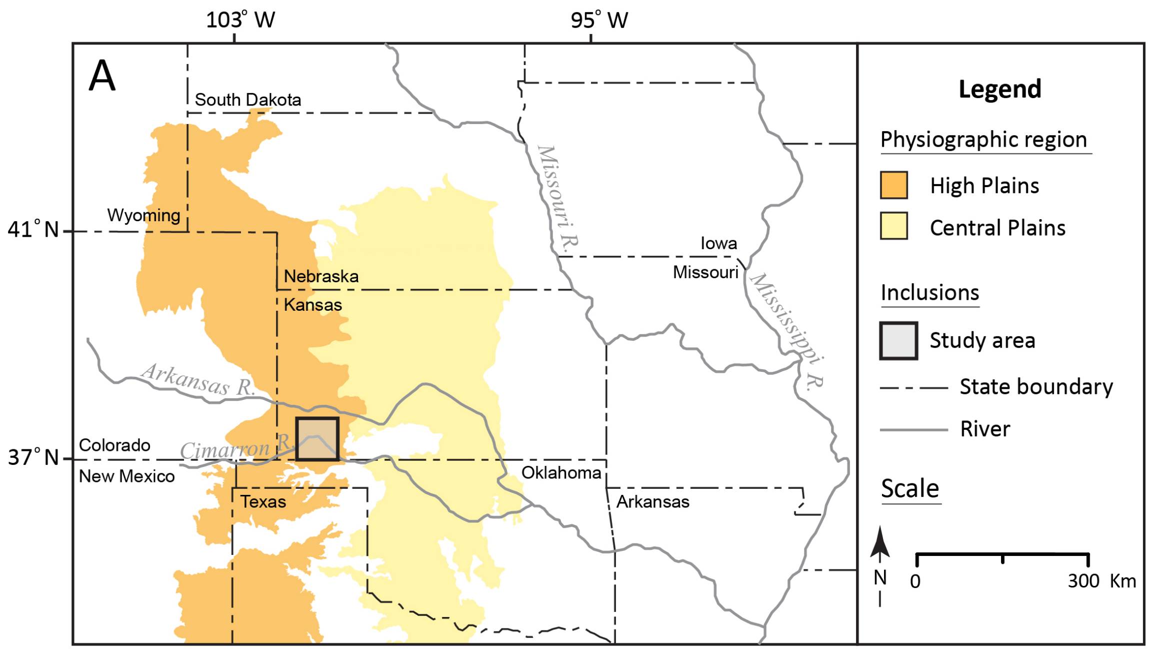


**Figure 1.1**. Map of study area location on the High Plains of southwestern Kansas. Physiographic regions from Fenneman (1931).

Pleistocene sediments and formation of buried soils; 3) Develop a paleoclimatic proxy record from Plio-Pleistocene deposits; 4) Investigate the relationship between landscape evolution and Plio-Pleistocene climate change.

The study area was chosen opportunistically to utilize a series of sand and gravel quarries that provide windows into the crosscutting relationships of Plio-Pleistocene deposits in the Cimarron River valley. In addition to the quarry outcrops, two 20-m deep cores were collected in close proximity to the outcrop face to ascertain valley fill thickness, and a 50-m deep core (CMC1) was taken on the High Plains surface. The CMC1 core was collected ~3 km from the quarry in which the Ogallala Formation is exposed and its location was determined by available access.

## 1.3. Background and rationale

### 1.3.1. Pleistocene alluvium

Previous research on alluvial deposits in the High Plains region has primarily been directed toward Holocene-aged fills (e.g., Johnson and Martin, 1987; Mandel, 1994; Bettis and Mandel, 2002). Relatively little work has been undertaken on the Pleistocene alluvium with the exception of studies in the mid-twentieth century that focused on basic lithostratigraphic and paleontological relationships (e.g., Smith, 1940; Frye and Hibbard, 1941; Frye and Leonard, 1952; Gutentag, 1963). This dissertation expands upon this early work by assessing stratigraphic, geomorphic, pedologic, and paleoenvironmental data from late-Pleistocene alluvial fills stored in the Cimarron River valley. These data provide a means to assess the geomorphic response of the Cimarron River to forcing mechanisms over a time interval for which such records are scarce in the Great Plains.

### 1.3.2. Pleistocene eolian deposits

Loess-paleosol sequences represent climatically controlled sedimentary extremes that can provide detailed terrestrial records of Quaternary climate change and landscape response (Muhs and Bettis, 2003). Several loess-paleosol sequences have been investigated in the Central and High Plains and at least four stratigraphically superposed Quaternary-aged loesses have been documented: the Loveland, Gilman Canyon, Peoria and Bignell loesses (e.g., Feng et al., 1994; Maat and Johnson, 1996; Muhs et al., 1999, 2008; Bettis et al., 2003; Rutter et al., 2006). Despite the recognition of multiple loess units, however, studies in the High Plains typically have focused on the youngest eolian deposits that comprise the surficial sediments of the region (e.g., Forman et al., 1995; Olson et al., 1997; Muhs et al., 1999; Mason et al., 2003; Muhs et al., 2008). Also, exposures of complete eolian stratigraphic sequences on the High Plains are rare, primarily due to the flat topography. Detailed analyses of soils and sediments from core, therefore, allow for investigation of late-Pleistocene paleoclimatic change and landscape response in this understudied part of the Great Plains.

### 1.3.3. Early Pliocene Ogallala Formation

In the High Plains of southwestern Kansas, the Miocene and early Pliocene sediments of the Ogallala Formation unconformably overlie Permian through Cretaceous strata (e.g., Frye at al., 1956; Merriam, 1963). The Ogallala Formation is the primary constituent of the High Plains aquifer, which provides almost 30% of all groundwater used for irrigation in the United States and is under increasing stress from developmental practices (e.g., Maupin and Barber, 2005; McGuire, 2009). The sedimentological properties and stratigraphic framework of the High Plains succession are derived from the formative processes and depositional histories of water-bearing strata (Smith et al., 2014). Documenting these properties, therefore, has important implications for management of the High Plains aquifer. This dissertation investigates the depositional history and paleoenvironments of the Ogallala Formation from a 50 m-deep core and presents preliminary findings from a new approach to date volcanogenic zircons from primary ash-fall tephra preserved in paleosols. Numerous paleosols have been identified in the Ogallala Formation (e.g., Diffendahl, 1982; Gustavson and Winkler, 1988; Gardner et al., 1992; Fox et al., 2012); hence this technique may provide a vital tool for establishing a chronostratigraphic framework for the High Plains succession.

### 1.4. Organization of dissertation

This dissertation is organized into five chapters, including this general introduction to the dissertation research (Chapter 1). Chapters 2–4 present individual studies focused on different depositional environments found on the High Plains of western Kansas. Chapter 2 focuses on Pleistocene alluvium stored in the Cimarron River valley and the geomorphic evolution of the Cimarron River. Chapter 3 discusses Pleistocene eolian sedimentation on the High Plains of western Kansas. Chapter 4 reports on the stratigraphy, depositional history and paleoenvironments of the Mio-Pliocene Ogallala Formation. Chapter 5 summarizes and concludes this dissertation, highlighting the main conclusions of chapters 2–4.

# CHAPTER 2

# LATE PLEISTOCENE GEOMORPHIC HISTORY OF THE CIMARRON RIVER, SOUTHWESTERN KANSAS

## 2.1. Introduction

Despite extensive research on the late-Pleistocene stratigraphy and paleoenvironments of the High Plains (e.g., Antevs, 1935; Frye and Leonard, 1952; Haynes and Agogino, 1966; Holliday, 1995, 2000; Holliday et al., 1994, 1996, 2011), significant gaps still exist. Previous studies in the central High Plains (western Kansas, southwestern Nebraska and eastern Colorado) have typically focused on late-Quaternary eolian sands and loess (e.g., Forman et al., 1995; Maat and Johnson, 1996; Olsen et al., 1997; Porter, 1997; Muhs et al., 1999, 2008; Olsen and Porter, 2002; Johnson et al., 2007) whereas research on alluvial deposits has primarily been directed toward Holocene-aged fills (e.g., Johnson and Martin, 1987; Mandel, 1994; Bettis and Mandel, 2002). In contrast, with the exception of studies during the mid-twentieth century that focused on basic lithostratigraphic and paleontological relationships (e.g., Smith, 1940; Frye and Hibbard, 1941; Frye and Leonard, 1952; Gutentag, 1963), relatively little work has been undertaken on the Pleistocene alluvium in this region. This study expands upon this early work by assessing stratigraphic, geomorphic, and pedologic data from late-Pleistocene (Marine Oxygen Isotope Stage (MIS) 4–2, ca. 77–12 ka) alluvial fills stored in the Cimarron River valley, southwestern Kansas. Also, stable carbon isotope ($\delta^{13}C$) data are used to assess paleoenvironmental change and subsequent alluvial response over a time interval for which such records are scarce in the Great Plains.

## 2.2. Study Area

### 2.2.1. Physiography and Geology

The study area is in the High Plains region of the Great Plains physiographic province (Fig. 2.1A; Fenneman, 1931). The High Plains generally comprises the western portion of the Great Plains, covering ~450,000 $km^2$, and represents the remnant of an extensive alluvial apron formed by sediment shed from the Rocky Mountains (e.g., Seni, 1980). In Kansas, the High Plains is predominantly underlain by the Miocene and early Pliocene-aged sediments of the Ogallala Formation together with Quaternary alluvial and eolian deposits (e.g., Merriam, 1963). Topographic relief is largely confined to stream valleys in which the Ogallala Formation crops out and Quaternary alluvium is stored (e.g., Mandel et al., 2004).

Interfluves and alluvial terraces in the High Plains are mantled by at least three late-Quaternary loesses: the Loveland, Gilman Canyon, and Peoria (e.g., Muhs et al., 1999; Bettis et al., 2003). The Loveland loess is typically the oldest loess unit exposed and dates to the penultimate glaciation (MIS 6). The Gilman Canyon Formation overlies the Loveland Loess and is usually < 2 m thick (Bettis et al., 2003). The Gilman Canyon Formation typically consists of a dark noncalareous silt loam that has been modified by pedogenesis, commonly with two or more soils forming a pedocomplex (e.g., Reed and Dreeszen, 1965; Mandel and Bettis, 1995; Johnson et al., 2007). Radiocarbon ages from sites in the Central Plains indicate that the Gilman Canyon Formation dates between ca. 40 and 20 ka (Muhs et al., 1999; Johnson et al., 2007). The Peoria Loess mantles the

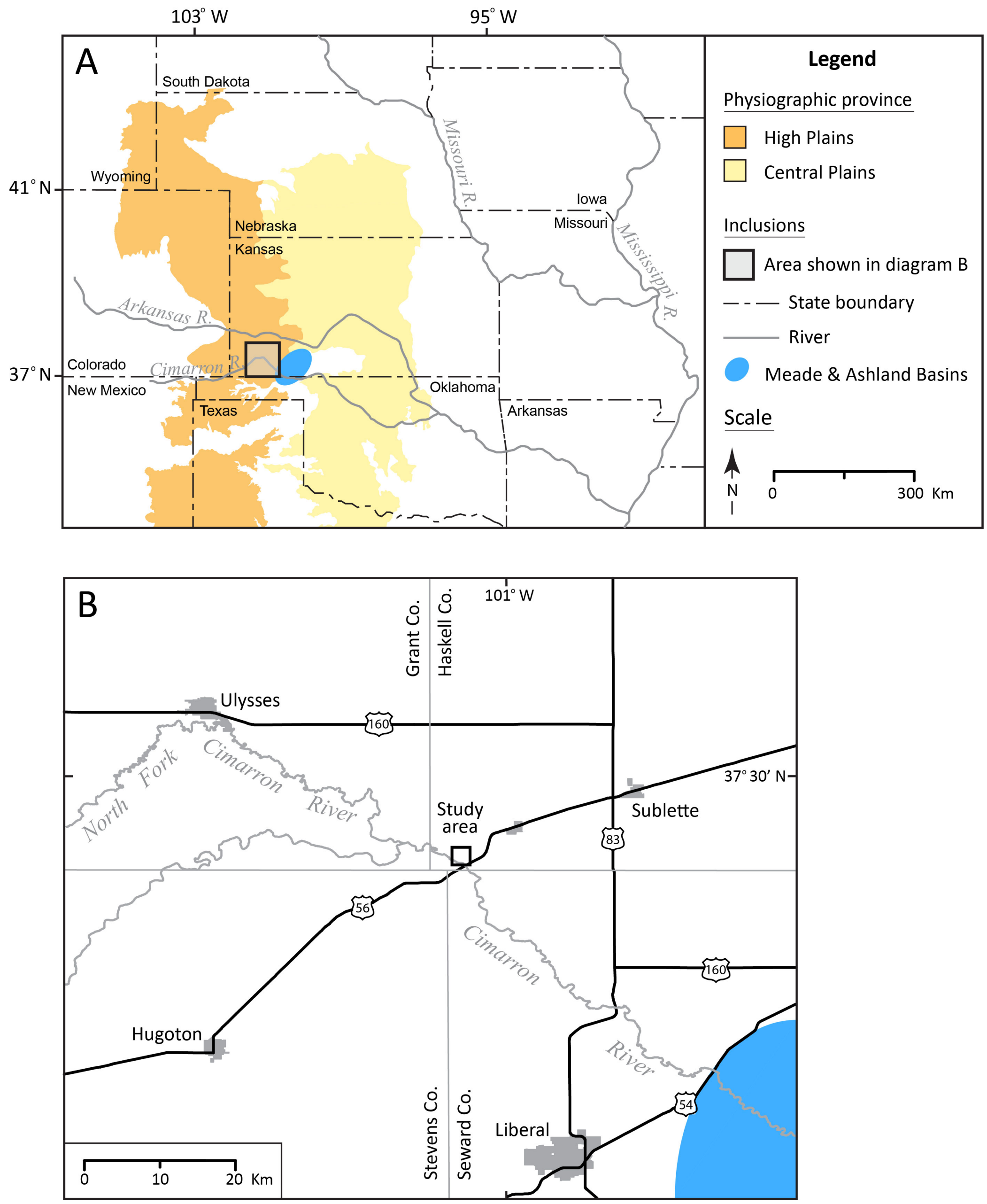


**Figure 2.1**. Study area location in the Central High Plains, southwestern Kansas. Physiographic regions from Fenneman (1931)

Gilman Canyon Formation and is the thickest and most areally extensive loess deposit in the Great Plains (Bettis et al., 2003). Radiocarbon ages indicate that Peoria Loess deposition began ~30 to 20 ka and continued to accumulate until ~13 ka (Bettis et al., 2003; Muhs et al., 2008).

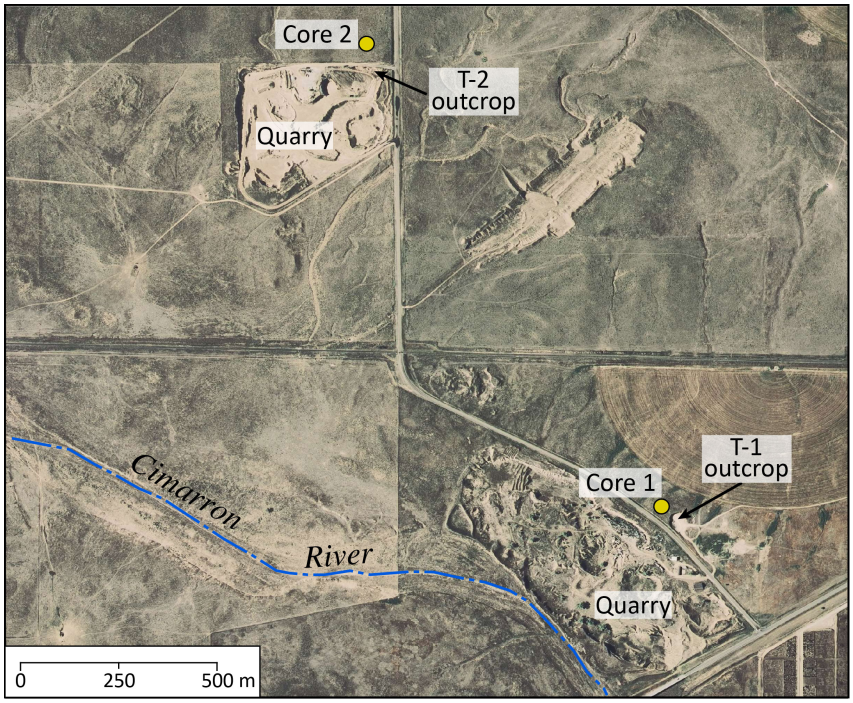


**Figure 2.2**. Aerial photograph of study area with quarry outcrop and core locations.

This study investigated late-Quaternary alluvium stored in the Cimarron River valley of southwestern Kansas. Valley fills underlying two terraces (T-1 and T-2) were investigated in two sand and gravel quarries in the southwest corner of Haskell County (Figs. 2.1 and 2.2). The T-1 and T-2 terrace treads stand 9 and 24 m above the modern river channel, respectively. The Cimarron River, a tributary of the Arkansas River, originates on the High Plains in northeastern New Mexico and drains ~49,000 km$^2$ (Fig. 2.1A). The Cimarron River has undergone significant morphological changes over the last 50 years, shifting from a wide, braided channel to a narrow, meandering one, with a 75% decline in mean channel width (VanLooy and Martin, 2005). Channel narrowing coincided with a decline in stream discharge owing to increased aridity and accelerated groundwater withdrawals from the High Plains Aquifer. In the study area, the valley width is ~3 km, with ~45 m of elevation change between the uplands and the valley floor.

2.2.2. Climate

The climate of southwestern Kansas is a semiarid steppe (BSk in the Köppen climate classification; Peel et al., 2007). Mean annual precipitation for the period of record at Sublette, Kansas is 47.3 cm (High Plains Regional Climate Center, 1918–2014). Mean July and January temperatures are 26 °C and 0 °C, respectively. Approximately 75% of the precipitation falls during the months of April through September. The collision of pacific and polar air masses with warm, moist, maritime-tropical air from the Gulf of Mexico often produces intense rainfall of short duration along the zone of convergence. Periodic intensification of westerly (zonal) airflow, however, prevents moist Gulf air from penetrating the Central Plains and tends to cause drought in the region. Drought frequency is modulated by positive and negative phases of the Atlantic Multidecadal Oscillation and Pacific Decadal Oscillation, respectively (e.g., McCabe et al., 2004). During late summer, high intensity, convectional storms are common. Periodic intensification of the North American Monsoon also brings peak summer rainfall to southwestern Kansas. Precipitation patterns are also affected by ENSO (El Niño–Southern Oscillation) variability where El Niño events tend to result in milder, wetter summers while La Niña episodes bring hot and dry summer conditions to the region (e.g., Hu and Huang, 2009).

2.2.3. Vegetation

The natural vegetation of southwestern Kansas is short grass prairie (e.g., Küchler, 1974). Uplands are dominated by $C_4$ plant communities, including blue gramma (*Bouteloua* *gracilis*) and buffalograss (*Buchloe dactyloides*). Big bluestem (*Andropogon gerardi*) and little bluestem (*Andropogon scoparius*) occur in dissected areas within the Cimarron River valley, and sandhill sage (*Artemisia filifolia*) is common on sandy soils. $C_3$ broadleaf deciduous trees, including cottonwood (*Populus sargentii*) and peachleaved willow (*Salix amygdaloides*), dominate riparian vegetation communities.

### 2.3. Methodology

Detailed stratigraphic, sedimentological, and pedological descriptions were prepared for two sections exposed in outcrop (Fig. 2.2). Also, a 20 m-deep core was collected from each of the alluvial fills underlying the T-1 and T-2 terraces. Cores were taken ~25 m from the outcrop face using an Acker hollow-stem auger drill rig equipped with a split-spoon sampler. Soils in outcrop were described in detail using standard terminology in Birkeland (1999) and Schoeneberger et al. (2012). Each soil horizon was measured and described in terms of its Munsell matrix color, texture, structure, consistency and boundary. Where present, clay films, roots, pores, secondary carbonate forms, and biogenic features were described. In addition, sedimentary features in C horizons were described where preserved. Soils were sampled by horizon for particle size (e.g., Schoeneberger et al., 2012). Where horizon thicknesses were >50 cm, subsamples were collected so that the sample interval was no greater than 50 cm. Air-dried (24–48 hrs) samples were ground to pass through a 2 mm sieve and 10 g of material was extracted for particle-size analysis using the pipette method (Soil Survey Staff, 1982). Calcium carbonate ($CaCO_3$) percent was determined by dry weight loss after HCl treatment and is reported as calcium carbonate equivalent (CCE).

Numerical-age control was provided by radiocarbon ($^{14}C$) dating of soil organic matter (SOM) and by optically stimulated luminescence (OSL) dating of sediments. Radiocarbon dating of SOM was selected because preferred materials, such as charcoal, are relatively scarce in buried soils on the High Plains. The $^{14}C$ samples from outcrop were submitted to the Illinois State Geological Survey (ISGS) and $^{14}C$ samples from core to the National Ocean Sciences Accelerator Mass Spectrometry (NOSAMS) facility at the Woods Hole Oceanographic Institute. All $^{14}C$ samples were pretreated to remove roots and carbonates. The ISGS dating was performed on the bulk organic fraction and $^{14}C$ activity was measured via the liquid scintillation technique. The NOSAMS samples were combusted in a high-temperature muffle furnace and the resultant $CO_2$ reacted with a Fe catalyst to create graphite. After conversion to graphite, $^{14}C$ activity was measured via Accelerator Mass Spectrometry (AMS).

Optically stimulated luminescence dating provides an age estimate of the time since sediment was last exposed to light (Huntley et al., 1985). Although fluvial environments can be challenging for OSL dating due to potential problems with solar resetting, termed partial bleaching, quartz small aliquot OSL dating has been successfully applied to numerous fluvial settings (e.g., Wallinga, 2002; Rittenour, 2008). The OSL samples were collected from the cores and analyzed at the Utah State University Luminescence Laboratory using the latest single-aliquot regenerative-dose (SAR) procedures for dating quartz sand (see Murray and Wintle, 2000). All samples were opened and processed under dim amber safelight conditions and were processed to isolate the fine-grained quartz sand fraction (using HCl to remove carbonates, household chlorine bleach to remove organics, heavy liquid to remove minerals (sodium polytungstate, 2.7 g/cm$^3$), and hydroflouric acid to etch the quartz and dissolve any remaining feldspars. Sample processing followed standard procedures outlined in Aitken (1998) and described in Rittenour et al. (2005).

Paleoenvironmental reconstructions were undertaken by analyzing stable carbon isotopes ($\delta^{13}C$) from SOM. This technique has been successfully applied in many paleoenvironmental studies conducted in alluvial settings (e.g., Nordt et al., 1994, 2002; Fredlund and Tieszen, 1997; Mandel, 2008; Cordova et al., 2010). During photosynthesis, plants fractionate carbon isotopes by differing amounts according to distinct metabolic pathways (i.e., $C_3$ and $C_4$ pathways) (Boutton, 1991). The $\delta^{13}C$ value of SOM from buried soils, therefore, reflects the relative contributions of $C_3$ and $C_4$ vegetation at the time of soil formation. Modern $C_3$ plant communities, which include cool season grasses and woody vegetation, produce SOM $\delta^{13}C$ values between -32‰ and -20‰ (average of -27‰) whereas $C_4$ plants, which typically comprise warm season grasses, produce SOM $\delta^{13}C$ values between -17‰ and -10‰ (average of -13‰) (e.g., Boutton, 1991). The relative contribution of $C_4$ plants to SOM is estimated with the following mass balance equation (Nordt et al., 1994)

$$\delta^{13}C_{SOM} = \delta^{13}C_{C4}(x) + \delta^{13}C_{C3}(x)\ (1\text{-}x) \qquad (1)$$

where $\delta^{13}C_{SOM}$ is the measured $\delta^{13}C$ value, $\delta^{13}C_{C4}$ = -13‰, $\delta^{13}C_{C3}$ = -27‰ and $x$ is the relative contribution of $C_4$ plants to SOM. Studies have shown a strong correlation between the proportion of $C_4$ vegetation and temperature (e.g., Terri and Stowe, 1976; Boutton, 1996), indicating that $\delta^{13}C$ values can function as an important proxy for paleoclimatic change.

$\delta^{13}C$ analysis was performed at the University of Kansas Keck Paleoenvironmental and Environmental Stable Isotope Laboratory. Bulk SOM samples were collected from outcrop at 10-cm intervals. Samples were oven-dried and then decarbonated with 10 ml of 0.5 M HCl. Samples were then centrifuged and rinsed with deionized water until attainment of a neutral pH. Samples were dried at 60°C and then ground to powder with a mortar and pestle. Between 5 and 35 mg of decarbonated sample was weighed into tin capsules, combusted using a Costech Elemental Analyzer at 1060°C, and analyzed with a continuous-flow ThermoFinnigan MAT 253 mass spectrometer. Final $\delta^{13}C$ data were calibrated with National Institute Standards and are expressed relative to the Vienna Peedee Belemnite standard.

## 2.4. Results

### 2.4.1. Stratigraphy and chronology

The highest and oldest terrace (T-2) stands ~24 m above the modern river channel (Fig. 2.3A). The T-2 fill is over 20 m thick and primarily consists of vertically stacked channel-fill sequences that fine upward and range in texture from fine gravel to loam (Fig. 2.3B and C). Horizontal bedding and cross-stratification are evident in outcrop.

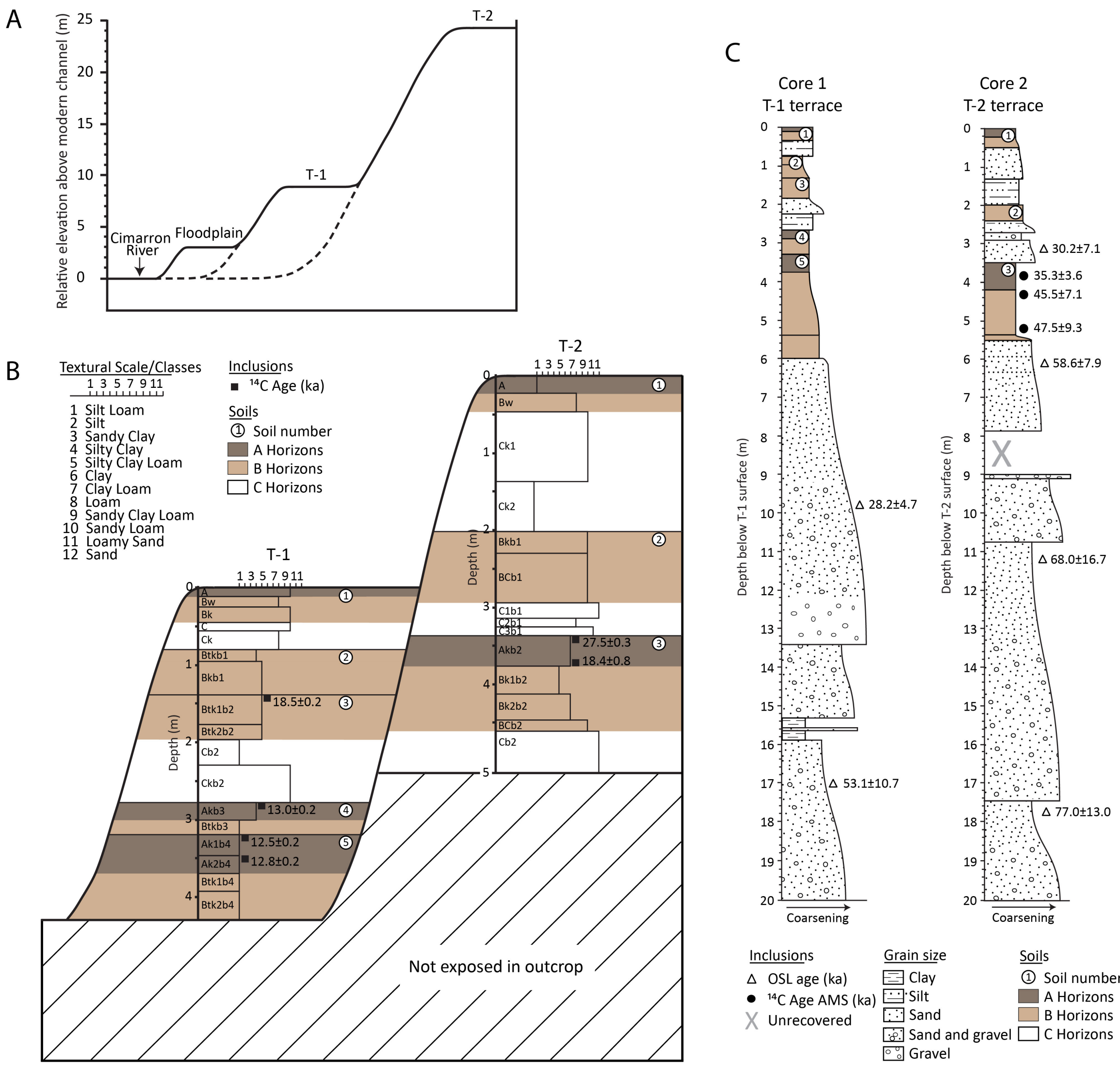


**Figure 2.3.** A) Terrace stratigraphy and tread elevations relative to the stream channel. B) Composite cross-section of alluvial fills exposed in quarries in the Cimarron River valley. Note that terrace fills are not to scale relative to each other. C) Stratigraphy of soils and sediments from core.

Sedimentological characteristics indicate deposition by a high-energy braided stream system. OSL ages of 77.0±13.0, 68.0±16.7 and 58.6±7.9 ka at 17.7, 11.1 and 6.2 m depths, respectively, indicate that this depositional environment prevailed in the study area during late MIS 5 and MIS 4 (Table 2.1).

**Table 2.1**. Optically Stimulated Luminescence age information

| Core | Lab no. | Depth (m) | Num. of aliquots[1] | Dose Rate[3] (Gy/ka) | Equivalent Dose, $D_E$[4] ± 2σ (Gy) | OD[5] (%) | OSL age ± 2σ (ka) |
|---|---|---|---|---|---|---|---|
| Core 1 | USU-1581 | 9.9 | 20 (34) | 1.82 ± 0.11 | 51.42 ± 6.42 | 25.7 ± 4.8 | 28.20 ± 4.68 |
| | USU-1582 | 17.1 | 12 (49) | 2.75 ± 0.17 | 145.7 ± 24.26 | 26.9 ± 6.4 | 53.07 ± 10.64 |
| Core 2 | USU-1588 | 3.2 | 15 (27) | 2.76 ± 0.14 | 83.46 ± 17.73 [6] | 37.3 ± 7.5 | 30.19 ± 7.11 |
| | USU-1589 | 6.2 | 15 (29) | 2.43 ± 0.15 | 142.5 ± 11.40 | 12.1 ± 3.5 | 58.61 ± 7.92 |
| | USU-1583 | 11.15 | 8 (47) | 2.51 ± 0.16 [7] | 170.9 ± 37.49 | 29.7 ± 8.1 | 68.04 ± 16.69 |
| | USU-1584 | 17.7 | 10 (44) | 2.59 ± 0.16 | 199.0 ± 25.54 | 17.4 ± 5.2 | 76.97 ± 13.03 |

[1] Number of aliquots used in age calculation and number of aliquots analyzed in parentheses.
[2] Radioelemental concentrations determined by ALS Chemex using ICP-MS and ICP-AES techniques.
[3] Dose rate is derived from concentrations by conversion factors from Guérin et al. (2011), and includes cosmogenic contribution to total dose rate using latitude, longitude, elevation and depth following Prescott and Hutton (1994). Assumed 13.8% as average moisture content for all samples below 5 m depth, assumed 5% for USU-1588, and in-situ 6% for USU-1518.
[4] DE calculated using the single-aliquot regenerative-dose procedure of Murray and Wintle (2000) on 1-mm small-aliquots of quartz sand (90-250μm). Weighted mean of DE calculated using the Central Age Model (CAM) of Galbraith et al. (2012), except where noted otherwise.
[5] Overdispersion (OD) calculated as part of the CAM and represents variance in DE data beyond measurement uncertainties, OD >20% may indicate significant scatter due to depositional or post-depositional processes.
[6] DE calculated using the Minimum Age Model of Galbraith et al. (2012).
[7] Dose rate calculated using chemistry data from USU-1584 and USU-1589.

Three soils, numbered 1 to 3 from top to bottom, occur in the T-2 fill (Table 2.2, Figs. 2.3B and 2.4). Soil $3_{T2}$ is a brown (10YR 5/3) to very pale brown (10YR 7/4) clay loam and silty clay loam, buried 3.38 m below the T-2 surface. Variability was observed in horizon thickness between outcrop and core, likely due to localized truncation by the stream channel. The soil has a moderately developed, 1.1 m-thick (2 m-thick in core) Ak-Bk profile. Calcium carbonate ($CaCO_3$) content ranges from 4 to 20% and is morphologically expressed in the form of fine to medium carbonate threads. Clay content in the soil is relatively high and uniform (31–37%). Organic content decreases progressively with depth from 0.21% in the Ak horizon to 0.04% in the C horizon. SOM from the upper and lower 10 cm of the Ak horizon in outcrop yielded ages of 23,330±170 $^{14}$C yr BP (27,800–27,290 cal yr BP) and 14,710±130 $^{14}$C yr BP (19,240–17,570 cal yr BP), respectively (Fig. 2.3B; Table 2.3). Three AMS $^{14}$C ages from SOM were also obtained from the middle of the Ak horizon and the top and bottom of the Bk horizon in

Table 2.2 – Soil descriptions from the T-2 outcrop profile

| Horizon | Depth (cm) | Color Dry | Color Moist | Texture[1] | Structure[2] | Consistence[3] | Clay Films | Boundary[4] | Pores[5] | Roots[5] | Notes |
|---|---|---|---|---|---|---|---|---|---|---|---|
| A | 0-22 | 10YR 4/2 | 10YR 3/2 | L | 1 f sbk | vfr | --- | c | 2vf | 1m 2f 3vf | Parts to 1 f gr; Common worm casts |
| Bw | 22-45 | 10YR 5/2 | 10YR 4/1 | SL | 2 f sbk | fr | --- | c | 1f 2vf | 1f 2vf | Parts to 2 f gr; Common worm casts |
| Ck1 | 45-137 | 10YR 6/4 | 10YR 5/4 | LS | sg | lo | --- | a | --- | 1f 2vf | Common carbonate nodules |
| Ck2 | 137-203 | 10YR 6/4 | 10YR 5/4 | SL | 1 f sbk | fr | --- | a | 2vf | 1f 1vf | Parts to sg; Few carbonate nodules |
| Bkb | 203-230 | 10YR 5/4 | 10YR 4/4 | SL | 2 m sbk | sh, vfr | --- | g | 1m 2f 3vf | 2vf | Parts to 1 f sbk and 1 f gr; Common fine threads and common patchy distinct coats on ped faces |
| BCb | 230-295 | 10YR 6/6 | 10YR 5/6 | SL | 2 f sbk | so, vfr | --- | c | 3f 2vf | 1vf | Parts to 1 f gr and sg |
| C1b | 295-316 | 10YR 6/6 | 10YR 5/6 | S | sg | lo | --- | a | --- | --- | Cross-stratification; gravel lenses |
| C2b | 316-326 | 10YR 6/4 | 10YR 5/4 | L | 1 f sbk | fr | --- | a | 2vf | --- | Parts to sg |
| C3b | 326-338 | 10YR 6/6 | 10YR 5/6 | LS | sg | lo | --- | a | --- | --- | Thin gravel lenses |
| Akb2 | 338-377 | 10YR 5/3 | 10YR 4/3 | CL | 2 m pr | h, fi | --- | g | 3f 3vf | --- | Parts to 1 f-m sbk; Few fine-medium carbonate threads |
| Bk1b2 | 377-414 | 10YR 6/3 | 10YR 5/3 | SICL | 2 m pr | h, fi | --- | g | 1m 3f 3vf | --- | Parts to 2 f-m sbk; Few fine carbonate threads; Few wormcasts in burrows |
| Bk2b2 | 414-448 | 10YR 7/3 | 10YR 6/4 | CL | 2 f pr | h,fr | --- | g | 2f 3vf | --- | Parts to 1 f sbk and 1 f gr; Common fine carbonate threads |
| BCb2 | 448-463 | 10YR 7/4 | 10YR 6/4 | SL | 1 m pr | so,vfr | --- | c | 3f 2vf | --- | Parts to 1 f sbk and sg |
| Cb2 | 463-500+ | 10YR 6/4 | 10YR 5/4 | S | sg | lo | --- | --- | --- | --- | |

[1]Texture: C – Clay, CL – Clay Loam, SiCL – Silty Clay Loam, SiC – Silty Clay, L – Loam, SiL – Silty Loam, LS – Loamy Sand
[2]Structure: 1 – weak, 2 – moderate, 3 – strong, m – massive, sg – single grain; f – fine, m – medium, c- coarse; abk – angular blocks, sbk – subangular blocks, pl – plates
[3]Consistence: so – soft, sh – slightly hard, h – hard, vh – very hard; lo – loose, vfr – very friable, fr – friable, fi – firm; vfi – very firm
[4]Boundaries: a – abrupt, c – clear, g – gradual
[5]Roots and pores: 1 – few, 2 – common, 3 – many; vf – very fine, f – fine, m – medium, c- coarse

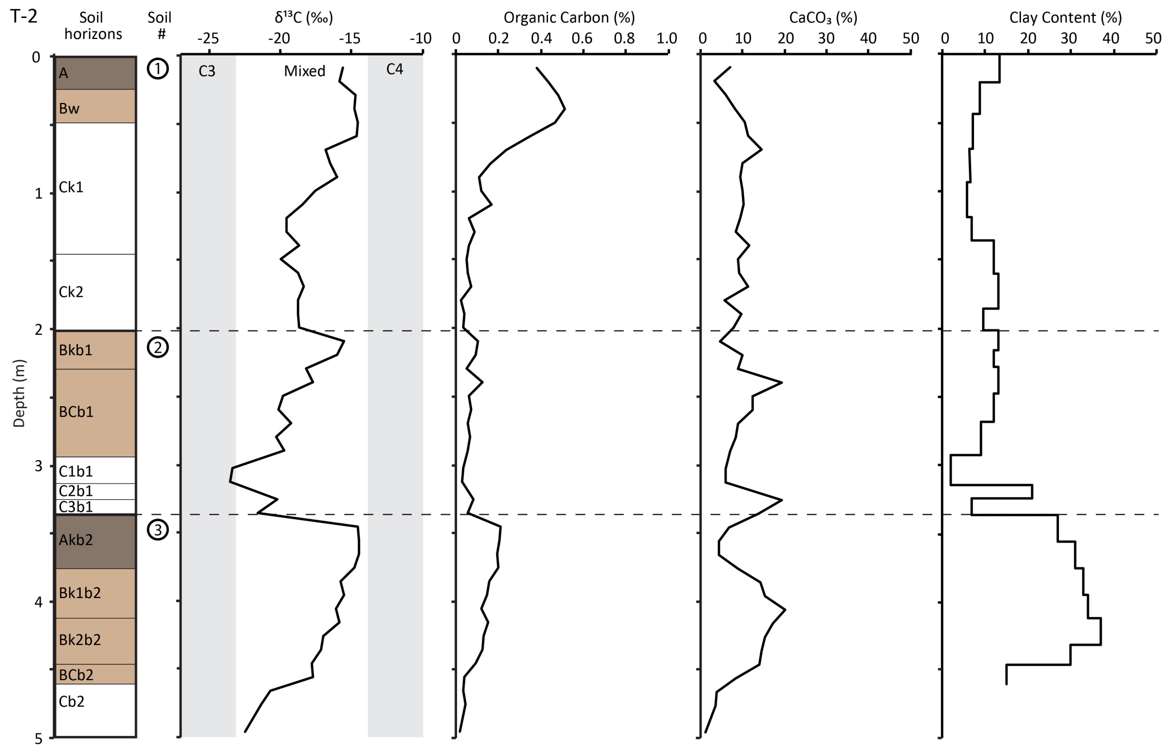


**Figure 2.4**. Soil stratigraphy and laboratory data ($\delta^{13}C$, organic carbon, $CaCO_3$ and clay content) from the T-2 outcrop profile.

core (Fig. 2.3C). AMS samples yielded ages of 31,300±1650 $^{14}C$ yr BP (38,950–31,720 cal yr BP), 42,400±6600 $^{14}C$ yr BP (52,620–38,380 cal yr BP) and 45,100±9300 $^{14}C$ yr BP (56,730–38,210 cal yr BP), respectively (Table 2.3). An OSL sample from the C horizon of soil 3 yielded an age of 58.6±7.9 ka (Table 2.1).

Soil $2_{T2}$ is a yellowish brown (10YR 5/4) sandy loam developed in sandy alluvium in which primary bedding structures (cross stratification and gravel lenses) are preserved. Gravel lenses consist of many stream-worn carbonate nodules that were likely derived from carbonate-rich paleosols developed in the Ogallala Formation. The soil is buried 2.03 m beneath the T-2 surface and has a truncated Bk horizon where the A horizon was

**Table 2.3.** Radiocarbon ages

| Landform | Depth (cm) | Horizon | $^{14}C$ age (yr B.P.) | Calibrated age range[1] (yr B.P.) | Median calibrated age (ka) | Lab no. | $\delta^{13}C$ |
|---|---|---|---|---|---|---|---|
| T-1 | 190-200 | Btk1b2 | 15,210±90 | 18,700-18,250 | 18.5±0.23 | ISGS-6998 | -6.4 |
| *(Outcrop)* | 278-288 | Akb3 | 11,110±70 | 13,100-12,800 | 13.0±0.15 | ISGS-6999 | -18.7 |
| | 320-330 | Ak1b4 | 10,520±70 | 12,670-12,370 | 12.5±0.15 | ISGS-7000 | -16.5 |
| | 348-258 | Ak2b4 | 10,930±70 | 12,980-12,700 | 12.8±0.14 | ISGS-7001 | -15.9 |
| T-2 | 338-348 | Akb2 | 23,330±170 | 27,800-27,290 | 27.5±0.26 | ISGS-7010 | -15.5 |
| *(Outcrop)* | 367-377 | Akb2 | 14,710±130 | 19,240-17,570 | 18.4±0.84 | ISGS-7011 | -13.4 |
| T-2 | 380 | Akb2 | 31,300±1650 | 38,950-31,720 | 35.3±3.62 | OS-111487 | -17.3 |
| *(Core)* | 420 | Bk1b2 | 42,400±6600 | 52,620-38,380 | 45.5±7.12 | OS-111488 | -14.3 |
| | 520 | Bk2b2 | 45,100±9300 | 56,730-38,210 | 47.5±9.26 | OS-111489 | -13.9 |

[1]Calibration to calendar years (2 sigma) was performed with CALIB 7.0 using calibration dataset IntCal13 (Reimer et al. 2013). $^{14}C$ ages older than 40,000 were calibrated with CalPal using the calibration dataset CalPal2007_HULU.

removed by erosion before subsequent burial. $CaCO_3$ content in the Bk horizon is between 5 and 10%. Carbonate morphology consists of fine carbonate threads and distinct patchy coats on ped faces. Clay content is relatively uniform throughout the Bk and BC horizons (12–13%) and organic content is relatively low (0.06–0.12%). An OSL sample from the C horizon of soil 2 yielded an age of 30.2±7.1 ka (Table 2.1).

The modern surface soil (soil $1_{T2}$) is a dark grayish brown (10YR 4/2) to grayish brown (10YR 5/2) loam and sandy loam with a weakly developed B horizon. In the A and Bw horizons, organic content is relatively high (0.38–0.51%) and clay content decreases with depth from 13.5 to 8.7%. The Ck1 and Ck2 horizons have loamy sand and sandy loam textures, respectively. Analysis of the particle-size distribution of the sand fraction indicates that the Ck1 and Ck2 horizons are mostly comprised of medium (500–355 μm) to fine (125–90 μm) and fine to very fine sand (125–63 μm), respectively. Also, no primary bedding structures were observed in these horizons. Eolian sediments and landforms typically blanket the upland landscape in the study area, leading one to suspect that the massive, unstratified sediments on the T-2 surface, which represent the parent material for the surface soil, are eolian. However, an alluvial origin for these sediments cannot be ruled out.

The youngest terrace (T-1) stands ~9 m above the modern river channel (Fig. 2.3A). The T-1 fill mostly consists of coarse-grained alluvium. A basal sample at ~17 m depth produced an OSL age of 53.1±10.7 ka and an OSL sample at ~10 m depth produced an age of 28.2±4.7 ka (Table 2.1). The upper portion of the T-1 alluvial fill exposed in outcrop has sandy loam, loamy sand and sand textures in which five soils have developed (Table 2.4, Figs. 2.3B and 2.5). The lowest soil (soil $5_{T1}$) is a silt loam that occurs 3.2 m beneath the T-1 surface. Soil $5_{T1}$ has a prominent grayish brown (10YR 5/2) to dark grayish brown (10YR 4/2) Ak horizon that is 50 cm thick and organic rich (0.42–0.48% organic carbon). Fine carbonate threads and distinct patchy coats are evident on ped faces. The Btk horizon is over 60 cm thick (1.15 m thick in core) and has yellowish brown (10YR 5/4) to light yellowish brown (10YR 6/4) matrix colors, common carbonate threads, and continuous brown (10YR 4/2) clay films on ped faces. Clay and $CaCO_3$ content peak at 21 and 11.9%, respectively. SOM from the upper 10 cm of the Ak1 and Ak2 horizons yielded ages of 10,520±70 $^{14}C$ yr BP (12,670–12,370 cal yr BP) and 10,930±70 $^{14}C$ yr BP (12,980–12,700 cal yr BP), respectively (Fig. 2.3B; Table 2.3).

**Table 2.4**. Soil descriptions from T-1 outcrop profile

| Horizon | Depth (cm) | Color Dry | Color Moist | Texture[1] | Structure[2] | Consistence[3] | Clay Films[4] | Boundary[5] | Pores[6] | Roots[6] | Notes |
|---|---|---|---|---|---|---|---|---|---|---|---|
| A | 0-7 | 10YR 4/2 | 10YR 3/2 | SL | 2 f gr | vfr | --- | c | 3f 3vf | 3f 3vf | |
| Bw | 7-25 | 10YR 4/2 | 10YR 3/2 | L | 2 f sbk | sh, vfr | --- | c | 1m 2f 3vf | 1m 2f 2vf | Parts to 1 f gr; Common worm casts, few open burrows |
| Bk | 25-45 | 10YR 6/4 | 10YR 5/4 | SL | 1 c pr | sh, vfr | --- | g | 1f 2vf | 1m 2f 2vf | Parts to 1 f sbk and 2 f gr; Few medium soft carbonate masses; Common worm casts, few open burrows |
| C | 45-55 | 10YR 6/4 | 10YR 5/4 | SL | 1 c pr | sh, vfr | --- | c | 2vf | 1f 2vf | Few medium soft carbonate masses |
| Ck | 55-80 | 10YR 7/4 | 10YR 5/4 | L | 1 c pr | sh, vfr | --- | a | 1f 3vf | 2vf | Few thin beds, gravel lens at 80 cm; Few medium hard carbonate masses, common fine threads |
| Btkb1 | 80-94 | 10YR 6/4 | 10YR 5/4 | SiC | 2 c pr | h, fr | 1 f pf, po | c | 1f 2vf | 1vf | Parts to 2 f-m abk; Patchy 10YR 4/4 clay films; Few fine hard carbonate masses, common distinct patchy coats on ped faces; Many wormcasts, Common open worm burrows |
| Bkb1 | 94-135 | 10YR 6/4 | 10YR 5/4 | SiCL | 2 c pr | h, fr | --- | c | 2f 3vf | 1f | Parts to 1 m sbk; Common fine hard carbonate masses, few fine threads and common distinct patchy coats on ped faces; Many wormcasts, common open worm burrows |
| Btk1b2 | 135-168 | 10YR 6/4 | 10YR 5/4 | SiCL | 2 m pr | h, fr | 2 d pf | g | 3f 3vf | 3vf | Parts to 2 f-m abk; Discontinuous 10YR 4/3 clay films; Few fine carbonate threads; Few faint 10YR 5/6 mottles along root paths; Many wormcasts, common open worm burrows |
| Btk2b2 | 168-194 | 10YR 7/4 | 10YR 6/4 | SiCL | 2 c pr | h, fr | 1 f pf, po | c | 2m 2f 2vf | 2f | Parts to 2 f-m sbk; Patchy 10YR 4/3 clay films; Few fine hard carbonate masses, few fine threads; Many wormcasts, common open worm burrows |
| Cb2 | 194-230 | 10YR 7/4 | 10YR 6/4 | SiL | 1 m pr | h, vfr | --- | a | 2vf | 1f | Few thin beds |
| Ckb2 | 230-278 | 10YR 7/4 | 10YR 6/4 | SL | 1 c pr | sh,,vfr | --- | c | 2f | 1f | Common fine gravel beds, Few fine carbonate threads; Common 10YR 6/3 flood coats on ped faces |

**Table 2.4 continued**. Soil descriptions from T-1 outcrop profile

| Horizon | Depth (cm) | Color Dry | Color Moist | Texture[1] | Structure[2] | Consistence[3] | Clay Films[4] | Boundary[5] | Pores[6] | Roots[6] | Notes |
|---|---|---|---|---|---|---|---|---|---|---|---|
| Akb3 | 278-300 | 10YR 5/2 | 10YR 4/2 | SiCL | 1 f pr | sh,fr | --- | g | 3f 3vf | 1f | Parts to 2 m-c gr; Common fine carbonate threads and common distinct patchy coats on ped faces |
| Btkb3 | 300-320 | 10YR 6/3 | 10YR 5/3 | SiL | 2 m pr | sh,fr | 1 f pf | g | 1m 3f 3vf | 1f | Parts to 2 f-m sbk; Discontinuous 10YR 4/2 clay films; Common fine carbonate threads and common distinct patchy coats on ped faces; Many wormcasts, common open worm burrows |
| Ak1b4 | 320-348 | 10YR 5/2 | 10YR 3/2 | SiL | 1 f-m pr | h, fr | --- | g | 2m 3f 3vf | 1vf | 50% 10YR 4/2 dry; Parts to 2 m-c gr; Common fine carbonate threads and many distinct patchy coats on ped faces; Many wormcasts, common open worm burrows |
| Ak2b4 | 348-369 | 10YR 4/2 | 10YR 3/2 | SiL | 1 f-m pr | h, fr | --- | g | 2m 3f 3vf | 1vf | Parts to 2 m-c gr; Common fine carbonate threads and many distinct patchy coats on ped faces; Many wormcasts, common open worm burrows |
| Btk1b4 | 369-393 | 10YR 5/4 | 10YR 4/4 | SiL | 1 m pr | h, fr | 2 d pf | g | 1m 2f 2vf | 1vf | Parts to 2 m sbk; Common fine and few medium carbonate threads; Continuous 10YR 4/2 clay films; Few wormcasts, few open worm burrows |
| Btk2b4 | 393-430+ | 10YR 6/4 | 10YR 5/4 | SiL | 1 m pr | h, fr | 1 f pf | --- | 1m 2f 2vf | 1vf | Parts to 1 f pr; Common fine and very fine carbonate threads; Patchy 10YR 5/2 clay films |

[1]Texture: C – Clay, CL – Clay Loam, SiCL – Silty Clay Loam, SiC – Silty Clay, L – Loam, SiL – Silty Loam, LS – Loamy Sand
[2]Structure: 1 – weak, 2 – moderate, 3 – strong, m – massive, sg – single grain; f – fine, m – medium, c – coarse; abk – angular blocks, sbk – subangular blocks, pl – plates
[3]Consistence: so – soft, sh – slightly hard, h – hard, vh – very hard; lo – loose, vfr – very friable, fr – friable, fi – firm; vfi – very firm
[4]Clay Films: 1 – few, 2 – common, 3 – many; d – distinct, p – prominent; pf – ped faces, po – pores
[5]Boundaries: a – abrupt, c – clear, g – gradual
[6]Roots and pores: 1 – few, 2 – common, 3 – many; vf – very fine, f – fine, m – medium, c – coarse

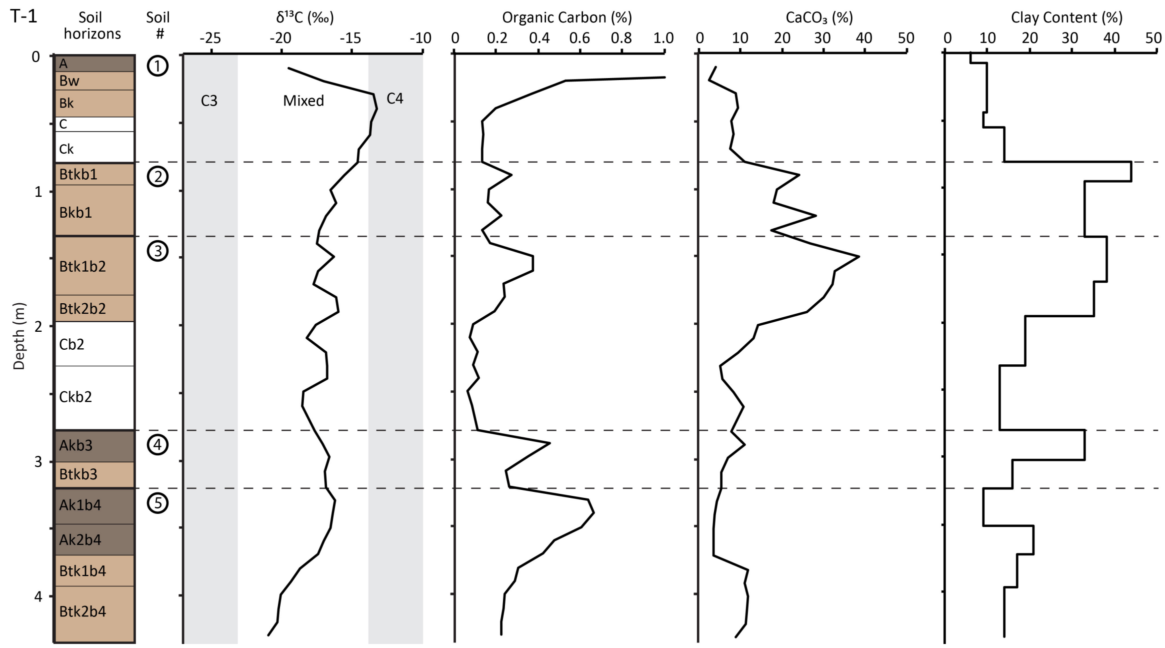


**Figure 2.5.** Soil stratigraphy and laboratory data ($\delta^{13}C$, organic carbon, $CaCO_3$ and clay content) from the T-1 outcrop profile.

Soil $4_{T1}$ is similar to soil $5_{T1}$ in terms of its morphological expression (i.e., horizonation, structure, consistence, and carbonate morphology). The Ak horizon of soil $4_{T1}$ has a higher clay content (33%) than soil $5_{T1}$ and is a silty clay loam. SOM from the upper 10 cm of the Ak horizon yielded a $^{14}C$ age of 11,110±70 yr BP (13,100–12,800 cal yr BP; Fig. 2.3B; Table 2.3).

Soil $4_{T1}$ is capped by upward-fining alluvium (sandy loam to silt loam) in which a moderately expressed soil (soil $3_{T1}$) developed and was subsequently truncated by erosion. Soil $3_{T1}$ is a light yellowish brown (10YR 6/4) and very pale brown (10YR 7/4) silty clay loam. The Btk horizon is 59 cm thick and has brown (10YR 4/3) discontinuous and patchy clay films on ped faces and in macropores. Clay content peaks at 38% in the Btk horizon. $CaCO_3$ content is relatively high (26–39%) and is expressed in the form of fine threads and hard nodules. SOM from the upper 10 cm of the profile yielded a $^{14}C$ age of 15,210±90 yr BP (18,700–18,250 cal yr BP; Fig. 2.3B; Table 2.3).

Soil 2 $_{T1}$ occurs 0.8 m below the T-1 surface and has a moderately developed Btk-Bk profile; the A horizon was likely stripped off by erosion before burial. The Btk horizon has the highest clay content (44%) in the section. Clay illuviation is evident in the form of patchy clay films on ped faces and in macropores. Carbonate morphology in both the Btk and Bk horizons is expressed in the form of hard carbonates nodules, fine threads, and distinct patchy coats on ped faces. $CaCO_3$ content ranges between 17 and 28%.

The modern surface soil (soil $1_{T1}$) developed in the T-1 fill is a dark grayish brown (10YR 4/2) to light yellowish brown (10YR 6/4) sandy loam and loam. Soil $1_{T1}$ has a moderately developed A-Bw-Bk profile. Organic content is relatively high in the Bw and Bk horizons (0.2–0.53%) and peaks in the A horizon at 2.4%. $CaCO_3$ content in the Bk horizon is about 9% and secondary accumulations consist of soft nodules.

2.4.2. Stable carbon isotopes

The $\delta^{13}C$ values of SOM from buried soils reflect the relative contributions of $C_3$ and $C_4$ vegetation at the time of soil formation and provide an important proxy for assessing paleoenvironmental change. $\delta^{13}C$ values of SOM from soil $3_{T2}$ in the T-2 fill increase progressively from -24.0‰ at the bottom of the soil to -14.6‰ at the top, indicating an substantial increase of 67% in the proportion of $C_4$ biomass (Fig. 2.4). $\delta^{13}C$ values become significantly more negative (-23.5‰) in the C horizon of soil $2_{T2}$, indicating that vegetation compositions shifted from a $C_4$-dominated community to a $C_3$-dominated community at this time (after ca. 28 ka). $\delta^{13}C$ values progressively increase to -15.5‰ at the top of soil $2_{T2}$ indicating another substantial increase (57%) in the amount of $C_4$ vegetation. In soil $1_{T2}$, $\delta^{13}C$ values initially decrease to -18.7‰ and progressively increase to -15.6‰ at the top of the soil (increase of 22% in $C_4$ biomass) (Fig. 2.4).

The $\delta^{13}C$ values from the T-1 fill range from -21.0 to -13.2‰, indicating that vegetation communities varied from $C_3$-dominated to strongly $C_4$-dominated over the last ca. 13 ka (Fig. 2.5). $\delta^{13}C$ values increase from -21.0‰ at the bottom of soil $5_{T1}$ to -16.3‰ near the top, indicating a 34% increase in the proportion of $C_4$ biomass beginning before ca. 13.0 ka and ending after 12.5 ka. $\delta^{13}C$ values decrease to -18.5‰ at the bottom of soil $3_{T1}$ before progressively increasing up section.

## 2.5. Discussion

### 2.5.1. Chronology and correlation

Due to the lack of macrofossils and charcoal preserved in the alluvial deposits, SOM was dated using both liquid scintillation and AMS techniques. Ages determined on SOM provide an assessment of mean resident time for organic carbon that, while not providing an absolute age, typically gives a minimum age for the period of soil development. The number of stratigraphically inverted $^{14}C$ ages in this study (3 ages out of 9) highlights some of the problems associated with $^{14}C$ dating SOM (see Mayer et al., 2008). Inputs of old detrital carbon, reworked from older alluvial fills or surrounding uplands, can cause the measured $^{14}C$ of bulk SOM to be older than the actual age of the soil. Younger carbon, however, also can be introduced into older buried soil horizons via root growth, bioturbation or the leaching of mobile organic compounds (e.g., Geyh et al., 1983; Halfen and Hasiotis, 2010).

With the exception of one $^{14}C$ age (14,710 $^{14}C$ yr BP), all $^{14}C$ ages from soil $3_{T2}$ in the T-2 fill are in stratigraphic order (Table 2.3). The anomalous age most likely reflects the input of younger carbon into the soil. Overall, the chronology indicates that soil 3 formed between 45,100 and 23,330 $^{14}C$ yr BP (ca. 48–28 ka) and is coeval with the Gilman Canyon Formation pedocomplex. Published $^{14}C$ ages for the Gilman Canyon Formation range from 40,600–19,770 $^{14}C$ yr BP (ca. 44–24 ka) from sites across the Central Great Plains (e.g., Souders and Kuzila, 1990; Muhs et al., 1999; Johnson et al., 2007).

The stratigraphically inverted ages from soils $3_{T1}$ and $4_{T1}$ in the T-1 fill likely represent the input of detrital carbon either eroded from older fills (e.g., the T-2 fill) or, in the case of soil $4_{T1}$, older carbon reworked from soil $5_{T1}$ due to their close proximity. The two $^{14}C$ ages from soil $5_{T1}$ are in correct stratigraphic order and are considered accurate based on $^{14}C$ ages determined on similar alluvial soils dating to 12.9–11.5 ka that represent a major episode of quasi-stability and cumulic soil development throughout the Central Plains (see Mandel, 2008).

2.5.2. Paleoenvironments

As $C_4$ plants have a competitive advantage over $C_3$ plants under conditions of higher temperatures and drought, the progressive increase in $\delta^{13}C$ values from soil $3_{T2}$ in the T-2 fill suggests climatic warming and likely drying during MIS 3 (ca. 48–28 ka). The significantly more negative $\delta^{13}C$ values in the C horizon of soil $2_{T2}$ suggest a shift to cooler and likely wetter conditions after ca. 28 ka. $\delta^{13}C$ values progressively increase at the top of soil $2_{T2}$ signifying warmer and likely drier climatic conditions during this period of soil formation.

The increase in $\delta^{13}C$ values in soil $5_{T1}$ from the T-1 fill, beginning before ca. 13.0 ka and ending after 12.5 ka, suggests a period of climatic warming and drying that likely correlates with the Bølling–Allerød interstadial. The slight decrease of ~2‰ in $\delta^{13}C$ values in soil $4_{T1}$ suggests a period of climatic cooling and may correspond to the Younger Dryas stadial. However, this decrease is relatively small and may be related to inherent soil processes rather than changes in vegetation composition (e.g., Krull and Skjemstad, 2003).

2.5.3. Regional comparisons

2.5.3.1. MIS 3: ca. 57–28 ka

Stable oxygen isotope ($\delta^{18}O$) records from Greenland ice cores indicate that MIS 3 experienced frequent and rapid climatic fluctuations known as Dansgaard–Oeschger (DO) events (Dansgaard et al., 1993). DO events are characterized by abrupt warming followed by a gradual return to cold, stadial conditions. During these events, different lobes of the Laurentide Ice Sheet retreated and advanced, resulting in the deposition of glaciogenic loess in the Missouri and Mississippi River valleys (e.g., Bettis et al., 2003). The manifestation and impact of DO events in the Central and High Plains, however, remains unclear due to the lack of high-resolution paleoenvironmental studies (see Voelker, 2002). In general, regional paleoenvironmental studies support the inference of increasingly warm and arid climatic conditions, documented in this study from stable carbon isotopes, during late MIS 3 that resulted in cumulic soil development and the formation of soil $3_{T2}$ in the T-2 fill.

A late-Quaternary pollen record from Cheyenne Bottoms in central Kansas indicates the existence of a persistent shallow-water marshland at ca. 34 ka that began to rapidly dry around 30 ka, with deposition ceasing in the basin by ca. 28 ka (Fredlund, 1995). Jacobs et al. (2007) document a similar record from the Cobb Basin in the Nebraska Sand Hills. Age control indicates that a lake was present in the Cobb basin at ca. 45 ka but was completely filled by 27 ka. A progressive decrease in lake level during the latter stages of the basin's history suggests a decrease in precipitation and diatom assemblages indicate slightly saline waters at this time indicative of evaporative conditions. Similarly, a summary of paleobotanical records from the eastern Great Plains (eastern Kansas and Nebraska, Iowa and Missouri) suggests cooler temperatures and increased moisture at ca. 38 ka, with more arid conditions prevailing between 37–29 ka as indicated by a decline in aquatic and weedy taxa and increased loess accumulation in wetland areas (Baker et al., 2009). Well-dated, high-resolution records of $\delta^{13}C$ and $\delta^{18}O$ data from speleothems at

Reed's Cave in South Dakota (Serefiddin et al., 2004) and Crevice Cave in southeastern Missouri (Dorale, 1998) also suggest warming from ca. 31–26 ka and after ca. 37 ka, respectively.

The warming and drying trend during MIS 3 inferred in this study and other regional paleoenvironmental investigations also are consistent with MIS 3 climate simulations from Van Meerbeeck et al. (2009), which suggest that MIS 3 climates across the Great Plains were substantially warmer and that annual precipitation was lower compared to the Last Glacial Maximum (LGM). Simulations indicate enhanced westerlies during MIS 3 over the region, which may have reduced the influx of moist subtropical air masses, as well as enhanced seasonality, with mainly warmer summers due to an increase in summer insolation.

Paleoenvironmental change in the mid-continent during MIS 3 also is indicated in mineralogical and sedimentological data from the Gulf of Mexico (GOM). Sionneau et al. (2013) identified distinct mineralogical provinces that contributed sediment at different times to the GOM. Between 42.6–37.3 ka and 31.4–29.6 ka, clay mineralogy indicates a dominance of illite and chlorite clay minerals derived from the northeastern Mississippi watershed and the Great Lakes region, which suggests that moisture inflow from the GOM into the Central and High Plains was prevented at this time and that the region experienced generally arid conditions.

One potential mechanism for increasing aridity in the Central Plains during late MIS 3 is meltwater discharge from the Laurentide Ice Sheet into the GOM. A $\delta^{18}O$ record from the GOM indicates five negative isotope excursions associated with increased meltwater discharge from ca. 44–28 ka (Hill et al., 2006) whereas sedimentological evidence from the northwest GOM indicates four meltwater events from ca. 53–32 ka (Tripsansas et al., 2007). Rittenour et al. (2007) also mapped extensive braidbelts in the lower Mississippi valley at this time (ca. 64–30 ka). Glacial meltwater discharge would have cooled sea surface temperatures in the GOM, resulting in reduced influx of subtropical air into the Central and High Plains during this period.

#### 2.5.3.2. MIS 2: ca. 28–14 ka

Climatic models indicate a bifurcation of the jet stream in response to the presence of the Laurentide ice sheet during late MIS 2 (e.g., Kutzbach, 1987; COHMAP, 1988; Bartlein et al., 1998). Paleowinds, originating from the northwest during this period, resulted in extensive loess deposition (Peoria Loess) across the Central and High Plains (e.g., Bettis et al., 2003; Muhs et al., 2008). Botanical and faunal studies from the Central Plains generally suggest colder climates during MIS 2, with greater effective moisture and less seasonality than today. These climatic conditions resulted in the deposition of the bulk of the T-1 fill in the Cimarron River valley.

In central Kansas, Fredlund (1995) reported an expansion of pine and spruce at ca. 28 ka, based on pollen data, suggesting a shift to colder climatic conditions. Similarly, in the eastern Plains, evidence exists for a region-wide shift in vegetation from open parkland to spruce forest after ca. 29 ka (Baker et al., 2009). In the Black Hills of South Dakota, $\delta^{18}O$ data suggests cooling from ca. 26–24 ka (Serefiddin et al., 2004). Wells and Stewart (1987) recorded spruce charcoal at three locations in south-central Nebraska and north-central Kansas that date to between ca. 21.5 and 17.6 ka. Also, land-snail and vertebrate fauna documented at these sites are typical of fauna found in modern subalpine taiga regions. Whereas other studies have argued against the presence of closed forests in the Central Plains at this time, they nonetheless affirm cool and moist conditions in the region. Fredlund and Jaumann (1987) reviewed late-Quaternary pollen and botanical data from the Central Plains and hypothesized an open parkland physiognomy composed of a mosaic of spruce and aspen with extensive prairie openings during the late Pleistocene. Rousseau and Kukla (1994) investigated mollusk assemblages at the Eustis Ash Pit in southwestern Nebraska that indicated relatively cool and moist conditions from ca. 24–16 ka, which resulted in a steppe prairie environment with scattered shrubs and trees. Inferences of colder climatic conditions from 24–14 ka in the Central Plains are also consistent with $\delta^{13}C$ data that indicate the dominance of $C_3$ plant communities during this period (e.g., Muhs, 1999; Johnson and Willey, 2000).

While there is general agreement that climatic conditions were colder from ca. 28–14 ka in the Central Plains, there is less certainty about moisture regimes. Although Wells and Stewart (1987) and Rousseau and Kukla (1994) suggest cold and moist conditions in north-central Kansas and southwest Nebraska, respectively, the pollen and sedimentological record from Cheyenne Bottoms suggests that climatic conditions were cold and dry during this period (Fredlund, 1995).

2.5.3.3. Early MIS 1: ca. 14–11 ka

The Pleistocene–Holocene transition was a period of considerable climatic variability on the Central Plains (e.g., Johnson and Willey, 2000; Mandel, 2008). Moreover, the stratigraphic records from the Central Plains during this time period show considerable temporal and spatial variability that reflect local paleoenvironmental conditions and probably complex response to the reorganization of mid-latitude climates following the collapse of the Laurentide ice sheet (Holliday et al., 2011). The shift to warmer and likely drier climatic conditions by ca. 12.4 ka inferred from the T-1 fill $\delta^{13}C$ record has, however, been documented by other regional paleoenvironmental studies. Cordova et al. (2010) suggest that a cool, wet environment prevailed in northwestern Kansas from ca. 14–12.9 ka and that conditions became more arid from ca. 12.9–12.2 ka, based on phytolith and $\delta^{13}C$ data. $\delta^{13}C$ analyses by Mandel (2008) at the Willem Ranch site in northwestern Kansas reveals a similar story of paleoenvironmental change. Bement et al. (2007) reported that $C_3$ plant communities dominated at Bull Creek in the Oklahoma Panhandle before ca. 12.9 ka followed by a shift to more mixed $C_3$ and $C_4$ communities at ca. 12.2 ka and $C_4$-dominated communities by ca. 11.2 ka. Pollen data indicate a sage scrubland environment mixed with hardwoods, sparse pines and junipers, and an understory of mixed grasses before ca. 12.9 ka. From ca. 12.9–12.7 ka grasslands begin to dominate and a drying of the environment is indicated by increases in high spine Asteraceae species. Further drying is indicated through ca. 11.2 ka by increases in Cheno-Am pollen.

### 2.5.4. Alluvial response to extrinsic and intrinsic forcing

Fluvial systems incise and aggrade based on the relationship between stream power (a function of discharge and slope) and sediment supply (Bull, 1991). Also, many studies have shown that changes in discharge and sediment supply are climatically driven (e.g., Knox, 1983; Bull, 1991; Mandel, 1994; Blum and Tornqvist, 2000). Consideration of both extrinsic and intrinsic forcing mechanisms on stream power and sediment supply, therefore, allows for investigation into the causes of incision and aggradation in the Cimarron River valley during the late Pleistocene.

Chronostratigraphic evidence (Fig. 2.3C) from core 2 indicates that the T-2 fill aggraded at least 12 m between ca. 77 and 58 ka followed by soil formation between ca. 48 and 28 ka, likely due to incision and terrace formation. Fluvial sediments from core 1, collected from the alluvium underlying the T-1 terrace, produced OSL ages of 53 ka at ~17m depth and 28 ka at ~10 m depth. The basal age is consistent with age estimates of the T-2 alluvial fill and is separated from the upper younger T-1 deposits by a coarse-grained unit interpreted to represent the base of channel incision into the T-2 alluvium at ~13.5 m.

During late MIS 5 through MIS 4 (ca. 77–58 ka) stratigraphic and sedimentological evidence indicate that the Cimarron River was an aggrading, braided stream. Paleoclimatic conditions were likely cool and wet at this time. Between ca. 48 and 28 ka, $\delta^{13}C$ data and regional paleoenvironmental records indicate a shift to warmer and more arid climatic conditions, resulting in slower rates of sedimentation and the formation of a cumulic soil (soil $3_{T2}$) in the T-2 fill.

One explanation for the slower rates of alluviation at this time is that the channel began to incise in response to the prevailing dry climatic conditions. The relationship between incision and aridity on the Great Plains has been demonstrated in several studies and is often explained in terms of vegetation response and the subsequent alteration of runoff characteristics (e.g., Knox, 1983; Hall, 1990; Daniels and Knox, 2005). Under this scenario, less effective moisture would have resulted in decreased vegetation cover, which in turn decreased interception rates and increased surface runoff. In order for surface runoff to result in channel incision, sediment transport must have exceeded sediment supply to the channel. In semiarid regions, this is typically achieved via high magnitude flood events, produced by high-intensity precipitation from convective storms capable of producing significant in-channel sediment transport (e.g., Tucker et al., 2006). Although convective storms are small in terms of their areal extent, higher order valley segments in a semiarid basin generally experience more frequent flood events, thereby favoring incision (Tucker et al., 2006). Furthermore, in terms of sediment supply, Langbein and Schumm (1958) showed that in semiarid regions sediment yield decreases with decreasing effective moisture, which would further favor channel incision during flood events. Overbank deposition, however, from high magnitude floods typically favors rapid sedimentation instead of soil cumulization on floodplains. Under this scenario, therefore, incision must have been to the extent that overbank flooding was minimal and that limited quantities of sediment were deposited on the T-2 surface during high-magnitude flood events. Another possibility, however, is that soil cumulization was facilitated through eolian deposition rather than alluviation on the T-2 surface after it was abandoned by incision. Eolian sedimentation is supported by the fact that this period coincides with the deposition of eolian sediments comprising the Gilman Canyon Formation across the Central Plains.

After ca. 28 ka, ~1.3 m of alluvium was deposited on the T-2 surface, burying soil $3_{T2}$. The chronology, however, indicates that the bottom of the T-1 fill was also aggrading at this time. Stratigraphic and chronologic relationships indicate that the Cimarron River incised over 25 m before the beginning of T-1 aggradation. This estimate is based on the difference between the terrace treads (~15 m) and assumes that the river incised below the 28 ka OSL sample interval at 10 m depth before subsequently aggrading. If the axial stream deposited alluvium on the T-2 surface at ca. 28 ka, then the bulk of valley incision must have occurred shortly after and progressed rapidly over a span of a few thousand years. Alternatively, a tributary stream flowing across the T-2 surface may have deposited the alluvium. This inference is supported by the presence of tributary streams and paleochannels that incised through the T-2 fill in close proximity to the study site. If correct, then valley incision could have begun as early as ca. 48 ka, resulting in the formation of soil $3_{T2}$ in the T-2 fill as previously discussed. Regardless of when channel incision was initiated, however, it is debatable whether climatic forcing alone could cause the magnitude of observed valley deepening. Considering alternative forcing mechanisms that could account for over 25 m of incision in the Cimarron River valley is therefore warranted.

One important consideration is the effect of local base level fall on the fluvial system. Base level lowering often results in channel incision and terrace generation through the creation and upstream migration of knickpoints (e.g., Schumm, 1977, 1993). Also, incision due to base level lowering has been shown to generate significant entrenchment over relatively short periods. For example, the South Fork of the Big Nemaha River, in southeastern Nebraska, incised 8–12 m in response to downvalley channelization during the last century (Mandel and Bettis, 2001). In the Cimarron River valley, evidence exists for local base level control in the Meade and Ashland basins located ~50 km downstream of the study area (Fig. 2.1). These basins were formed by the coalescence of dissolution-subsidence depressions that became integrated during the Pleistocene (Frye and Schoff, 1942; Frye, 1950). In this area, deep-seated dissolution of Permian salt and gypsum deposits is favored by the presence of early Pleistocene faults that allow surface water access to deeply buried soluble beds (Frye and Hibbard, 1941; Frye, 1950). It is suggested, therefore, that local base level lowering, produced by the integration of drainages from formerly isolated dissolution-subsidence areas during the late Pleistocene, resulted in significant headward valley deepening in the Cimarron River valley and caused the abandonment of the T-2 surface shortly after ca. 28 ka. Gustavson (1986) tested a similar hypothesis of subsidence-controlled valley deepening in the Canadian River valley, located in the Texas Panhandle, and concluded that dissolution processes have been ongoing in the region since the late Pliocene.

Although a fall in local base level would tend to produce a response in one direction (i.e., incision), stratigraphic evidence indicates that the river re-aggraded at least 10 m to form the T-1 terrace, and possibly as much as 13.5 m, presuming the coarse-grained unit in core 1 represents the base of the T-1 fill. Whereas post-incisional aggradation typically favors a climatic driver, this mechanism assumes sediment bypass during knickpoint migration. As the knickpoint migrated upstream following base level fall, however, it is feasible that the sediment generated by the wave of incision was subsequently stored in the Cimarron River valley, forming the bulk of the T-1 fill.

The Cimarron River deposited the bulk of the T-1 fill between ca. 28 and 13 ka. During this period regional paleoclimatic proxy data suggest a more mesic climate, with greater effective moisture than present in the Central Plains (e.g., Wells and Stewart, 1987; Rousseau and Kukla, 1994). Furthermore, this period of aggradation coincides with the timing of extensive loess deposition (Peoria Loess) across the Central Plains.

Around 13 ka, sedimentation rates declined, resulting in the formation of a cumulic soil (soil $5_{T1}$) in the T-1 fill. The period from 12.9 to 11.5 ka has been identified as a major period of quasi-stability, characterized by cumulic soil development in stream valleys throughout the Central Plains (Mandel, 2008). The $\delta^{13}C$ record, together with regional paleoenvironmental reconstructions, suggests that climatic conditions during this time were warmer and drier in the study area. Effective moisture, however, must have been high enough to promote continued alluviation, albeit at a slower pace that favored cumulic soil formation (soil $5_{T1}$). Mandel (2008) hypothesized that zonal flow during this time may have restricted the northward penetration of moist air masses from the Gulf of Mexico into the Central Plains and that weak Pacific storms may have generated enough precipitation to promote slow alluviation and soil cumulization.

### 2.6. Summary and conclusions

The purpose of this study was to investigate stratigraphic, geomorphic, and sedimentological relationships from late-Pleistocene alluvial fills stored in the Cimarron River valley, southwestern Kansas. Stable carbon isotope ($\delta^{13}C$) analyses were also used to assess paleoenvironmental change and the subsequent alluvial response during this period. Two distinct valley fills (T-1 and T-2) were investigated from outcrop and core. Fluvial deposits consist primarily of vertically stacked, upward fining channel-fill sequences. Three soils were documented in the T-2 fill and five soils in the T-1 fill that indicate periods of slow sedimentation and landscape stability in the Cimarron River valley. Of particular interest was the presence of two cumulic soils: one dating to ca. 48–28 ka, the other dating to ca. 13–12.5 ka. $\delta^{13}C$ values are consistent with regional paleoenvironmental proxy data and confirm that cool, wet conditions prevailed in the study area before ca. 48 ka, followed by progressive warming and drying until ca. 28 ka. A return to cool, wet conditions occurred from ca. 28–14 ka, followed by a shift to warm, dry climates at ca. 13 ka.

The data collected in this study illustrate how the Cimarron River responded to changes in climate as well as to local base level control. Results indicate that 1) aggradation was facilitated by cool, wet climatic conditions (e.g., before ca. 48 ka and from ca. 28–13 ka), 2) slow sedimentation and cumulic soil formation, together with possible channel incision, occurred under warm, dry climatic conditions (e.g., from ca. 48–28 ka), and 3) significant valley deepening (~25 m) likely resulted from a lowering of local base level caused by deep-seated dissolution of Permian salt and gypsum deposits downstream of the study area. Overall, stratigraphic, paleopedologic, and paleoenvironmental data from the Cimarron River valley offer important insights into the late-Pleistocene geomorphic evolution of this fluvial system.

# CHAPTER 3

# LATE PLEISTOCENE EOLIAN SEDIMENTATION, SOIL DEVELOPMENT AND CLIMATE CHANGE ON THE HIGH PLAINS OF SOUTHWESTERN KANSAS

## 3.1. Introduction

Loess-paleosol sequences represent climatically controlled sedimentary extremes that can provide detailed terrestrial records of Quaternary climate change and landscape response (Muhs and Bettis, 2003). Several loess-paleosol sequences have been investigated in the Central and High Plains and at least four stratigraphically superposed Quaternary-aged loesses have been documented: the Loveland, Gilman Canyon, Peoria and Bignell loesses (e.g., Feng et al., 1994; Maat and Johnson, 1996; Muhs et al., 1999, 2008; Bettis et al., 2003; Rutter et al., 2006). Despite the recognition of multiple loess units, however, regional studies typically have focused on younger eolian deposits that comprise the surficial sediments of the region (e.g., Forman et al., 1995; Olson et al., 1997; Muhs et al., 1999; Mason et al., 2003; Muhs et al., 2008).

In this paper, we interpret data from two cores that record late-Pleistocene eolian sedimentation and soil formation on the High Plains of southwestern Kansas. Exposures of eolian stratigraphic sequences on the High Plains are rare, primarily due to the flat topography. Detailed descriptions, dating, and stable isotopic analyses of soils and sediments from core, therefore, allow for investigation of paleoclimatic change and landscape response in this understudied part of the Great Plains.

## 3.2. Study area

### 3.2.1. Geology and loess stratigraphy

The study area (Fig. 3.1) is in the High Plains region of the Great Plains physiographic province (Fenneman, 1931). The High Plains covers ~450,000 $km^2$ of the central United States, extending from South Dakota to northwest Texas. The region is characterized by predominantly flat terrain and represents the remnant of a vast alluvial plain formed by sediment shed eastward from the Rocky Mountains (e.g., Seni, 1980). These deposits predominantly comprise the Miocene and early Pliocene-aged sediments of the Ogallala Formation together with Quaternary alluvial and eolian units (e.g., Merriam, 1963). Loess deposits blanket the High Plains surface, ranging in thickness from > 20 m in parts of Nebraska to < 5 m in southwestern Kansas (Bettis et al., 2003). At least four stratigraphically superposed Quaternary-aged loesses have been documented in the region: the Loveland, Gilman Canyon, Peoria and Bignell loesses (e.g., Frye and Leonard, 1951; Feng et al., 1994; Bettis et al., 2003). Topographic relief (5–15 m) is largely confined to river valleys, dune fields and numerous small playa basins.

The Loveland Loess is typically the oldest loess unit exposed in the Great Plains, usually only a few meters thick, and has an eolian sand facies in some localities (Bettis et al., 2003). The typical age assignment of the Loveland Loess is to the penultimate glaciation (MIS 6). Thermoluminescene and cosmogenic ($^{10}Be$) ages from the Missouri and Mississippi River valleys indicate that most of the Loveland Loess accumulated between

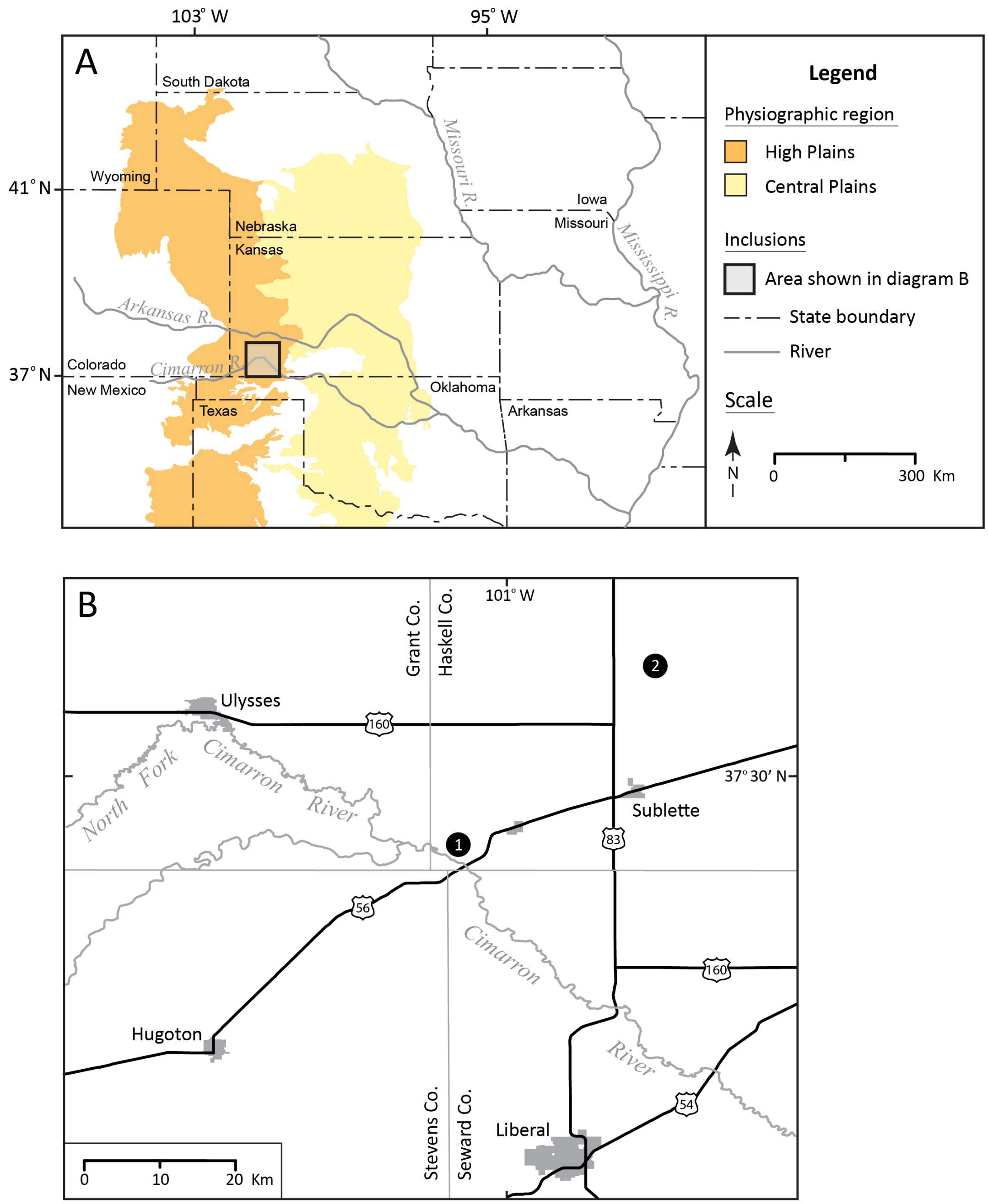


**Figure 3.1**. A) Study area location in the central High Plains, southwestern Kansas. B) Coring locations (1) CMC1 core, (2) HP1A core. Physiographic regions from Fenneman (1931).

190 and 130 ka with intermittent deposition from ca. 95 to 74 ka (Markewich et al., 2011). The Loveland Loess is commonly identifiable by the well-developed, rubified soil formed in its upper part. This soil, referred to as the Sangamon Soil, has been

documented throughout the Midwest (e.g., Leighton and Willman, 1950; Willman and Frye, 1970; Ruhe, 1974; Follmer, 1978; McKay, 1986; Jacobs and Knox, 1994; Grimley et al., 2003; Rutter et al., 2006; Wang et al., 2009; Markewich et al., 2011). The Sangamon Soil typically is a 1–2 m thick silt loam or silty clay loam, with 7.5YR to 5YR hues, thick Bt horizons and well-developed prismatic or angular blocky structure. $^{10}Be$ ages from the Mississippi River valley indicate that the Sangamon Soil formed between ca. 130–90 ka with continued pedogenesis from ca. 74–54 ka (Markewich et al., 2011).

The Gilman Canyon Formation overlies the Loveland-Sangamon complex and is usually less than 2 m thick on the Great Plains (Bettis et al., 2003). The Gilman Canyon Formation typically consists of a dark noncalareous silt loam that has been modified by pedogenesis, commonly with two or more soils forming a pedocomplex (e.g., Reed and Dreeszen, 1965; Mandel and Bettis, 1995; Johnson et al., 2007). Radiocarbon ($^{14}C$) ages from sites in the Central Plains range from ca. 40 to 20 ka (Muhs et al., 1999; Johnson et al., 2007).

The Peoria Loess buries the Gilman Canyon Formation and is the thickest and most areally extensive loess deposit in the Great Plains (Bettis et al., 2003). This loess unit typically is a calcareous, massive, light yellowish tan to brown colored silt loam. $^{14}C$ ages indicate that Peoria Loess began to accumulate in the Great Plains from 30–20 ka and continued to accumulate until about 12 ka (Bettis et al., 2003; Mason et al., 2007). The Brady Soil, developed in the Peoria loess and only detectable when buried by the Bignell Loess, typically is a dark gray to grayish brown soil with a well-developed B horizon

(Johnson and Willey, 2000). Published $^{14}C$ ages indicate that the Brady soil formed from ca. 13.3 to 8.8 ka (Johnson and Willey, 2000; Mason et al., 2003) and was buried by the Bignell Loess beginning ca. 9.9–8.8 ka, with continued loess deposition spanning much of the Holocene in some locations (Mason et al., 2003).

### 3.2.2. Climate

The climate of southwestern Kansas is semiarid steppe (BSk in the Köppen climate classification; Peel et al., 2007). Mean annual precipitation is 47.3 cm for the period of record (1918–2014) at Sublette, Kansas (High Plains Regional Climate Center, 2014). Mean July and January temperatures are 26°C and 0°C, respectively. The majority of precipitation occurs due to frontal activity, when warm, moist maritime-tropical air from the Gulf of Mexico collides with pacific and polar air masses, producing intense rainfall of short duration along the convergence zone. Approximately 75% of the precipitation falls between the months of April and September. During late summer, high intensity, convectional storms are common. Periodic intensification of the North American Monsoon also brings peak summer rainfall to southwestern Kansas. Droughts are also frequent in the region, produced by the periodic intensification of westerly (zonal) airflow, which prevents moist Gulf air from penetrating into the Central Plains. Drought frequency is modulated by positive and negative phases of the Atlantic Multidecadal Oscillation and Pacific Decadal Oscillation, respectively (e.g., McCabe et al., 2004).

3.2.3. Vegetation

The natural vegetation of southwestern Kansas is a short grass prairie (e.g., Küchler, 1974). In the study area, uplands are dominated by $C_4$ plant communities, including blue gramma (*Bouteloua gracilis*), buffalograss (*Buchloe dactyloides*) and sand sage (*Artemisia filifolia*) species. $C_3$ plants, including needle-and-thread (*Stipa comata*), yucca (*Yucca glauca*) and western wheatgrass (*Agropyron smithii*), and the CAM plant prickly pear cactus (*Opuntia polyacantha*) are also present in the region.

**3.3. Methodology**

Two cores were collected on the High Plains surface in Haskell County, Kansas (Fig. 3.1B) as part of the High Plains Ogallala Drilling Program at the Kansas Geological Survey. In this chapter, we describe the upper 20 m from these cores, which contain a late-Quaternary record of eolian sedimentation and soil development on the High Plains. Drilling and core retrieval were accomplished using an Acker hollow-stem auger and wireline, split-spoon core sampler.

Soils were described in detail using standard terminology in Birkeland (1999) and Soil Survey Staff (1993). Each soil horizon was described in terms of thickness, Munsell color, texture, structure, consistence and boundaries. Where present, clay films, secondary carbonate forms, and biogenic features were described. Horizon Development Indices (HDI), developed by Harden (1982), were calculated to quantitatively measure the degree of soil development based on color paling and lightening, texture, consistence, clay films, structure and carbonate morphology. Soils were sampled by horizon for particle size (e.g., Soil Survey Staff, 1993). Where horizon thicknesses were > 50 cm, subsamples were collected so that the sample interval was no greater than 50 cm. Particle size analyses were performed using the pipette method (Soil Survey Staff, 1982). Calcium carbonate ($CaCO_3$) percent was determined by dry weight loss after HCl treatment and is expressed as calcium carbonate equivalent (CCE).

Stable carbon isotopes ($\delta^{13}C$) from soil organic matter (SOM) and both $\delta^{13}C$ and stable oxygen isotopes ($\delta^{18}O$) from pedogenic carbonate were analyzed to investigate potential paleoclimatic trends. $\delta^{13}C$ values of SOM ($\delta^{13}C_{org}$) from buried soils reflect the relative contributions of $C_3$ and $C_4$ vegetation at the time of soil formation. Modern $C_3$ plant communities include cool season grasses and woody vegetation and have $\delta^{13}C_{org}$ values between -32‰ and -20‰ (average of -27‰) (e.g., Boutton, 1991). In contrast, $C_4$ plants, which include warm season grasses, have $\delta^{13}C_{org}$ values between -17‰ and -10‰ (average of -13‰). We estimate the relative contribution of $C_4$ plants to SOM with the following mass balance equation (Nordt et al., 1994)

$$\delta^{13}C_{SOM} = \delta^{13}C_{C4}(x) + \delta^{13}C_{C3}(x)\ (1\text{-}x) \qquad (1)$$

where $\delta^{13}C_{SOM}$ is the measured $\delta^{13}C$ value, $\delta^{13}C_{C4}$ = -13‰, $\delta^{13}C_{C3}$ = -27‰ and $x$ is the relative contribution of $C_4$ plants to SOM.

$\delta^{13}C$ values from pedogenic carbonate ($\delta^{13}C_{carb}$) also can be used to assess past vegetation compositions. Pedogenic carbonate forms in carbon isotopic equilibrium with soil $CO_2$, which is derived mainly from root respiration and therefore reflects the relative contributions of $C_3$ and $C_4$ species. $\delta^{13}C_{carb}$ values are offset, however, by 14–17‰ relative to $\delta^{13}C_{org}$ due to molecular diffusion and isotopic equilibria reactions (e.g., Cerling et al., 1989). Studies have shown a strong correlation between the proportion of $C_4$ vegetation and temperature (e.g., Terri and Stowe, 1976; Boutton, 1996) indicating that $\delta^{13}C$ data can function as an important proxy for paleoclimatic change.

The analysis of $\delta^{18}O$ from pedogenic carbonate also provides a potential source of important paleoclimatic data. The $\delta^{18}O$ of pedogenic carbonate is controlled by the $\delta^{18}O$ value of soil water and temperature (e.g., Cerling and Wang, 1996). Soil water is derived from meteoric water but can differ in its $\delta^{18}O$ value due to evaporation and mixing with isotopically distinct water sources (Cerling and Quade, 1993). In general, lower (higher) carbonate $\delta^{18}O$ values indicate 1) lower (higher) temperatures through lower (higher) $\delta^{18}O$ values of meteoric water, 2) a greater fraction of winter (summer) season recharge of soil water, 3) wetter (drier) conditions and a decrease (an increase) in evaporative enrichment of soil water, or 4) a combination of some or all of these factors (Fox et al., 2012). Changes in atmospheric circulation patterns can also affect $\delta^{18}O$ values through changes in the relative importance of different moisture sources. In the Great Plains, precipitation from Pacific moisture sources has lighter $\delta^{18}O$ values than moisture sources from the Gulf of Mexico (e.g., Simpkins, 1995).

All stable isotopic analyses were performed at the University of Kansas W. M. Keck Paleoenvironmental and Environmental Stable Isotope Laboratory. SOM samples were collected at regular intervals (15–30 cm) from the core and decarbonated with 0.5 M HCl. Decarbonated samples were combusted using a Costech Elemental Analyzer at 1060 °C and the resultant $CO_2$ analyzed by a continuous-flow ThermoFinnigan MAT 253 mass spectrometer. Pedogenic carbonate samples were collected at regular intervals where present in buried soils. Samples were analyzed with a Kiel III device coupled to a dual inlet ThermoFinnigan MAT 253 mass spectrometer.

Numerical-age control was provided by radiocarbon ($^{14}C$) dating of SOM and optically stimulated luminescence (OSL) dating. All $^{14}C$ samples were submitted to the National Ocean Sciences Accelerator Mass Spectrometry facility at the Woods Hole Oceanographic Institute. Samples were pretreated to remove roots and carbonates, combusted in a high-temperature muffle furnace, and the resultant $CO_2$ reacted with a Fe catalyst to create graphite. After conversion to graphite, $^{14}C$ activity was measured via Accelerator Mass Spectrometry.

Optically stimulated luminescence dating provides an age estimate of the time since sediment was last exposed to light (Huntley et al., 1985). The OSL samples were collected from core and analyzed at the Utah State University Luminescence Laboratory using the latest single-aliquot regenerative-dose (SAR) procedures for dating quartz sand (see Murray and Wintle, 2000). All samples were opened and processed under dim amber safelight conditions and were processed using HCl to remove carbonates, household chlorine bleach to remove organics, and heavy liquid (sodium polytungstate, 2.7 g/$cm_3$) to remove minerals and isolate the fine-grained quartz sand fraction. Hydroflouric acid was used to etch the quartz and dissolve any remaining feldspars. Sample processing followed standard procedures outlined in Aitken (1998) and described in Rittenour et al. (2005).

## 3.4. Results and interpretations

### 3.4.1. HP1A Core

#### 3.4.1.1. Stratigraphy, chronology and correlation

The upper 20 m of the HP1A core contains 8 eolian units and intercalated soils (Fig. 3.2; Table 3.1). Three OSL ages (76.8±13.1, 76.1±13.5, and 75.7±11.3 ka) from the middle of the HP1A core indicate that units 4, 5, and 6 are coeval with the Loveland Loess (Fig. 3.2; Table 3.2). Although the Loveland Loess has been interpreted as essentially a single depositional unit in the Missouri River valley (e.g., Mason et al., 2007), multiple carbonate-rich soils have been identified in this loess deposit in Kansas and Nebraska (e.g., Feng et al., 1994). Also, Markewich et al. (2011) suggest that although much of the Loveland was deposited from 190 to 130 ka in the Mississippi River valley, loess accumulation continued intermittently through MIS 5 from ca. 95 to 74 ka. The OSL ages reported in this study, therefore, together with the presence of multiple buried soils in the HP1A core, confirm the episodic nature of eolian deposition during late MIS 5 on the High Plains.

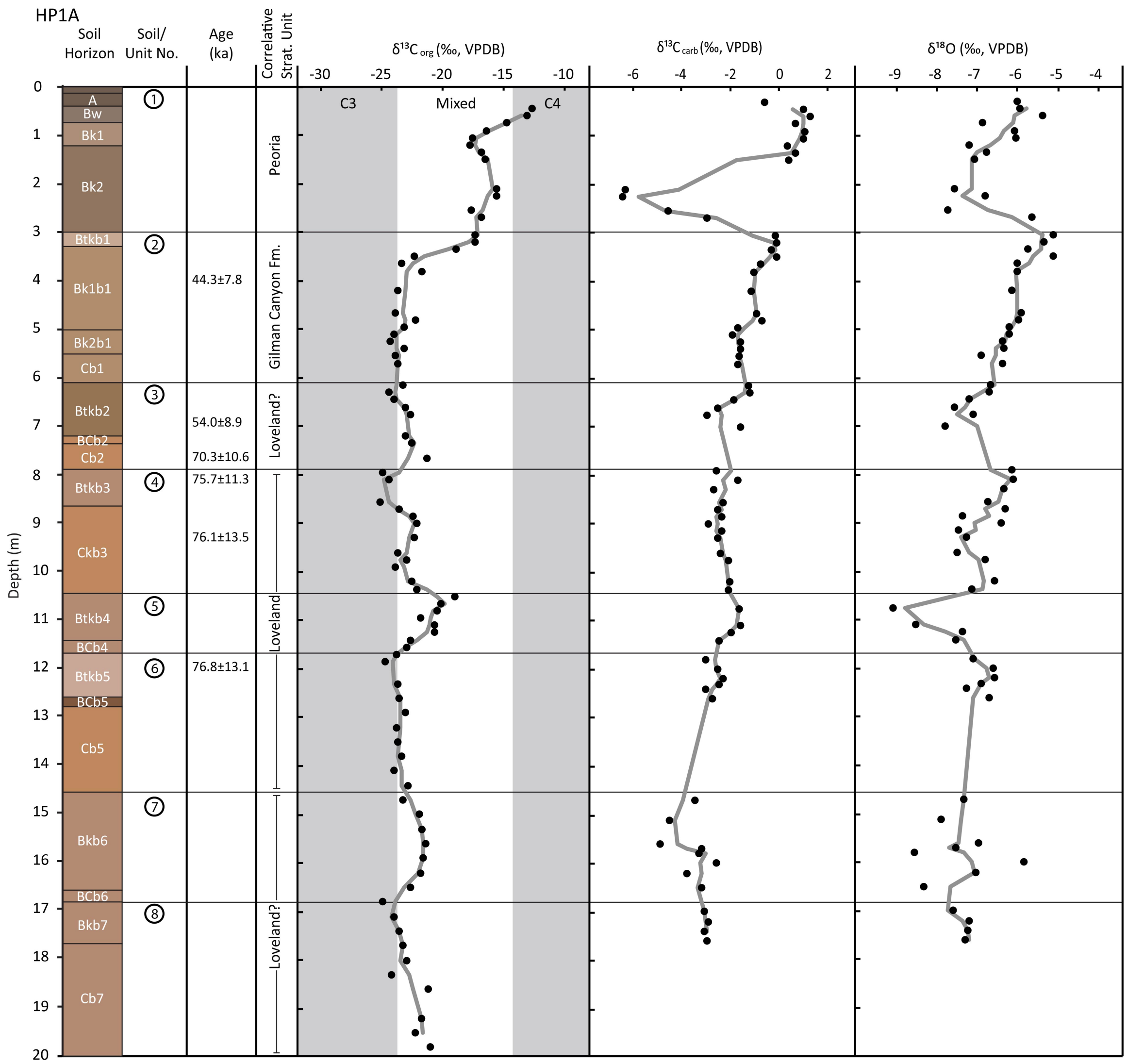


**Figure 3.2**. Stratigraphy, chronology, and stable isotope data from the HP1A core. Gray line represents 3 pt moving average. Stable isotope data and chronology from Harlow (2013).

Two OSL ages constrain the age of unit 3 to between 70.3±10.6 and 54.0±8.9 ka (Fig. 3.2; Table 3.2). Similar ages have been reported for the Loveland-Sangamon complex in the Mississippi River valley (e.g., Rodbell et al., 1997). Markewich et al. (2011) date the end of the Sangamon soil-forming interval in the Mississippi River valley to no later than ca. 50 ka. Soil 3, therefore, may be the stratigraphic equivalent of late-Sangamon soils identified in the Mississippi River valley. Alternatively, soil 3 may correlate to an

**Table 3.1**. Soil descriptions from the HP1A core

| Soil No. | Horizon | Depth (m) | Matrix Color | Texture[a] | Structure[b] | Consistence[c] | Clay Films[d] | Boundary[e] | Notes |
|---|---|---|---|---|---|---|---|---|---|
| 1 | Ap | 0-0.1 | 10YR 4/2 | SiL | 1 f sbk | fr | --- | g | Parts to 2 f gr |
| | A | 0.1-0.4 | 10YR 4/2 | SiL | 2 f sbk | fr | --- | c | Parts to 1 f gr |
| | Bk1 | 0.4-0.72 | 10YR 5/2 | SiCL | 2 m sbk | fi | --- | g | Few carbonate nodules, common fine threads |
| | Bk2 | 0.72-1.2 | 10YR 6/3 | SiCL | 2 m abk | fi | --- | g | Few carbonate nodules, few fine threads |
| | Bk3 | 1.2-3.0 | 10YR 5/3 | SiCL | 2 m abk | fi | --- | a | Few fine-medium carbonate threads |
| 2 | Btkb1 | 3.0-3.3 | 10YR 7/3 | CL | 3 m abk | vfi | 1 d po | g | Common carbonate nodules, few fine threads |
| | Bk1b1 | 3.3-5.0 | 10YR 6/4 | L | 3 m abk | vfi | --- | g | Common carbonate nodules, few fine threads |
| | Bk2b1 | 5.0-5.48 | 10YR 6/4 | SL | 2 m sbk | fr | --- | c | Few carbonate nodules |
| | Cb1 | 5.48-6.08 | 10YR 6/4 | SL | 1 f sbk | vfr | --- | a | |
| 3 | Btkb2 | 6.08-7.2 | 10YR 5/4 | L | 3 m pl | fi | 2 d po | g | Parts to 2 m abk; Common carbonate nodules |
| | BCb2 | 7.2-7.35 | 7.5YR 6/6 | L | 1 m sbk | fr | --- | c | Parts to 1 f gr |
| | Cb2 | 7.35-7.9 | 7.5 YR 6/6 | SL | sg | lo | --- | a | |
| 4 | Btkb3 | 7.9-8.66 | 7.5YR 6/4 | SL | 3 m pl | fi | 2 d po, pf | c | Parts to 2 m sbk; Common carbonate nodules |
| | Ckb3 | 8.66-10.5 | 7.5YR 6/6 | SL | sg | lo | --- | a | Few carbonate nodules |
| 5 | Btkb4 | 10.5-11.4 | 7.5YR 6/4 | SiCL | 2 m abk | fi | 2 p po | c | Parts to 1 f sbk; Few carbonate nodules |
| | BCb4 | 11.4-11.68 | 7.5YR 6/4 | SiL | 2 f sbk | fi | --- | a | Parts to 1 f gr |
| 6 | Btkb5 | 11.68-12.6 | 7.5YR 7/3 | L | 3 m abk | vfi | 2 d pf, po | c | Many coalescing carbonate nodules |
| | BCb5 | 12.6-12.8 | 7.5YR 4/4 | L | 1 m sbk | fr | --- | g | |
| | Cb5 | 12.8-14.58 | 7.5YR 6/6 | SL | sg | lo | --- | a | |
| 7 | Bkb6 | 14.58-16.6 | 7.5YR 6/4 | SL | 2 m sbk | fr | --- | c | Common fine carbonate threads |
| | BCb6 | 16.6-16.8 | 7.5YR 6/4 | SL | 1 f sbk | vfr | --- | c | |
| 8 | Bkb7 | 16.8-17.7 | 7.5YR 6/4 | SL | 2 m sbk | fr | --- | g | Few carbonate nodules, few fine threads |
| | Cb7 | 17.7-20.0 | 7.5YR 6/4 | LS | sg | lo | --- | a | |

[a] Texture: SiL–Silt Loam, SiCL–Silty Clay Loam, CL–Clay Loam, L–Loam, SL–Sandy Loam, LS–Loamy Sand

[b] Structure: 1–weak, 2–moderate, 3–strong; f–fine, m–medium, c–coarse; abk–angular blocks, sbk–subangular blocks, pl–plates, gr–granular, sg–single grain

[c] Consistence: lo–loose, vfr–very friable, fr–friable, fi–firm; vfi–very firm

[d] Clay Films: 1–few, 2–common, 3–many; d–distinct, p–prominent; pf–ped faces, po–pores

[e] Boundaries: a–abrupt, c–clear, g–gradual

**Table 3.2**. Optically Stimulated Luminescence age information

| Core | Lab no. | Depth (m) | No. of aliquots[1] | Dose Rate (Gy/ka) | De[2] ± 2σ (Gy) | OD[3] (%) | OSL age ± 2σ (ka) |
|---|---|---|---|---|---|---|---|
| HP1A | USU-1110 | 3.9 | 29 (46) | 3.39 ± 0.16 | 150.08 ± 21.79 | 37.2 ± 5.4 | 44.3 ± 7.8 |
| | USU-1111 | 6.9 | 20 (46) | 3.47 ± 0.19 | 187.57 ± 24.24 | 27.5 ± 4.8 | 54.0 ± 8.9 |
| | USU-1112 | 7.5 | 29 (55) | 2.94 ± 0.15 | 206.90 ± 23.13 | 26.4 ± 4.4 | 70.3 ± 10.6 |
| | USU-1113 | 8.2 | 30 (54) | 3.06 ± 0.14 | 231.38 ± 25.89 | 27.5 ± 4.4 | 75.7 ± 11.3 |
| | USU-1114 | 9.3 | 24 (65) | 3.16 ± 0.16 | 240.11 ± 35.20 | 33.5 ± 5.5 | 76.1 ± 13.5 |
| | USU-1115 | 11.9 | 26 (59) | 2.78 ± 0.14 | 213.76 ± 29.55 | 31.9 ± 5.4 | 76.8 ± 13.1 |
| CMC1 | USU-1518 | 4.4 | 8 (55) | 2.79 ± 0.14 | 145.36 ± 22.24 | 17.2 ± 6.5 | 52.2 ± 9.6 |
| | USU-1519 | 11.7 | 15 (45) | 2.66 ± 0.17 | 200.83 ± 39.44 | 36.1 ± 7.3 | 75.5 ± 16.9 |
| | USU-1569 | 18.65 | 13 (44) | 2.78 ± 0.17 | 233.27 ± 42.69[4] | 33.6 ± 7.2 | 84.0 ± 17.9 |

[1] Number of aliquots used in age calculation and number of aliquots analyzed in parentheses.
[2] Equivalent dose (De) calculated using the Central Age Model of Galbraith et al. (1999), except where noted otherwise.
[3] Overdispersion (OD) represents variance in De data beyond measurement uncertainties, OD >20% may indicate significant scatter due to depositional or post-depositional processes.
[4] $D_e$ calculated using arithmetic mean.

unnamed paleosol that has been identified between the Sangamon Soil and the Gilman Canyon Formation (see Feng et al., 1994) and the Roxana Silt (the stratigraphic equivalent of the Gilman Canyon Formation in the Mississippi River valley) (see Markewich et al., 2011) at certain localities. In particular, the ages of unit 3 correlate well with the dating of a reddish pedocomplex (69±6.4 ka) below the Gilman Canyon Formation at the Barton Landfill in central Kansas (e.g., Feng et al., 1994).

An OSL age of 44.3±7.8 ka from unit 2 indicates that this unit is likely equivalent to the Gilman Canyon Formation (Fig. 3.2; Table 3.2). In Kansas and Nebraska, the Gilman Canyon Formation has yielded $^{14}C$ ages ranging from ca. 40 to 20 ka (Muhs et al., 1999; Johnson et al., 2007). Although the OSL age for unit 2 falls outside this range, the basal age of the Gilman Canyon Formation is poorly constrained. Johnson et al. (1998) extrapolate a basal age of about 45 ka for the Gilman Canyon Formation in central

Nebraska. Furthermore, the Roxana Silt, the stratigraphic equivalent of the Gilman Canyon Formation in the Mississippi River valley, has an age range of ca. 60 to 30 ka (Forman and Pierson, 2002).

3.4.1.2. Soil morphology

Soils from the HP1A core are developed in predominantly sandy loam textured sediments with sand contents ranging between 63 and 82% (Table 3.1; Fig. 3.3). Soils developed in eolian deposits interpreted to be stratigraphically equivalent to the Loveland Loess (soils 4–6) are well developed and have 7.5 YR hues, ~1 m-thick Btk horizons, and either platy or angular blocky structure. Soil textures are loams, sandy loams and silty clay loams. $CaCO_3$ contents peak in the Btk horizon and range from 4 to 30% (Fig. 3.3). Pedogenic carbonate is morphologically expressed in the form of nodules and fine threads. Nearly continuous clay films occur either on ped faces or in pores. Clay contents in Btk horizons range from 18 to 32% (Fig. 3.3). Soil 3, representing either the Sangamon Soil or an unnamed paleosol between the Gilman Canyon Formation and the Sangamon Soil, is morphologically similar to soil 4. Soil 3, however, lacks the presence of clay films on ped faces and has 10YR Btk coloration. HDI values indicate that soils 3, 4 and 6 are the most developed (Fig. 3.3)

Soils 7 and 8 may also be of Loveland-age but direct age control is lacking. These soils are morphologically less developed than soils 3–6, as indicated by relatively low HDI values, and are characterized by subangular blocky structure, friable consistence, sandy loam textures, and a lack clay films. $CaCO_3$ contents are also lower in soils 7 and 8

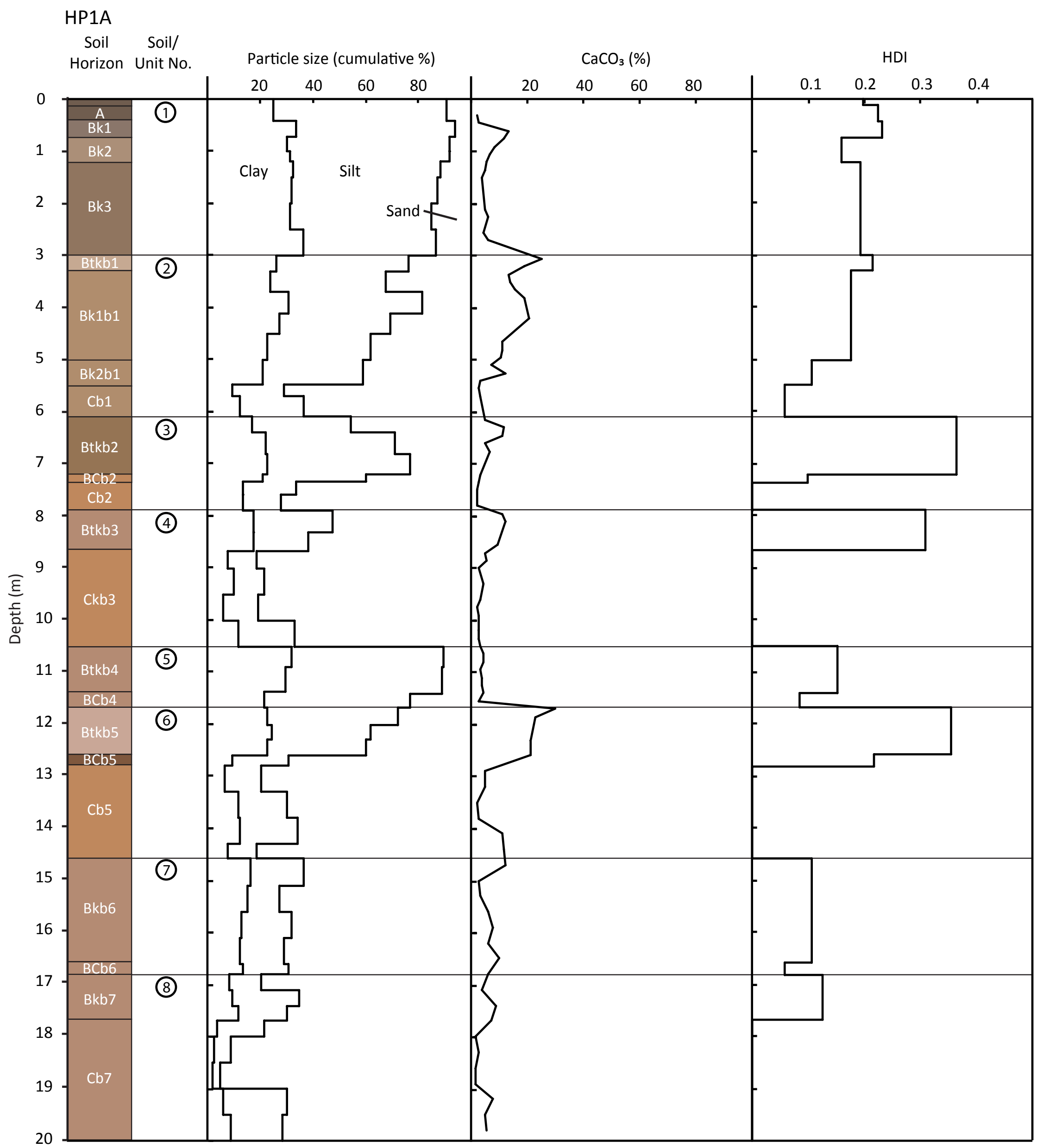


**Figure 3.3**. Particle size, carbonate content and HDI data for the HP1A core

(3 to 11%) compared to soils 3–6 and pedogenic carbonate is only present in the form of fine threads.

Soil 2, interpreted as representing a soil developed in the Gilman Canyon Formation, is well developed with a 2.5 m-thick profile, Btk-Bk horizonation, and angular blocky structure. Soil texture fines upward from sandy loam to clay loam. Soil 2 is likely welded to the overlying soil as no A horizon, a typical characteristic of soils developed in the Gilman Canyon Formation, is evident. $CaCO_3$ content is relatively high peaking at 25% in the Btk horizon. Clay content ranges from 21 to 33% and there are distinct clay films lining pores.

The surface soil is moderately developed with A-Bk horizonation and subangular to angular blocky structure. A and B horizon textures are silt loams and silty clay loams, respectively. $CaCO_3$ and clay contents in the Bk horizon range between 3–12% and 30–36%, respectively (Fig. 3.3).

3.4.1.3. Stable isotopes and paleoclimatic trends

$\delta^{13}C_{org}$ values are relatively consistent from the bottom of unit 8 to the top of unit 6 (average of -23.5‰; 24% $C_4$ biomass), with a slight increase to -22‰ (35% $C_4$ biomass) in unit 7 (Fig. 3.2). $\delta^{13}C_{carb}$ and $\delta^{18}O$ values average -3‰ and -7.4‰, respectively, over this interval but are highly variable in unit 7. The stable isotope data indicate a predominance of $C_3$ biomass (76%) in the study area before 76.8±13.1 ka and suggest cold climatic conditions at this time. The increase in $C_4$ biomass during the formation of soil 7 may indicate a slight increase in temperature during this soil-forming interval.

Both $\delta^{13}C_{org}$ and $\delta^{13}C_{carb}$ values increase in soil 5 from -22.9 to -19‰ (29 to 57% $C_4$ biomass) and -2.4 to -1.6‰, respectively. $\delta^{18}O$ values, however, indicate a sharp decrease from -7.5 to -9.1‰. These contrasting trends are best explained by a scenario of overall climate warming with a reduction in evaporative enrichment (i.e., warm and wet). The lower $\delta^{18}O$ values may also reflect a change in the seasonal distribution of precipitation, to the effect that a greater proportion of soil water was derived from isotopically light winter precipitation. Alternatively, the lower $\delta^{18}O$ values may indicate in change in moisture sources with an increase in precipitation derived from Pacific air masses. The timing of this period of climate change is constrained by two OSL ages from units 4 and 6 (76.1±13.5 and 76.8±13.1 ka), indicating that the change occurred during late MIS 5.

The isotopic data from soil 4 shows the opposite trends to those discussed for soil 5. In soil 4, $\delta^{13}C_{org}$ values generally decrease upward through the soil, representing a decrease in $C_4$ biomass of 20%, whereas $\delta^{18}O$ values increase. These disparate trends likely suggest cooler but drier conditions, resulting in greater evaporative enrichment of soil water. Alternatively, the increase in $\delta^{18}O$ values may indicate a shift in moisture source from Pacific to Gulf of Mexico sources. Whereas $\delta^{13}C_{org}$ values decrease in soil 4, $\delta^{13}C_{carb}$ values remain relatively constant. This consistency is likely due to the effect of increased aridity, which can increase $\delta^{13}C_{carb}$ values without a concomitant increase in the relative abundance of $C_4$ biomass (e.g., Fox et al., 2012).

$\delta^{13}C_{org}$ values decline upward through unit 3 with a decrease in $C_4$ biomass from 41 to 20%, indicating general climatic cooling. A shift to cooler climatic conditions from ca.

70–54 ka is also indicated by $\delta^{18}O$ values that show a sharp decrease from -6.1 to -7.8‰ in the lower half of unit 3. Whereas $\delta^{13}C_{org}$ values decline upward through soil 3, however, $\delta^{13}C_{carb}$ and $\delta^{18}O$ values increase after ca. 54 ka. These trends are similar to those observed in soil 4 and may indicate that whereas climatic conditions were generally cool, thereby supporting more $C_3$ vegetation, aridity likely increased progressively after ca. 54 ka.

$\delta^{13}C_{org}$ values remain fairly constant around -23‰ (28% $C_4$ biomass) from the top of unit 3 through much of unit 2 before increasing significantly at the top of soil 2 to -17.3‰ (69% $C_4$ biomass). Both $\delta^{13}C_{carb}$ and $\delta^{18}O$ values also generally increase over this interval with sharper increases coinciding with the significant increase in $\delta^{13}C_{org}$ values at the top of soil 2. These data suggest significantly warmer and drier climatic conditions after ca. 44 ka. A similar warming trend was documented from a cumulic soil developed in late-Pleistocene alluvium in the Cimarron River valley that dates between ca. 48–28 ka (see chapter 2). The inference of warm and dry conditions in the Central Plains during late MIS 3 is also supported by several paleoenvironmental studies. For example, sedimentological records from central Kansas and the Nebraska Sand Hills indicate rapid drying from 34–29 ka and 45–27 ka, respectively (Fredlund, 1995; Jacobs et al., 2007), and paleobotantical records from the eastern Plains also suggest more arid conditions between 37–29 ka (Baker et al., 2009). A significant negative isotopic shift is evident in the $\delta^{13}C_{carb}$ and $\delta^{18}O$ data from the bottom of soil 1. This shift is also observable in the CMC1 core and discussion is deferred to the following section.

3.4.2. CMC1 core

3.4.2.1. Stratigraphy, chronology and correlation

In the CMC1 core, a 19.6 m eolian succession overlies a 7.5 m-thick, well-developed pedocomplex formed in alluvium (see chapter 4). This pedocomplex is interpreted as representing slow sedimentation accompanied by pedogenesis during the final aggradational phase of the Ogallala Formation. The 19.6 m-thick eolian sequence includes 8 eolian units and intercalated soils (Fig. 3.4) that are developed in either sandy loam or loamy sands (Table 3.3). Eolian sands were likely sourced from the Cimarron and Arkansas River valleys as well as from local reworking of alluvial deposits of the Ogallala Formation.

Two OSL ages from the bottom of the CMC1 core (84.0±17.9 and 75.5±16.9 ka) indicate that units 5–8 are coeval with the Loveland Loess (Fig. 3.4; Table 3.2). As previously noted, the presence of multiple eolian units and intercalated soils indicates episodic deposition and soil formation during late MIS 5.

Although we have no direct age control for unit 3, based on stratigraphic relationships, this unit likely correlates with unit 3 in the HP1A core, which has OSL ages of ca. 70–54 ka. Unit 2 is interpreted as representing the Gilman Canyon Formation based on OSL and $^{14}C$ samples that yielded ages of 52.2±9.6 and 34.6±3.6 ka, respectively (Fig. 3.4; Tables 3.2 and 3.4). The 52.2 ka age is older than previously published ages for the Gilman Canyon Formation in Kansas and Nebraska; however, the Roxana Silt has yielded an age

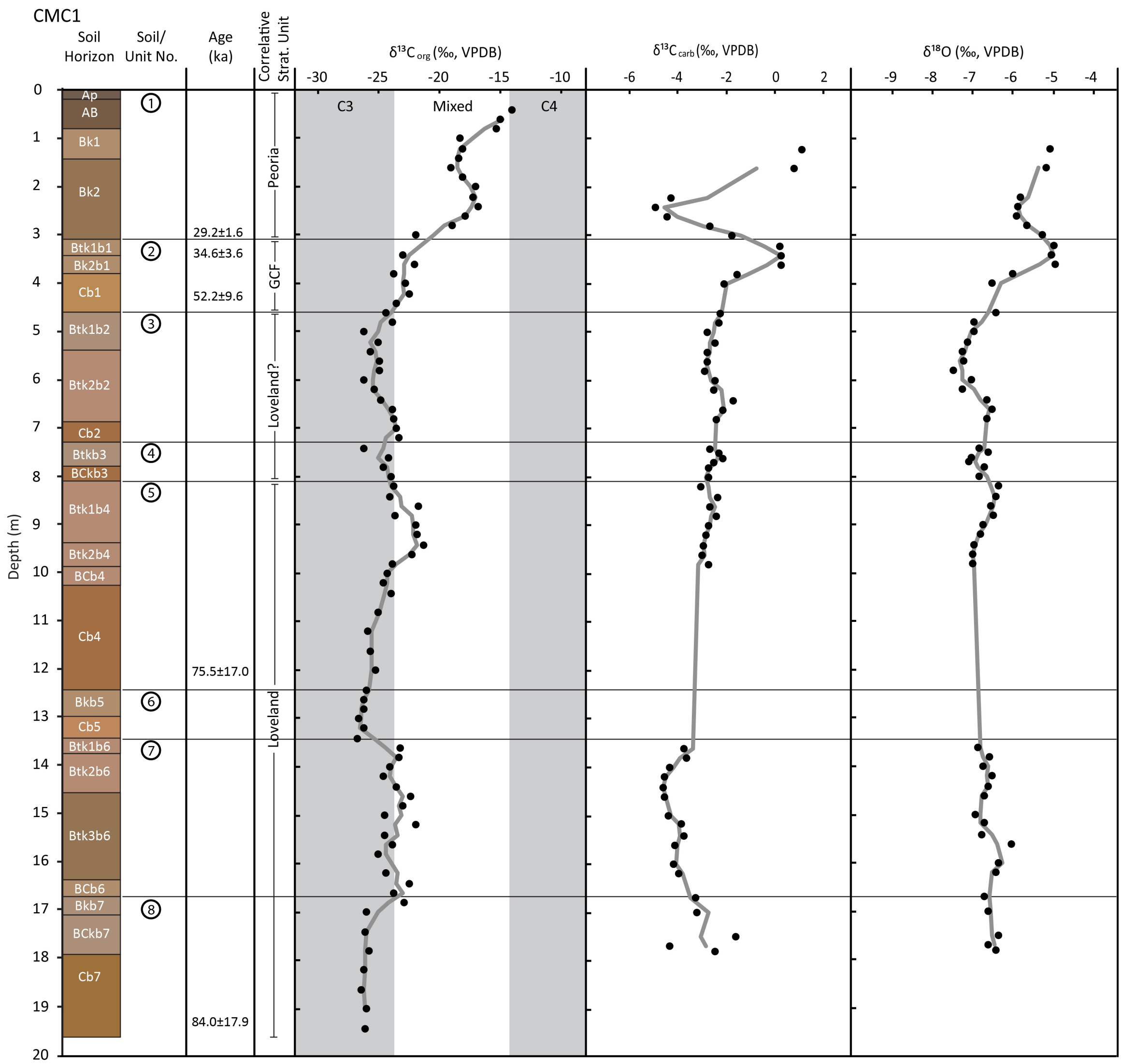


**Figure 3.4**. Stratigraphy, chronology, and stable isotope data from the CMC1 core. GCF = Gilman Canyon Formation. Gray line represents 3 pt moving average

of ca. 60 ka in the Mississippi River valley as previously noted. A $^{14}C$ sample from the bottom of unit 1 yielded an age of ca. 29.2 ka (Table 3.4) and indicates that this unit is coeval with the Peoria Loess, which began to accumulate in the Great Plains ca. 30–20 ka (e.g., Bettis et al., 2003).

**Table 3.3**. Soil descriptions from the CMC1 core

| Soil No. | Horizon | Depth (m) | Matrix Color | Texture[a] | Structure[b] | Consistence[c] | Clay Films[d] | Boundary[e] | Notes |
|---|---|---|---|---|---|---|---|---|---|
| 1 | Ap | 0-0.2 | 10YR 4/2 | L | 2 m gr | fr | --- | c | |
| | AB | 0.2-1.1 | 10YR 4/3 | SiCL | 2 m sbk | fr | --- | c | Parts to 2 m gr |
| | Bk1 | 1.1-1.45 | 10YR 6/4 | SiCL | 2 m abk | fi | --- | g | Few carbonate nodules |
| | Bk2 | 1.45-3.1 | 10YR 5/4 | SiCL | 2 m abk | fi | --- | a | Common carbonate nodules, few fine threads |
| 2 | Btkb1 | 3.1-3.4 | 10YR 6/4 | L | 2 m abk | fr | 1 d po | g | Parts to 2 m gr; Few carbonate nodules, common fine threads |
| | Bkb1 | 3.4-3.84 | 10YR6/4 | L | 3 m sbk | vfi | --- | g | Few carbonate nodules |
| | Cb1 | 3.84-4.6 | 10YR 6/6 | SL | sg | lo | --- | c | |
| 3 | Btk1b2 | 4.6-5.4 | 10YR 6/3 | CL | 2 m sbk | fi | 2 d pf | g | Parts to 1 f sbk; Many coalescing carbonate nodules, common fine threads |
| | Btk2b2 | 5.4-6.9 | 7.5YR 6/4 | SL | 2 m abk | fi | 2 d pf | g | Common carbonate nodules |
| | Cb2 | 6.9-7.29 | 7.5YR 5/6 | SL | sg | lo | --- | a | |
| 4 | Btkb3 | 7.29-7.8 | 10YR 6/3 | CL | 2 m abk | fi | 2 d pf | g | Many coalescing carbonate nodules, few fine threads |
| | BCkb3 | 7.8-8.1 | 7.5YR 5/6 | L | 1 f sbk | fr | --- | a | Parts to 2 m gr; Few carbonate nodules |
| 5 | Btk1b4 | 8.1-9.4 | 7.5 YR 6/4 | SiCL | 3 m abk | vfi | 3 d pf | g | Many coalescing carbonate nodules |
| | Btk2b4 | 9.4-9.9 | 7.5YR 6/4 | SiL | 2 m abk | fr | 2 d pf | g | Common carbonate nodules |
| | BCb4 | 9.9-10.28 | 7.5YR 6/4 | L | 1 f sbk | fr | --- | g | Parts to 2 m gr |
| | Cb4 | 10.28-12.45 | 7.5YR 5/6 | SL | sg | lo | --- | c | |
| 6 | Bkb5 | 12.45-12.9 | 10YR 6/4 | L | 2 m sbk | fr | --- | g | Parts to 1 f sbk and 2 m gr; Common fine carbonate threads |
| | Cb5 | 12.9-13.42 | 7.5YR 6/6 | LS | sg | lo | --- | a | |
| 7 | Btk1b6 | 13.42-13.8 | 7.5YR 6/6 | L | 2 f sbk | fr | 1 d pf | g | Parts to 2 m gr; Few carbonate nodules, common fine threads |
| | Btk2b6 | 13.8-14.6 | 7.5YR 6/6 | SL | 2 m abk | fi | 2 d pf | g | Few carbonate nodules, few fine threads |
| | Btk3b6 | 14.6-16.4 | 7.5YR 6/4 | L | 2 f sbk | fi | 2 d pf | c | Few carbonate nodules, common fine threads |
| | BCb6 | 16.4-16.7 | 7.5YR 6/4 | SL | 1 f sbk | vfr | --- | a | Parts to sg |
| 8 | Bkb7 | 16.7-17.1 | 10YR 6/3 | SL | 1 f sbk | fr | --- | c | Parts to 2 m gr; Few carbonate nodules, few fine threads |
| | BkCb7 | 17.1-17.9 | 10YR 6/3 | LS | 1 f sbk | fr | --- | c | Parts to sg |
| | Cb8 | 17.1-19.59 | 10YR 5/6 | LS | sg | lo | --- | a | |

[a] Texture: SiL–Silt Loam, SiCL–Silty Clay Loam, CL–Clay Loam, L–Loam, SL–Sandy Loam, LS–Loamy Sand
[b] Structure: 1–weak, 2–moderate, 3–strong; f–fine, m–medium, c–coarse; abk–angular blocks, sbk–subangular blocks, pl–plates, gr–granular, sg–single grain
[c] Consistence: lo–loose, vfr–very friable, fr–friable, fi–firm; vfi–very firm
[d] Clay Films: 1–few, 2–common, 3–many; d–distinct, p–prominent; pf–ped faces, po–pores
[e] Boundaries: a–abrupt, c–clear, g–gradual

**Table 3.4**. Radiocarbon age information from the CMC1 core

| Soil # | Horizon | Depth (m) | $^{14}C$ age (yr B.P.) | Calibrated age range[1] (yr B.P.) | Median calibrated age (ka) | Lab no. | $\delta^{13}C$ |
|---|---|---|---|---|---|---|---|
| 1 | Bk2 | 3.0 | 24,900±840 | 27,600-30,760 | 29.2±1.6 | OS-112461 | -17.4 |
| 2 | Btk1b1 | 3.4 | 30,300±1700 | 31,070-38,170 | 34.6±3.6 | OS-112462 | -15.9 |

[1]Calibration to calendar years (2 sigma) was performed with CALIB 7.0 using calibration dataset IntCal13 (Reimer et al. 2013).

3.4.2.2. Soil morphology

Soils from the CMC1 core are developed in predominantly sandy loam with sand contents ranging between 63 and 95% (Table 3.3; Fig. 3.5). Soils developed in eolian deposits interpreted to be coeval with the Loveland Loess (soils 5–8; Fig. 3.4) typically are characterized by 7.5 YR hues, > 2 m-thick Btk horizons, and angular blocky structure (Table 3.3). Soils 6 and 8, however, are less developed as indicated by relatively low HDI values (Fig. 3.5). These soils are characterized by 10 YR hues, relatively thin Bk horizons (< 0.5 m thick), and subangular blocky structure. Soil 7 is also morphologically less developed but is distinguished from soils 6 and 8 by the presence of clay films. Soil 5 is well developed and is a silty clay loam and silty loam with prominent clay films on ped faces. Clay and $CaCO_3$ contents peak at 40 and 43%, respectively (Fig. 3.5).

Soil 3 is morphologically similar to soil 5 and have the highest HDI values in the uppermost Btk horizon (Fig. 3.5). Soil 3 may therefore represent a late-Sangamon soil. Soil 3 is a clay loam to sandy loam and has a 2.3 m-thick Btk horizon with subangular to

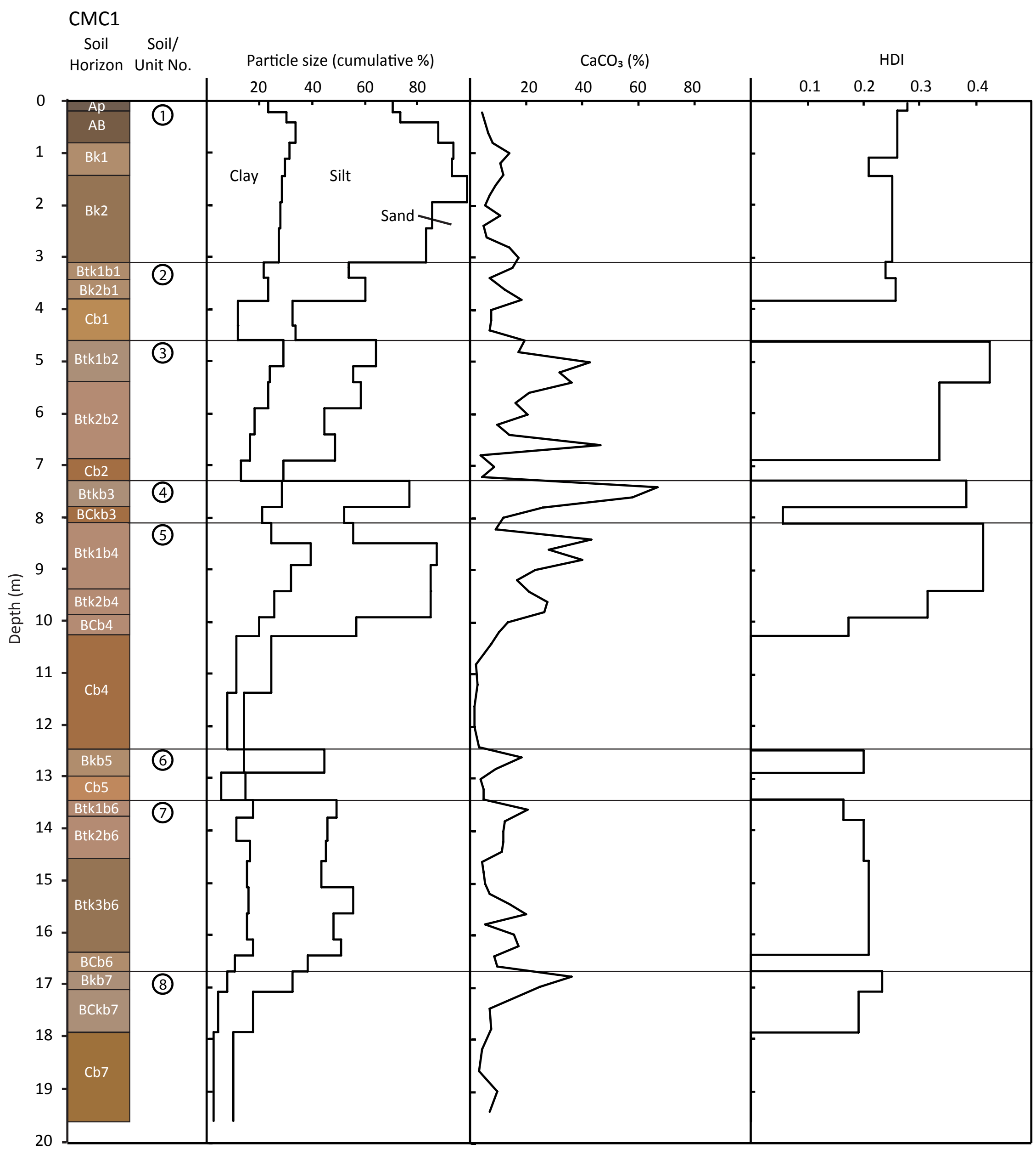


**Figure 3.5**. Particle size, carbonate content and HDI data for the CMC1 core

angular blocky structure. Clay content is less than in soil 5, ranging from 16 to 29%, and distinct clay films occur on ped faces. $CaCO_3$ content peaks at 46% and is morphologically expressed in the form of nodules and fine threads.

Soil 2 is developed in sandy loam sediments that are coeval with the Gilman Canyon Formation. The soil is 0.74 m thick and has a moderately developed Btk-Bk profile. $CaCO_3$ content is relatively low (7–18%) and is present in the form of nodules and fine threads. Although the modern surface soil (soil 1) is likely welded onto soil 2, soil 2 is distinguishable based on the presence of distinct clay films in pores and a change in soil texture.

The surface soil is 3.1 m thick and is a silty clay loam. The soil has moderately developed A-AB-Bk horizonation with subangular and angular blocky structure. $CaCO_3$ and clay contents peak at 17 and 35%, respectively.

3.4.2.3. Stable isotopes and paleoclimatic trends

$\delta^{13}C_{org}$ values show a relatively consistent $C_3$ signal throughout much of the CMC1 core, suggesting that late-Pleistocene climates were generally cooler than modern conditions (Fig. 3.4). Despite this consistent signal, certain isotopic trends and shifts are evident. A positive isotopic shift is apparent in unit 7 where $\delta^{13}C_{org}$ values increase to an average of -23.7‰, indicating an increase of 24% in the proportion of $C_4$ biomass compared to units 6 and 8. $\delta^{13}C_{org}$ values in units 8 and 6 are isotopically lighter (6% $C_4$ biomass) and indicate a dominance of $C_3$ vegetation. The positive isotopic shift in unit 7 likely indicates a change to warmer conditions during the formation of soil 7. This shift is similar to the one documented in unit 7 from the HP1A core. OSL ages from the C horizons of soils 8 and 5 indicate this period of climatic change occurred during late MIS 5 (ca. 84–75 ka).

$\delta^{13}C_{org}$ values increase through unit 6 and most of unit 5 from -26.7 to -21.3‰. This trend of overall increasing $C_4$ biomass (2 to 40%) suggests that temperatures were rising after ca. 75 ka,. At the top of soil 5, $\delta^{13}C_{org}$ values decline to -23.8‰, indicating a decline of 17% in $C_4$ biomass, whereas $\delta^{18}O$ values increase from -7.0 to -6.4‰. These opposite trends are similar to those observed in unit 4 from the HP1A core and likely represent colder but drier climatic conditions. The slight increase in $\delta^{13}C_{carb}$ values supports the inference of increased aridity at this time as water stress can increase the $\delta^{13}C$ value of pedogenic carbonate without an increase in the relative proportion of $C_4$ biomass (e.g., Fox et al., 2012).

The $\delta^{13}C_{org}$ values continue to decrease slightly overall through units 4 and 3 from -23.4 to -26.3‰ (26 to 5% $C_4$ biomass). Slight positive shifts are observable at the bottom of unit 3 and at the top of soil 3. $\delta^{13}C_{carb}$ values, however, remain relatively constant. $\delta^{18}O$ values decrease in the middle of soil 3 to -7.5‰ before increasing to -6.4‰ at the top of the soil. Overall, isotopic data suggests warmer climatic conditions at the onset of unit 3 deposition, followed by climatic cooling during most of the formation of soil 3. The increase in $\delta^{13}C$ and $\delta^{18}O$ values at the top of soil 3 suggests that conditions became warmer and more arid conditions during the latter stages of soil formation.

$\delta^{13}C_{org}$ values increase significantly from the top of soil 3 (-24.4‰) to the bottom of soil 1 (-17‰), indicating a considerable increase from 19 to 71% in the amount of $C_4$ biomass. Sharp increases are also apparent in the $\delta^{13}C_{carb}$ and $\delta^{18}O$ records for most of unit 2. These data suggest that warming and increasing aridity occurred during MIS 3 (between ca. 52–35 ka). A similar shift to warmer, drier conditions was observed in unit 2 from the HP1A core. As previously noted, warm and dry conditions during late MIS 3 have been documented from a late Pleistocene (ca. 48–28 ka) buried soil in the Cimarron River valley (see chapter 2) and by several regional paleoenvironmental studies (e.g., Fredlund, 1995; Jacobs et al., 2007; Baker et al., 2009).

Whereas the $\delta^{13}C_{org}$ values continue to increase at the bottom of soil 1 the other isotope records show a significant shift to more negative values. The sharp negative isotopic excursions in the $\delta^{13}C_{carb}$ and $\delta^{18}O$ record are also observable in the HP1A core. Several explanations can be advanced to explain the documented trends. First, the $\delta^{13}C_{org}$ and $\delta^{18}O$ trends could indicate warmer but wetter conditions with either an increase in the fraction of isotopically light winter precipitation or perhaps an increase in precipitation derived from Pacific moisture sources. This scenario, however, does not explain the sharp decrease in $\delta^{13}C_{carb}$ values.

An alternative explanation is that the pedogenic carbonate in soil 1 formed in water-saturated conditions. A study by Mintz et al. (2011) investigated calcite precipitation in vertisols on the Texas Coastal Plain and showed that luminescent phases of calcite growth, reflecting formation during water-saturated parts of the year, had significantly more negative values than the non-luminescent phases that indicated well-drained conditions. There is no morphological evidence, however, of water-saturated conditions (e.g., gleying) during the formation of soil 1 in either core.

A final explanation is that this signal reflects a change in the source of the eolian parent material. Eolian sands in much of the core are likely locally derived from either the Cimarron and Arkansas River valleys or from the alluvial sediments of the Ogallala Formation. In contrast, studies have shown that most Peoria Loess in the Central Plains is primarily sourced from the Oligocene White River Group in South Dakota (e.g., Aleinikoff et al., 2008; Muhs et al., 2008). $\delta^{13}C_{carb}$ values for White River Group pedogenic carbonates have been shown to range between -6 and -7‰ (Mullin, 2010). The negative shift in $\delta^{13}C_{carb}$ and $\delta^{18}O$ observed in the cores may therefore reflect the onset of Peoria Loess deposition rather than a change in climatic conditions. This interpretation is supported by a $^{14}C$ age of ca. 29 ka from unit 1 in the CMC1 core that is consistent with the timing of Peoria Loess deposition in the Great Plains (see Bettis et al., 2003).

### 3.5. Conclusions

The stratigraphy of two 20 m-deep cores from the High Plains of southwestern Kansas provide a record of eolian sedimentation and soil formation during the late Pleistocene. Both cores contain 8 eolian units and intercalated soils that span the period from late MIS 5 to present. The chronology indicates that ~ 10 m of eolian sediments were episodically deposited during late MIS 5 (ca. 84–70 ka). Paleoenvironmental reconstructions indicate that this episodic deposition was concomitant with climatic variability. In particular, $\delta^{13}C$ and $\delta^{18}O$ analyses indicate distinct shifts to both warmer and cooler and temperatures during this time period. Furthermore, relationships between $\delta^{13}C$ and $\delta^{18}O$ values suggest that periods of climatic warming were likely relatively humid with greater amounts of isotopically light winter precipitation. In contrast, periods of climatic cooling during late

MIS 5 were likely relatively dry, resulting in greater evaporative enrichment of soil water.

Paleoenvironmental data indicate cool conditions during early MIS 3 with a subsequent increase in temperature and aridity. A significant negative isotopic excursion in the $\delta^{13}C_{carb}$ and $\delta^{18}O$ record was observed at the top of both cores. This shift is hypothesized to represent a change in the source of the eolian parent material, with the isotope values recording the deposition of Peoria Loess derived from the White River Group. Overall, $\delta^{13}C$ and $\delta^{18}O$ analyses provide an important means to investigate paleoenvironmental change and landscape response during the late Quaternary, and the inferred paleoclimatic changes in this study correlate well with other paleoclimatic reconstructions from the Great Plains.

# CHAPTER 4

# STRATIGRAPHY, DEPOSITIONAL HISTORY AND PALEOENVIRONMENTS OF THE LATE MIOCENE TO EARLY PLIOCENE OGALLALA FORMATION, SOUTHWESTERN KANSAS

## 4.1. Introduction

In the High Plains of southwestern Kansas, the Miocene and early Pliocene sediments of the Ogallala Formation unconformably overlie Permian through Cretaceous strata and are locally overlain by Quaternary alluvial and eolian deposits (e.g., Frye at al., 1956; Merriam, 1963). The Ogallala Formation is the primary constituent of the High Plains aquifer, which provides almost 30% of all groundwater used for irrigation in the United States and is under increasing stress from developmental practices (e.g., Maupin and Barber, 2005). Over the last 50 years, groundwater withdrawals from the aquifer for irrigation have resulted in significant water level declines in some areas, including southwestern Kansas where declines of over 150 ft have been reported (e.g., McGuire, 2009; High Plains Aquifer Atlas, 2014; Fig. 4.1). Adequate management of this vital resource is best achieved through numerical modeling of predicted hydrological response to different management strategies, which in turn depends on an accurate characterization of sedimentary deposits comprising the aquifer and their stratigraphic framework (Smith et al., 2014).

This study is part of the High Plains Ogallala Drilling Program at the Kansas Geological Survey, which is designed to advance the scientific understanding of the sedimentary facies, stratigraphy, depositional history, and paleoenvironments of the High Plains

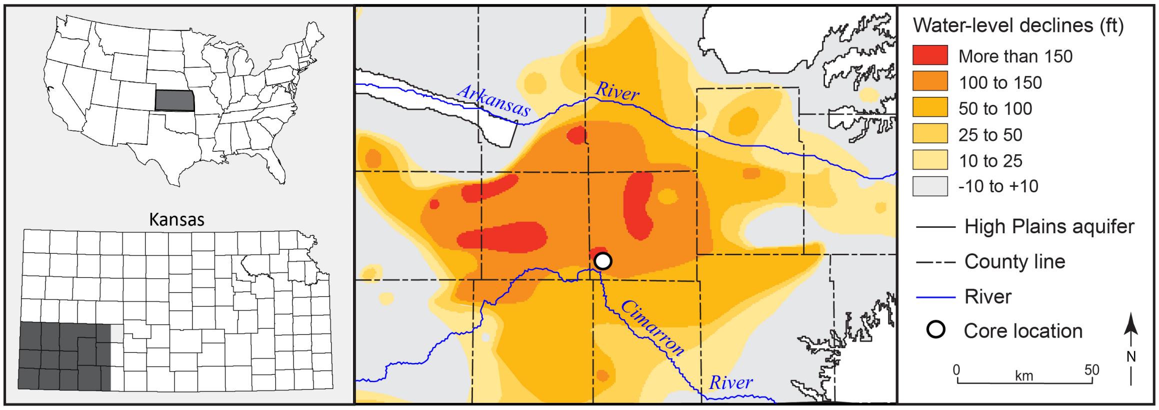


**Figure 4.1**. Study area location in Haskell County, southwestern Kansas and water level changes in the High Plains aquifer from predevelopment to 2007 (modified from McGuire, 2009).

succession. The sedimentological properties and stratigraphic framework of the High Plains succession are derived from the formative processes and depositional histories of water-bearing and confining strata (Smith et al., 2014). Previous studies have highlighted complexities in the depositional histories of Ogallala Formation strata (e.g., Chapin, 2008; Eaton, 2008) and, therefore, in order to develop accurate stratigraphic correlation a detailed temporal framework is required. This study investigates the lithostratigraphy and paleoenvironments of the Ogallala Formation from a 50-m-deep core collected from Haskell County, southwestern Kansas (Fig. 4.1) and presents preliminary findings from a new approach to date volcanogenic zircons from primary ash-fall tephra preserved in paleosols. Numerous paleosols have been identified in the Ogallala Formation (e.g., Diffendal, 1982; Gustavson and Winkler, 1988; Gardner et al., 1992; Fox et al., 2012); hence, this technique may provide a vital tool for establishing a chronostratigraphic framework for the High Plains succession.

## 4.2. Background and rationale

### 4.2.1 Geology

The Ogallala Formation extends from Texas to South Dakota and represents the remnant of an extensive alluvial apron formed by clastic sediments shed eastward from the uplifting Rocky Mountains. Ogallala strata have been interpreted as being deposited through the coalescence of alluvial fans that aggraded from trunk streams discharging from the Rocky Mountain front (e.g., Seni, 1980). Later investigations in New Mexico and Texas indicated that the Ogallala Formation consisted of fluvial sediments, deposited by high-energy braided streams that filled broad paleovalleys, and eolian sediments that bury fluvial sediments and paleouplands (e.g., Gustavson and Winkler, 1988). Recent studies have highlighted differences in local rates of aggradation and uplift, as well as sedimentary provenience, suggesting that streams feeding the depositional system of the Ogallala Formation likely experienced different depositional histories (e.g., Chapin, 2008; Eaton, 2008). These observations necessitate the development of a detailed temporal framework in order to construct accurate stratigraphic correlations for the High Plains aquifer.

### 4.2.2 Chronology

Terrestrial vertebrate fossil assemblages commonly have been used to date Ogallala Formation deposits. In Kansas, vertebrate faunas indicate that the Ogallala Formation includes Miocene and early Pliocene strata with an age range of approximately 16.3–4.9 Ma (Ludvigson et al., 2009). Volcanic ash bed tephrochronology also has been used to provide age control for the deposition of Ogallala sediments. Published fission track ages and chemical fingerprinting of volcanic glass shards from ash beds across the Great Plains constrain Ogallala deposition to between 12.5 and 5.0 Ma (Boellstorff, 1978; Perkins et al., 1995). Volcanic ash beds, however, typically are preserved in isolated swales and depressions with limited lateral extent. In over 500 m of core, collected as part of the High Plains Ogallala Drilling Program, no ash beds have been intercepted. In order to overcome the poor preservation of ash-fall tephra, this study specifically targets volcanogenic zircons preserved in paleosols. Ash-fall zircons are more likely to be concentrated in well-developed paleosols as they represent time-rich intervals in the stratigraphic record and, therefore, are most likely to overlap with past periods of volcanic activity.

### 4.2.3 Paleosols

In Kansas, a thick carbonate-rich horizon, developed in the Ogallala Formation through pedogenic processes (Swineford et al., 1958), typically maintains the very low relief (5–15 m) of the upland surface. Early investigations attempted to use the presence of carbonate-rich horizons as a stratigraphic marker for the top of the Ogallala Formation (e.g., Merriam and Frye, 1954; Frye et al., 1956). Later studies, however, showed that carbonate-rich paleosols are common throughout the whole formation (e.g., Diffendal, 1982).

Paleosols reflect the complex interplay of sedimentation, erosion, and non-deposition (e.g., Kraus, 1999). As the rate of sedimentation varies over time, and is controlled by autogenic and allogenic mechanisms that initiate and terminate sedimentation, paleosols can be helpful in reconstructing and interpreting depositional history, landscape evolution, and paleoclimatic change in sedimentary successions. In terms of Neogene paleoclimatic change, the analysis of stable carbon ($\delta^{13}C$) and oxygen ($\delta^{18}O$) isotopes in paleosols has been shown to provide important paleoenvironmental information, including the documentation of an increasing abundance of $C_4$ biomass throughout the Neogene (e.g., Fox and Koch, 2003; Fox et al., 2012).

### 4.3. Methodology

A 50-m-deep core was collected as part of the High Plains Ogallala Drilling Program at the Kansas Geological Survey. In this paper, the lower 30 m of the core, comprising the fluvial deposits of the Ogallala Formation, is described. Additional descriptions (Table 4.1) were obtained from exposures in a quarry located ~3 km from the coring location. Drilling and core retrieval were accomplished using an Acker hollow-stem auger and wireline, split-spoon core sampler. Sedimentary descriptions included assessment of lithology, color, bedding characteristics and sedimentary structures. Paleosols were described in detail using standard terminology in Birkeland (1999) and Soil Survey Staff (1993). Soil horizons were described in terms of their color, texture, structure, consistency and boundaries. Where present, clay films, secondary carbonate forms and biogenic features were described. Paleosols were sampled by horizon for particle size. Where horizon thicknesses were > 50 cm, subsamples were collected so that the sample interval was < 50 cm. Samples were air-dried (24–48 hrs) and ground to pass through a 2-mm-sieve for particle-size analysis using the pipette method (Soil Survey Staff, 1982).

Stable carbon isotopes ($\delta^{13}C$) from organic matter and both $\delta^{13}C$ and stable oxygen isotopes ($\delta^{18}O$) from pedogenic carbonate were analyzed to investigate potential paleoclimatic trends. $\delta^{13}C$ values of organic matter ($\delta^{13}C_{org}$) preserved in paleosols reflect the relative contributions of $C_3$ and $C_4$ vegetation at the time of soil formation. Modern $C_3$ plant communities have $\delta^{13}C_{org}$ values between -32‰ and -20‰ (average of -27‰) and include cool season grasses and woody vegetation (e.g., Boutton, 1991). In contrast, $C_4$ plants have $\delta^{13}C_{org}$ values between -17‰ and -10‰ (average of -13‰) and are primarily comprised of warm season grasses. The relative contribution of $C_4$ plants to SOM is estimated with the following mass balance equation (Nordt et al., 1994):

$$\delta^{13}C_{SOM} = \delta^{13}C_{C4}(x) + \delta^{13}C_{C3}(x)\ (1\text{-}x) \qquad (1)$$

where $\delta^{13}C_{SOM}$ is the measured $\delta^{13}C$ value, $\delta^{13}C_{C4}$ = -13‰, $\delta^{13}C_{C3}$ = -27‰ and $x$ is the relative contribution of $C_4$ plants to SOM.

$\delta^{13}C$ values from pedogenic carbonate ($\delta^{13}C_{carb}$) also can be used to assess past vegetation compositions. Pedogenic carbonate forms in carbon isotopic equilibrium with soil $CO_2$, which is derived primarily from root respiration and therefore reflects the relative contributions of $C_3$ and $C_4$ species. $\delta^{13}C_{carb}$ values, however, are offset by 14–17‰ relative to $\delta^{13}C_{org}$ due to molecular diffusion and isotopic equilibria reactions (e.g., Cerling et al., 1989). Strong correlations have been found between the proportion of $C_4$

vegetation and temperature (e.g., Terri and Stowe, 1976; Boutton, 1996) indicating that $\delta^{13}C$ data can function as an important proxy for paleoclimatic change.

The analysis of $\delta^{18}O$ from pedogenic carbonate also provides a potential source of important paleoclimatic data. The $\delta^{18}O$ of pedogenic carbonate is controlled by the $\delta^{18}O$ value of soil water and temperature (e.g., Cerling and Wang, 1996). Soil water is derived from meteoric water but can differ in its $\delta^{18}O$ value due to evaporation and mixing with isotopically distinct water sources (Cerling and Quade, 1993). In general, lower (higher) carbonate $\delta^{18}O$ values indicate: 1) lower (higher) temperatures through lower (higher) $\delta^{18}O$ values of meteoric water; 2) a greater fraction of winter (summer) season recharge of soil water; 3) wetter (drier) conditions and a decrease (an increase) in evaporative enrichment of soil water; or 4) a combination of some or all of these factors (Fox et al., 2012).

All stable isotopic analyses were performed at the University of Kansas W. M. Keck Paleoenvironmental and Environmental Stable Isotope Laboratory. Organic matter samples were collected at 60-cm intervals from sediments and 20 cm from paleosols. Samples were decarbonated with 0.5 M HCl and combusted using a Costech Elemental Analyzer at 1060° C. The resultant $CO_2$ was analyzed by a continuous-flow ThermoFinnigan MAT 253 mass spectrometer. Pedogenic carbonate samples were collected at regular intervals where present in buried paleosols. Dried, ground samples were analyzed with a Kiel III device coupled to a dual inlet ThermoFinnigan MAT 253 mass spectrometer. Final $\delta^{13}C$ and $\delta^{18}O$ data were calibrated with National Institute Standards and are expressed relative to the Vienna Peedee Belemnite standard.

U-Pb dating of volcanogenic zircon grains was utilized to provide age control for the High Plains succession. Although this technique has commonly been used to date ash beds (e.g., Bowring et al., 1998; Reid and Coath, 2000) and detrital zircon populations in fluvial sandstones (e.g., Blum and Pacha, 2014), here, a new approach is employed that aims to isolate volcanogenic zircon grains preserved in paleosols for U-Pb analyses. Conceptually, zircons from ash-fall deposits should be preserved in paleosols through soil-forming processes (i.e., translocation and bioturbation) (Fig. 4.2). Attempts to isolate these zircons are made by selecting grains with euhedral, prismatic shapes that lack evidence of abrasion via sediment transport (i.e., non-detrital populations). U-Pb dating of detrital zircons typically provides maximum depositional ages (e.g., Dickinson and Gehrels, 2009), however, focusing on primary ash-fall grains in paleosols potentially provides a means to minimize the difference between maximum and true depositional ages.

Samples from paleosols were initially disaggregated using water, and dilute HCl was used to remove pedogenic carbonate. Clay-sized and very coarse fractions were removed on a water table before heavy mineral separation. Heavy, non-magnetic minerals were isolated using a Frantz Isodynamic magnetic separator and heavy liquid separation techniques. Euhedral, prismatic grains were then handpicked and mounted on double-

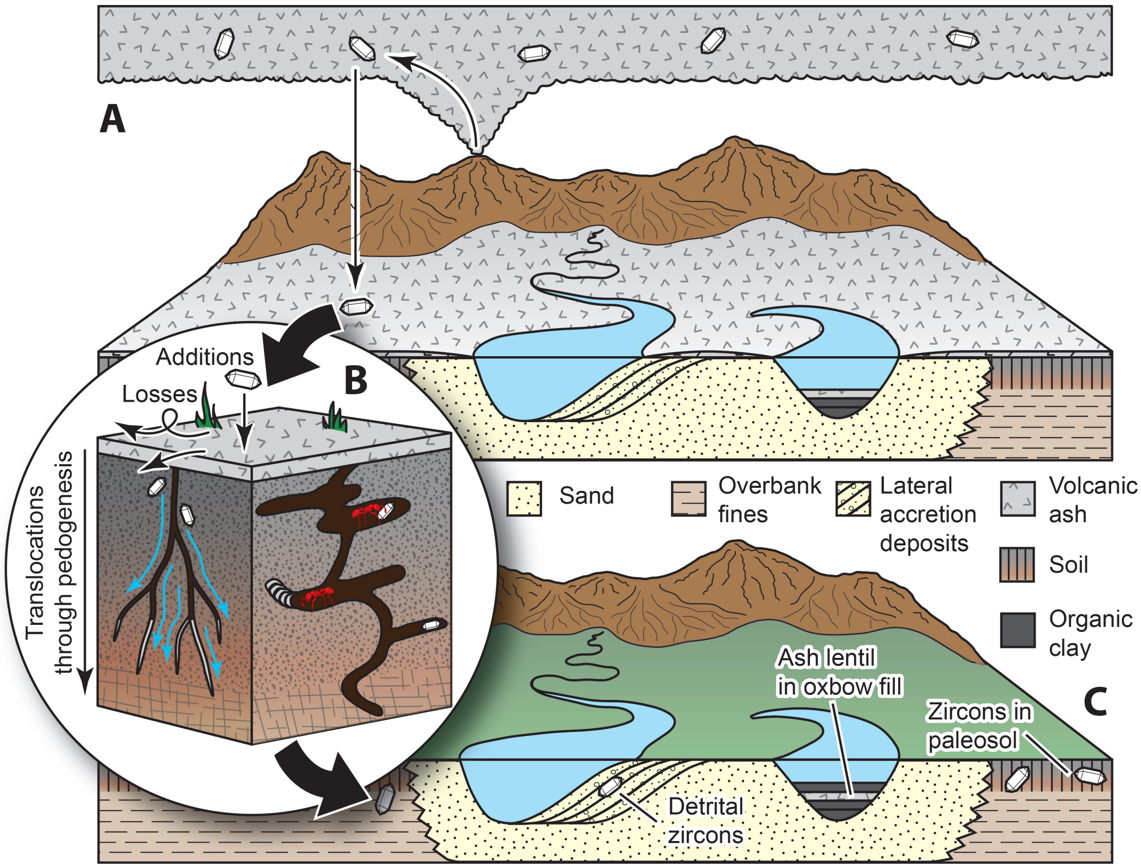


**Figure 4.2**. Conceptual diagram of A) the deposition of primary ash-fall tephra across a landscape, B) the incorporation of zircons into a paleosol via soil-forming processes, and C) the likely locations of preserved zircon grains in paleosols, swales and fluvial deposits. Image courtesy of Brian Platt, University of Mississippi.

sided tape for U-Pb analysis by laser ablation inductively couples mass spectrometry (LA-ICP-MS) at the University of Kansas Isotope Geochemistry Laboratory.

## 4.4. Results

### 4.4.1. Stratigraphy and paleosols

The upper 19.6 m of the core (see chapter 3) consists sediments that are typically brown (7.5 YR 5/4) with sandy loam or loamy sand textures. These sediments have been strongly modified by pedogenesis and the succession contains seven paleosols as well as the modern soil. Thick (> 1 m) Bt horizons with moderate angular blocky structure and distinct clay films on ped faces are common. Bk horizons are also common with few to many carbonate nodules and threads. Ro-Tap sieve analyses (see Appendix A) indicate that sediments in the upper 19.6 m of the core are finer (lower mean phi values) and better sorted (lower coefficient of variation) than the rest of the core. The upper sediments are therefore interpreted as eolian in origin based on textural characteristics and landscape position.

About 20 m of eolian sediments bury the fluvial deposits of the Ogallala Formation. The fluvial deposits consist of vertically stacked, upward-fining sequences that range in texture from coarse gravel to fine sand (Fig. 4.3). These sediments are typically yellowish brown (10YR 5/4) to very pale brown (10YR 7/4) in color. No primary sedimentary structures were observable in core.

Three paleosols are developed in the fluvial sediments of the Ogallala Formation (Fig. 4.3). No A horizons were preserved in these paleosols, having either been eroded before burial or oxidized after burial. The lowest paleosol (paleosol 3) is 1 m thick and is buried 40.7 m below the surface. Paleosol 3 has well expressed Btkss-Btss horizonation with angular blocky structure, firm to very firm consistence, many prominent clay films on ped faces, and common distinct slickensides. Matrix colors of the Btkss and Btss horizons are very pale brown (10YR 7/4) and reddish yellow (7.5YR 6/8), respectively. Pedogenic carbonate in the Btkss horizon is expressed in the form of few, very fine threads. The Btss horizon exhibits common, medium sized, prominent gray (10YR 5/1)

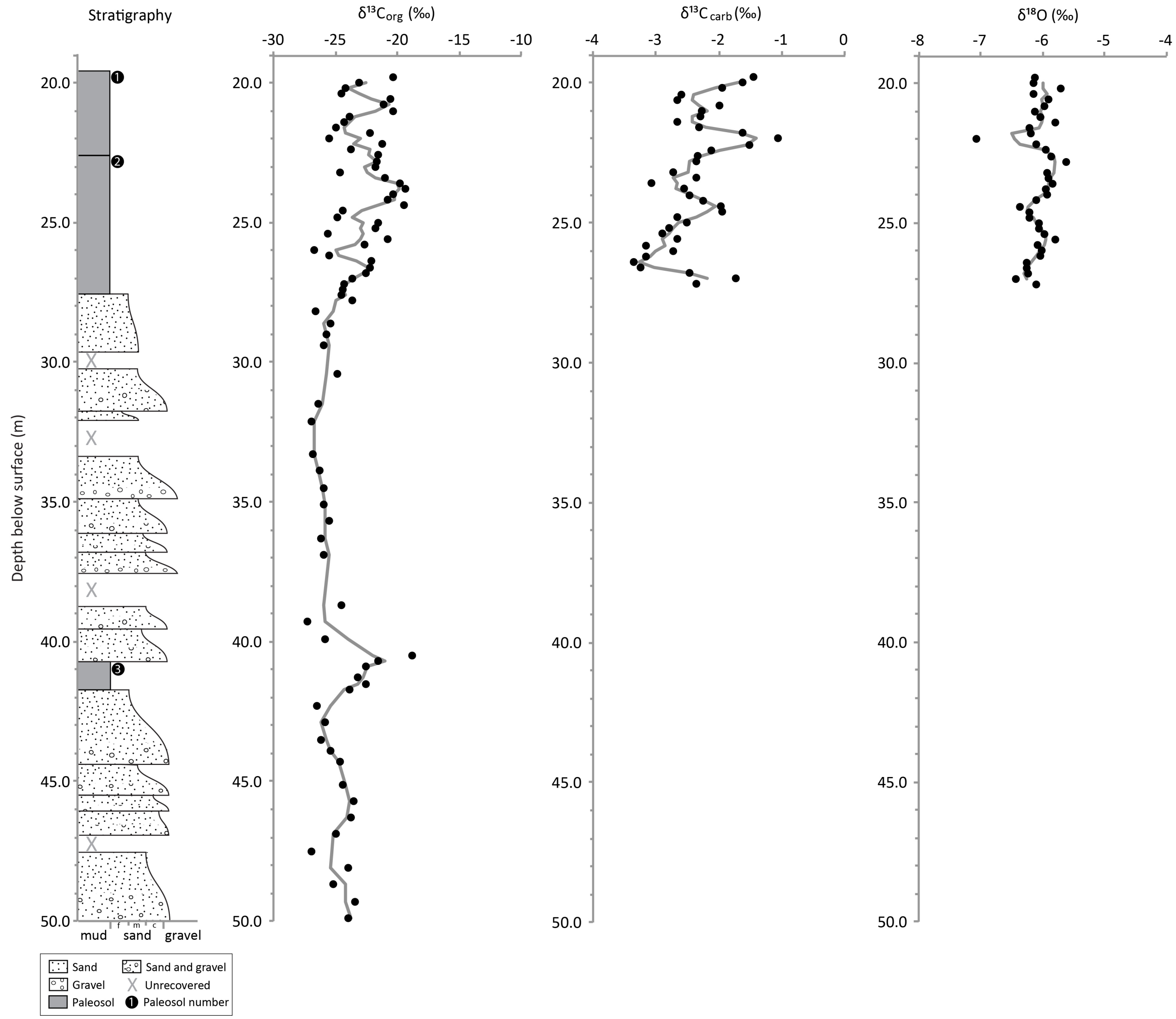


**Figure 4.3**. Stratigraphy and stable isotope data from core

mottles. The Btkss and Btss horizons have silty clay loam to clay loam and clay textures, respectively.

Paleosols 1 and 2 are buried 19.6 and 23.3 m, respectively, below the High Plains surface in core. Paleosol 2 has a 4.3 m-thick Btk horizon with a sandy clay loam texture, well-developed angular blocky structure and firm consistence. Well-expressed coarse prismatic structure is evident in outcrop (Table 4.1). Common, prominent, continuous clay films occur in macropores and on ped faces. The paleosol is strongly indurated with carbonate (up to 53%) that is morphologically expressed in the form of many large carbonate nodules. In outcrop, the profile thickness is only 0.83 m (Table 4.1), indicating that paleosol 2 has been truncated at this location. This inference is supported by the presence of an abrupt wavy boundary, indicative of an erosion surface.

Paleosol 1 is similar to paleosol 2 in terms of its morphology. The paleosol has a 3.6 m thick, well-developed Btk horizon with a sandy clay loam texture, well-expressed angular blocky structure and very hard, firm consistence. In outcrop, the profile thickness is 2.4 m and coarse prismatic structure is evident (Table 4.1). Prominent clay films are present in macropores and on ped faces. Carbonate content is relatively high (up to 27.9%) and is present in the form of many to common nodules that range in size from 0.5 to 2 cm. Paleosols 1 and 2 are separated by a relatively thin BCk horizon and, therefore, represent a pedocomplex in accordance with the definition proposed by the Paleopedology Working Group to the International Union for Quaternary Research (INQUA) (e.g., Catt, 1998).

**Table 4.1** – Soil profile description from outcrop

| Horizon | Depth (cm) | Color Dry | Color Moist | Texture[1] | Structure[2] | Consistence[3] | Clay Films[4] | Boundary[5] | Pores[6] | Roots[6] | Notes |
|---|---|---|---|---|---|---|---|---|---|---|---|
| A | 0-20 | 10YR 5/3 | 10YR 4/2 | SL | 2 m gr | sh, vfr | --- | g | 1f, 2vf | 2f, 3vf | |
| AB | 20-70 | 10YR 5/3 | 10YR 4/2 | SL | 2 vc pr | sh, fr | --- | a | 3m, 1f, 3vf | 3m, 1f, 2vf | Parts to 2 c sbk; Many wormcasts |
| 2Btk1b1 | 70-156 | 7.5YR 7/6 | 7.5YR 6/6 | SCL | 3 m pr | vh, fi | 2 p po | g | 1m, 1f, 3vf | 2vf | Parts to 3 c abk; Continuous 5YR 5/6 clay films; Many (60% surface area) large soft 10YR 8/1 carbonate nodules, weakly cemented; Few wormcasts in burrows |
| 2Btk2b1 | 156-196 | 5YR 6/6 | 5YR 5/6 | SCL | 3 vc pr | vh, fi | 3 p pf, po | g | 3vf | --- | Parts to 3 m abk; Discontinuous 5YR 5/8 clay films; Common (35% surface area) large hard 10YR 8/1 carbonate nodules weakly cemented |
| 2Btk3b1 | 196-314 | 5YR 6/6 | 5YR 5/6 | SCL | 3 vc pr | vh, fi | 3 p pf, po | g | 1m, 3vf | --- | Parts to 3 m abk; Discontinuous 5YR 5/8 clay films; Common (25% surface area) large hard 10YR 8/1 carbonate nodules, weakly cemented |
| 2BCkb1 | 314-336 | 7.5YR 7/6 | 7.5YR 6/6 | SL | 2 m pr | vh, fi | --- | a | 1m, 3vf | 3vf | Parts to 2 m abk; Few sand and fine gravel beds 5cm thick, 1cm thick mud bed; Few medium hard carbonate nodules |
| 2Btkb2 | 336-419 | 7.5YR 7/4 | 7.5YR 6/4 | SCL | 3 c pr | vh, fi | 2 p po | g | 2vf | --- | Parts to 3 c abk; Continuous 5YR 5/8 clay films; Many (75% surface area) large hard 10YR 8/1 carbonate nodules, strongly cemented |
| 2Cb2 | 419-507+ | 10YR 7/4 | 10YR 5/4 | S | sg | lo | --- | --- | --- | --- | |

[1]Texture: SL–Sandy Loam, SCL–Sandy Clay Loam, S–Sand
[2]Structure: 1–weak, 2–moderate, 3–strong, sg–single grain; f–fine, m–medium, c–coarse, vc–very coarse; gr–granular, abk–angular blocks, sbk–subangular blocks, pr–prismatic
[3]Consistence: sh–slightly hard, h–hard, vh–very hard; lo–loose, vfr–very friable, fr–friable, fi–firm; vfi–very firm
[4]Clay Films: 1–few, 2–common, 3–many; d–distinct, p–prominent; pf–ped faces, po–pores
[5]Boundaries: a–abrupt, c–clear, g–gradual
[6]Roots and pores: 1–few, 2–common, 3–many; vf–very fine, f–fine, m–medium, c–coarse

4.4.2. Stable isotopes

From 50–40.7 m in the core, $\delta^{13}C_{org}$ values decline upward from -24‰ to -26.5‰ before increasing to -18.8‰ at the top of paleosol 3 (Fig. 4.3). These values represent an initial reduction in $C_4$ biomass from 22 to 3% with a subsequent increase to 59%. From 40.7–27.6 m, $\delta^{13}C_{org}$ values are relatively constant with a mean value of -25.9‰, representing ~8% $C_4$ biomass. Between 27.6–19.6 m, $\delta^{13}C_{org}$ values generally increase upward from -24.6 to -20.3‰ (17 to 48% $C_4$ biomass) through paleosols 1 and 2; however, distinct isotopic intervals are also evident (Fig. 4.4).

In paleosol 2, $\delta^{13}C_{org}$ values generally increase from -24.6‰ in the C horizon to about -20‰ at the top of the paleosol (increase of 15 to 50% in $C_4$ biomass) (Fig. 4.4). Near the bottom of the soil (isotopic interval A), however, $\delta^{13}C_{org}$ values decline upward from -22.1 to -26.7‰ (35 to 2% $C_4$ biomass) before subsequently increasing to -19.4% in interval B. This trend is also observable in the $\delta^{13}C_{carb}$ record where values decline from -1.7 to -3.4‰ (interval A) before increasing to -2.0‰ (interval B). In interval C, near the top of paleosol 2, $\delta^{13}C_{org}$ values remain relatively constant around -20‰ (50% $C_4$ biomass) but $\delta^{13}C_{carb}$ values decline upward from -2.0 to -3.1‰. $\delta^{18}O$ values are relatively constant around -6‰ in paleosol 2, however some subtle shifts occur. In isotopic interval A, $\delta^{18}O$ values increase upward from -6.4 to -6.0‰, whereas $\delta^{13}C$ values decline. The opposite trend is observable in interval B where $\delta^{18}O$ values decline upward from -5.8 to -6.4‰ whereas $\delta^{13}C$ values increase. At the top of the paleosol (interval C), $\delta^{18}O$ values increase upward to -5.9‰, mirroring the trend in $\delta^{13}C_{org}$, however $\delta^{13}C_{carb}$ values show the opposite trend.

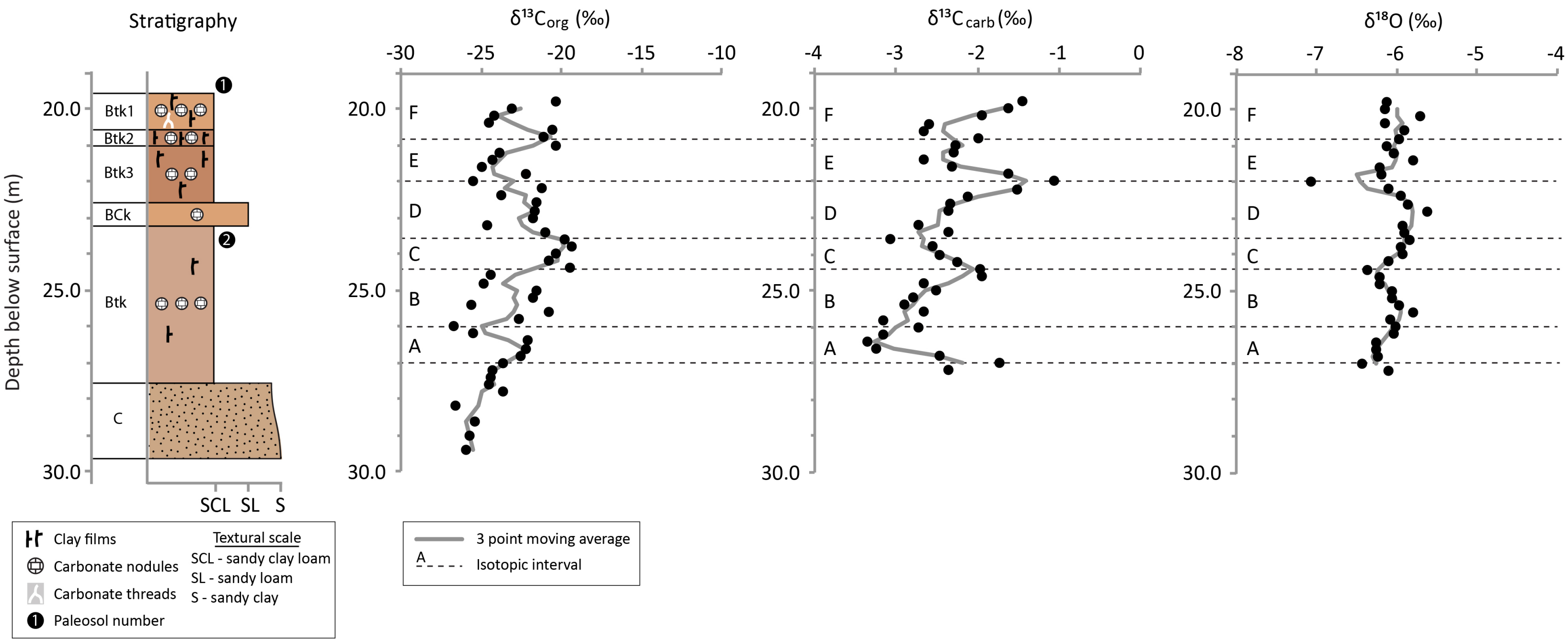


**Figure 4.4**. Stratigraphy and stable isotope data from paleosols 1 and 2

At the bottom of paleosol 1 (interval D), $\delta^{13}C_{org}$ values decrease upward from -19.8 to -25.6‰ (51 to 10% $C_4$ biomass) (Fig, 4.4). This decline is mirrored in the $\delta^{18}O$ record where values decrease from -5.6 to -7.1‰. $\delta^{13}C_{carb}$ values, however, show the opposite trend, increasing upward from -2.7 to -1.1‰. In interval E, $\delta^{13}C_{org}$ values increase upward to -20.6‰ (46% $C_4$ biomass) whereas $\delta^{13}C_{carb}$ values decrease to -2.7‰. At the top of the paleosol (interval F), $\delta^{13}C_{org}$ values initially decrease to -24.2‰ (20% $C_4$ biomass) then increase to -20.3‰ (48% $C_4$ biomass) whereas $\delta^{13}C_{carb}$ values increase to -1.5‰.

4.4.3. Chronology

$\delta^{13}C_{org}$ values indicate up to 46, 54 and 59% contributions to SOM from $C_4$ vegetation for paleosols 1, 2, and 3, respectively. Given that ecosystems with >50% $C_4$ biomass only appeared in the Great Plains during the Pliocene (Fox and Koch, 2003), the three paleosols identified in core are inferred to be Pliocene in age. Furthermore, based on a shift from fluvial to eolian sediments above paleosol 1, the pedocomplex (paleosols 1 and 2) is interpreted as representing slow sedimentation accompanied by pedogenesis during the final aggradational phase of the Ogallala Formation. If correct, then the pedocomplex represents the abandoned High Plains surface after the onset of incision in the Great Plains, which is estimated to have occured between 4 and 6 Ma (e.g., Chapin, 2008).

In order to confirm the timing of late Cenozoic incision, volcanogenic zircons from primary ash-fall tephra preserved in paleosols were dated. A total of 32 zircons were extracted from paleosol 2 for U-Pb dating. Isolated zircons were euhedral and prismatic

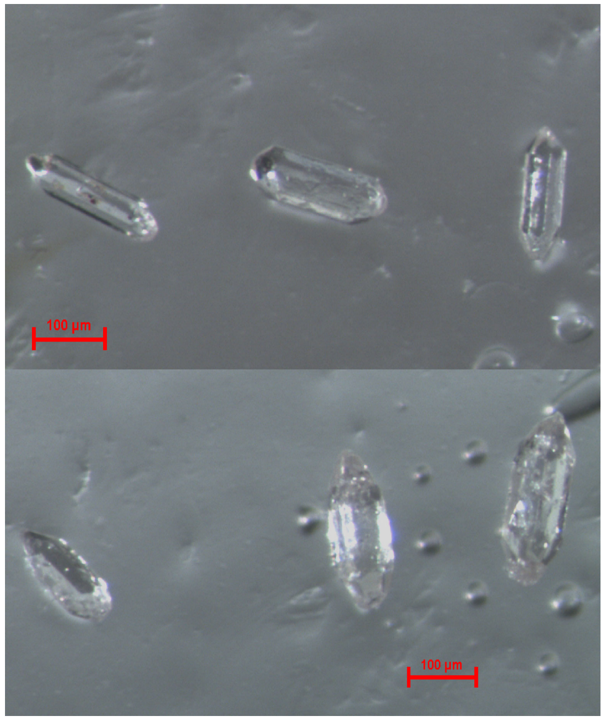


**Figure 4.5**. Example zircon grains selected for U-Pb dating from paleosol 2

in shape and typically 100–200 µm in size (Fig. 4.5). U-Pb dating of these zircons via LA-ICP-MS yielded a youngest population of five grains with a concordia age of 64.2±3.9 Ma (Fig. 4.6).

## 4.5. Discussion

### 4.5.1. Paleoenvironments and paleosols

The paucity of paleosols and presence of coarse textured (sand and gravel) deposits throughout much of the 30 m succession of the Ogallala Formation indicates that sedimentation was relatively rapid and continuous. The depositional environment was likely a rapidly aggrading, high-energy, braided fluvial system with frequent channel shifting. The paucity of paleosols suggests that periods of landscape stability were either of insufficient duration to form soils or that weakly developed soils formed in the sandy alluvium were eroded before burial or oxidized after burial.

The fine-grained texture of paleosol 3 is indicative of steady depositional conditions where the rate pedogenesis exceeded the rate of sedimentation, resulting in a cumulative soil profile (e.g., Kraus, 1999). This type of paleosol typically forms in floodplain deposits distal to the active channel. $\delta^{13}C_{org}$ values of up to -18.8‰ (59% $C_4$ biomass) in paleosol 3 are suggestive of warmer climatic conditions during this interval of soil formation. Also, evidence of mottling and slickensides in paleosol 3 indicate that water tables were fluctuating seasonally.

The morphology and magnitude of development of paleosols 1 and 2 implies long periods of landscape stability that may be related to the creation of an unconformity due to valley incision at the end of Ogallala Formation aggradation. The presence of pedogenic carbonate in this pedocomplex suggests that relatively arid climatic conditions prevailed during these periods of soil formation. This inference is supported by $\delta^{13}C$ data that indicate a general increase in the proportion of $C_4$ biomass, which have a competitive advantage under conditions of increased aridity and temperature.

Discrete intervals in the isotopic record from paleosols 1 and 2 suggest that these soils experienced multiple climatic episodes during their formation; hence, they are polygenetic. In isotopic interval A, $\delta^{13}C$ values decrease upward whereas $\delta^{18}O$ values increase. These trends suggest climatic cooling with either enhanced aridity or perhaps a decrease in the proportion of isotopically light winter precipitation at the onset of paleosol 2 development. In interval B the opposite trends are evident where $\delta^{13}C$ values increase upward but $\delta^{18}O$ values decrease. These trends most likely indicate climatic warming with a concomitant decrease in aridity or an increase in the proportion of isotopically light winter precipitation. Isotopic trends in intervals C and E are similar where $\delta^{13}C_{org}$ values and $\delta^{18}O$ values increase upward but $\delta^{13}C_{carb}$ values decrease. The decoupling of $\delta^{13}C_{org}$ and $\delta^{13}C_{carb}$ may be due to organic matter decomposition, which results in enrichment of $\delta^{13}C_{org}$ with respect to the original biomass (Wynn, 2007). If correct, then the trends in $\delta^{13}C_{carb}$ and $\delta^{18}O$ from these intervals suggest climatic cooling together with increased aridity. In interval D, the opposite trends to C and E are observable with both $\delta^{13}C_{org}$ values and $\delta^{18}O$ values declining upward but $\delta^{13}C_{carb}$ values increasing. In this case, the decoupling of $\delta^{13}C_{org}$ and $\delta^{13}C_{carb}$ may be due to increased aridity, which can increase $\delta^{13}C_{carb}$ values without a concomitant increase in the relative abundance of $C_4$ biomass (Fox et al., 2012). If correct, then climatic conditions during interval D were likely characterized by cooler but drier conditions. In interval F, $\delta^{13}C$ values initially decrease before increasing at the top of paleosol 1 whereas $\delta^{18}O$ values remain relatively constant. These trends may indicate initial climatic cooling followed by warming during interval F with an evaporative balance that remained relatively constant.

4.5.2. Chronology

The Paleocene concordia age of 64.2±3.9 Ma obtained from zircons preserved in paleosol 2 (Fig. 4.6) may represent the time that this paleosol was exposed at the surface. If correct, then the part of the High Plains succession investigated in this study is equivalent

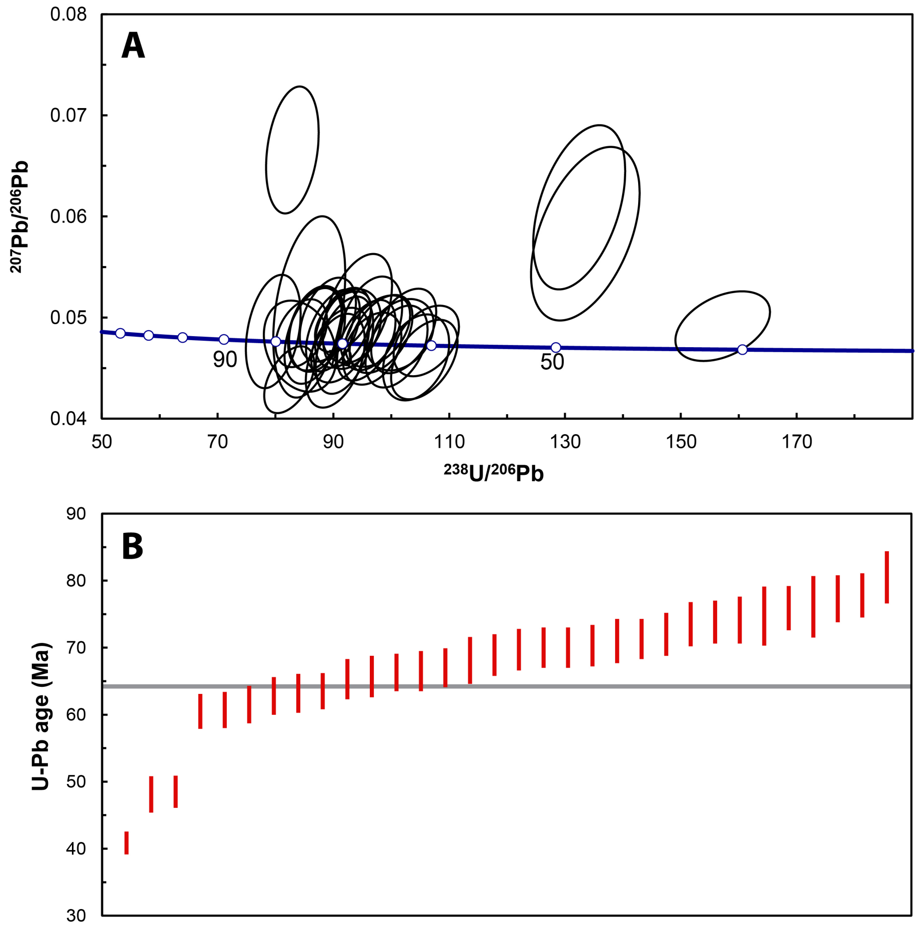


**Figure 4.6**. A) Concordia age plot from paleosol zircons. Data point ellipses are 2σ. B) U-Pb age diagram. Gray line shows weighted mean U-Pb age (64.2±3.9 Ma). Red columns represent single analyses.

in age to the fluvial strata of the Arapahoe and Denver Formations in the Denver Basin, Colorado (the D1 sequence of Raynolds, 2002) and previously has been unrecognized in Kansas. The Arapahoe and Denver Formations represent the first phase of synorogenic sedimentation that spanned the Cretaceous-Tertiary boundary and extended into the early Paleocene. Several radiometric dates have been obtained from ash beds preserved in these units that range between 65.7±0.4 and 63.6±3.9 Ma (Obradovich, 2002).

This association is improbable, however, for the following reasons: 1) the units in the High Plains succession are unconsolidated sands whereas correlative units in the Denver Basin are lithified sandstones and conglomerates (cf., Raynolds, 2002); 2) paleosols formed at the top of the D1 sequence are morphologically dissimilar to paleosols described in this study (cf. Farnham and Kraus, 2002); 3) previous studies in Kansas have noted that the Ogallala Formation rests unconformably on Cretaceous or older bedrock (e.g., Frye at al., 1956; Merriam, 1963); 4) the presence of > 50% $C_4$ biomass in paleosols 1–3 precludes a Paleocene age for these units (cf., Fox an Koch, 2003).

The zircons analyzed in this study are therefore interpreted as detrital populations that were eroded and subsequently transported by streams discharging from the Rocky Mountain front. The presence of detrital grains is supported by the range of concordia ages reported, which spans over 40 Ma. It is highly improbable that paleosol 2 was exposed at the surface for this length of time and therefore the range of concordia ages indicates the presence of detrital zircons in the analyzed population.

Although the zircons dated were euhedral and prismatic in shape, and showed no evidence of mechanical abrasion, the size of grains (~100–200 μm) may be too large to accurately represent distal air-fall tephra. Perkins and Nash (2002) compiled a synthesis of Yellowstone hotspot ash-fall compositions from Neogene sedimentary basins that indicates a range of 30–100 μm for the mean grain size of hotspot tuffs in the Great Plains. Procedural modifications are therefore proposed regarding the type and size of zircon grains analyzed in future research. Future processing of zircons will focus on grains that are <50 μm in length with a 6:1 aspect ratio. This type of grain most likely represents distal air-fall from events that did not produce widespread, thick ash beds. This processing methodology will also utilize an ultrasonic clay separator that is designed to minimize the loss of zircons through flocculation during settling of diluted slurries.

Future geochronological work will also focus on utilizing $^{26}Al$ and $^{10}Be$ nuclides produced in quartz to date periods of soil burial. These nuclides are commonly used in exposure-dating studies, but this method has recently been modified to date the burial ages of paleosols (e.g., Balco and Rovey, 2008) and has been successfully used to date early-Pleistocene glacial till sequences (e.g., Balco and Rovey, 2010).

**4.6. Summary and conclusions**

This study investigates the lithostratigraphy and paleoenvironments of the Ogallala Formation from a 50 m-deep core collected from Haskell County, southwestern Kansas. The fluvial deposits of the Ogallala Formation consist of vertically stacked, upward-fining sequences that range in texture from coarse gravel to fine sand. Three calcic paleosols occur in these fluvial sediments. A new approach was utilized to date volcanogenic zircons from primary ash-fall tephra preserved in paleosols. U-Pb dating of 32 zircon grains via LA-ICP-MS yielded a youngest population of five grains with a concordia age of 64.2±3.9 Ma from paleosol 2. This age indicates that the paleosols and sediments investigated in this study are equivalent in age to the fluvial strata of the Arapahoe and Denver Formations in the Denver Basin, Colorado and previously have been unrecognized in Kansas. It is concluded, however, that this association is improbable because of 1) differences in sediment consolidation and lithification (cf., Raynolds et al., 2002), 2) differences in paleosol morphology and maturity (cf. Farnham and Kraus, 2002), 3) the unconformable relationship between the Neogene Ogallala Formation and Cretaceous or older bedrock noted in previous studies (e.g., Merriam, 1963), and 4) the presence of > 50% $C_4$ biomass in paleosols that precludes a Paleocene age for these units (cf., Fox and Koch, 2003). The zircon grains analyzed, therefore, most likely represent detrital populations.

Despite problems with developing a numerical chronology, this study provides important stratigraphic and paleoenvironmental data from the High Plains succession. $\delta^{13}C$ data from paleosols indicate a shift to greater contributions of $C_4$ vegetation, suggestive of climate warming during soil-forming periods. Based on the > 50% contributions to SOM from $C_4$ vegetation, together with a shift from fluvial to eolian sediments, the upper pedocomplex is interpreted as representing the abandoned High Plains surface after the onset of incision in the Great Plains, which is estimated to have occurred between ca. 4–6 Ma (e.g., Chapin, 2008). Discrete intervals in the isotopic record suggest that the uppermost paleosols are polygenetic and experienced multiple climatic episodes during their formation. The isotopic intervals suggest distinct periods of 1) climatic cooling with either enhanced aridity or a greater degree of summer precipitation (intervals A, C, D and E), 2) climatic warming with a concomitant decrease in aridity or increase in the proportion of winter precipitation (interval B), and 3) a period of climatic cooling and subsequent warming but with an evaporative balance that remained relatively constant (interval F).

# CHAPTER 5

# SUMMARY AND CONCLUSIONS

The overarching goal of this dissertation research was to investigate patterns and forcing mechanisms of Plio-Pleistocene landscape evolution in the Cimarron River valley. The main conclusions relating to each of the four specific research objectives are presented below.

## 5.1. Objective 1

The first objective was to determine the characteristics and stratigraphic relationships of alluvial and eolian deposits, together with associated buried soils, in the Cimarron River valley. The oldest alluvial deposits in the study area comprise the Ogallala Formation. These deposits are over 30 m thick and consist of vertically stacked, upward-fining sequences that range in texture from coarse gravel to fine sand. Three well-expressed paleosols are developed in the fluvial sediments of the Ogallala Formation. Paleosols 1 and 2 have ~1–4 m thick Btk horizons with sandy clay loam textures and well-expressed angular blocky structure. Paleosol 3 has well-expressed Btkss-Btss horizonation with soil textures ranging from silty clay loam to clay.

Pleistocene alluvial fills stored in the Cimarron River valley are inset into the Ogallala Formation. Valley fills beneath two terraces (T-1 and T-2) were investigated. The highest and oldest terrace (T-2) stands ~24 m above the modern river channel. The T-2 fill is over 20 m thick and consists primarily of vertically stacked channel-fill sequences that fine upward and range in texture from fine gravel to loam. The youngest terrace (T-1) stands ~ 9 m above the modern river channel. The T-1 fill mostly consists of coarse-grained alluvium that ranges in texture from loam to sand. Three soils were documented in the T-2 fill and five soils in the T-1 fill. Of particular interest was the presence of two cumulic soils developed in the valley fills. The cumulic soil developed in the T-2 fill (soil $3_{T2}$) has a ~1–2 m thick Ak-Bk profile and dates to ca. 48–28 ka. This soil represents the alluvial stratigraphic equivalent of the Gilman Canyon Formation pedocomplex. The cumulic soil developed in the T-1 fill (soil $5_{T1}$) has a 1.1 m thick Ak-Btk profile and dates to ca. 13–12.5 ka. Cumulic soils of a similar age have been identified in stream valleys throughout the Central Plains (e.g., Mandel, 2008).

The Ogallala Formation is mantled by ~20 m of eolian sediments. Two cores taken on the High Plains surface both contain eight eolian units and intercalated soils. Most of the eolian sediments have a sandy loam texture. Buried soils developed in the eolian deposits typically have >1 m thick Btk or Bt horizons, and stratigraphic equivalents of the Sangamon Soil and the Gilman Canyon Formation pedocomplex occur in both cores.

5.2. Objective 2

The second objective of this dissertation was to establish a numerical chronology for the deposition of Plio-Pleistocene sediments and the formation of buried soils. In the study area, the uppermost paleosols developed in the Ogallala Formation are interpreted to represent the abandoned High Plains surface after the onset of regional incision between ca. 4–6 Ma (cf. Chapin, 2008). $\delta^{13}C_{org}$ values from this pedocomplex indicate up to 59%

contributions to SOM from $C_4$ vegetation. Given that ecosystems with >50% $C_4$ biomass only appeared in the Great Plains during the Pliocene (Fox and Koch, 2003), it is concluded that the portion of the Ogallala Formation investigated in this study is at least Pliocene in age. In order to better constrain the end of Ogallala Formation aggradation, a new technique to date volcanogenic zircons from primary ash-fall tephra preserved in paleosols was utilized. A concordia age of 64.2±3.9 Ma was obtained from zircons preserved in paleosol 2. This Paleocene age, however, appears to represent detrital zircon populations that were eroded and subsequently transported by the ancestral Cimarron River.

The eight eolian units and intercalated soils mantling the Ogallala Formation span the period from late MIS 5 to present. Chronological control indicates that deposition of ~10 m of eolian sediments occurred episodically during late MIS 5 (ca. 84–70 ka) and that these sediments and associated soils are coeval with the Loveland-Sangamon complex. Eolian sediments representing the stratigraphic equivalent of the Gilman Canyon Formation have ages ranging from ca. 53–44 ka. Although this age range is older than previously published ages for the Gilman Canyon Formation in Kansas (e.g., Johnson et al., 2007), the stratigraphically equivalent Roxana Silt has yielded ages as old as ca. 60 ka in the Mississippi River valley (e.g., Forman and Pierson, 2002). A soil representing the Gilman Canyon Formation pedocomplex yielded an age of ca. 35 ka, which is consistent with other published ages from the region. This soil was buried by Peoria Loess, which began to accumulate in the study area at ca. 29 ka.

Evidence of late-Pleistocene alluviation is present in the form of two distinct valley fills (T-1 and T-2 fills). Chronological control indicates that the T-2 fill was aggrading during late MIS 5 through MIS 4 (ca. 77–58 ka) and that at least 12 m of alluvium was deposited over this period. The cumulic soil (soil $3_{T2}$) developed in the T-2 fill dates to between ca. 48 and 28 ka and indicates slow rates of sedimentation during this interval. A ca. 53 ka age from sediments underlying the T-1 terrace surface at a depth of 17 m is consistent with ages from the T-2 fill, indicating the presence of an unconformity. The Cimarron River deposited the bulk of the T-1 fill between ca. 28 and 13 ka. Around 13 ka, sedimentation rates declined, resulting in the formation of a cumulic soil (soil $5_{T1}$) in the T-1 fill.

5.3. Objective 3

The third objective was to develop a paleoenvironmental proxy record from Plio-Pleistocene deposits by utilizing stable carbon ($\delta^{13}C$) and oxygen ($\delta^{18}O$) isotopes. $\delta^{13}C_{org}$ data from the Ogallala Formation indicate a predominant $C_3$ signal, suggesting that early Pliocene climates were generally cooler than modern conditions. $\delta^{13}C_{org}$ data from paleosols developed in the Ogallala Formation, however, indicate a shift to greater contributions of $C_4$ vegetation, and therefore climatic warming, during periods of soil formation. Discrete intervals in the $\delta^{13}C$ and $\delta^{18}O$ isotopic record from the upper two paleosols, however, indicate that these paleosols are polygenetic and likely experienced multiple climatic shifts during their formation.

Paleoenvironmental reconstructions for the late Pleistocene were developed from alluvial fills in the Cimarron River valley and eolian deposits on the High Plains surface. $\delta^{13}C$ and $\delta^{18}O$ data from eolian deposits indicate climatic variability during late MIS 5 (ca. 84–70 ka). In particular, isotopic analyses suggest distinct shifts to both warmer and cooler and temperatures during this time period. Relationships between $\delta^{13}C$ and $\delta^{18}O$ values suggest that periods of climatic warming probably were relatively humid with greater amounts of isotopically light winter precipitation. In contrast, periods of climatic cooling during late MIS 5 probably were relatively dry, resulting in greater evaporative enrichment of soil water.

Paleoenvironmental proxy data from eolian deposits indicate cool conditions during early MIS 3, with a subsequent increase in temperature and aridity. Similar results were obtained from alluvial deposits that indicate climatic warming and likely drying between ca. 48 and 28 ka followed by a shift to cooler and likely wetter conditions after ca. 28 ka. Another period of climatic warming was inferred between ca. 13.0 and 12.5 ka.

Overall, the inferred paleoclimatic changes during the late Pleistocene correlate well with other paleoclimatic reconstructions from the Great Plains. Attempts were made to correlate pedogenic $\delta^{18}O$ data with global $\delta^{18}O$ benthic records, marine $\delta^{18}O$ records from the Gulf of Mexico, and Greenland ice core $\delta^{18}O$ records (see Appendix B). No clear correlations were apparent, however, suggesting that the pedogenic $\delta^{18}O$ data provide a signal of Pleistocene paleoenvironmental change that is driven by regional and local forcing mechanisms.

5.4. Objective 4

The final objective of this dissertation was to investigate the relationship between landscape evolution and Plio-Pleistocene climate change on the High Plains of western Kansas. Particular attention was given to the geomorphic history of the Cimarron River and the alluvial response to environmental forcing. During the Miocene and early Pliocene, the ancestral Cimarron River was a high-energy braided stream that transported vast quantities of sediment from the Rocky Mountains (e.g., Seni, 1980). These sediments were likely deposited in a broad paleovalley and represent the alluvial sediments of the Ogallala Formation. The aggradation of the Ogallala Formation is believed to have ceased during the early Pliocene (~ 5 Ma) and was concomitant with regional incision of fluvial systems across the Great Plains (e.g., Chapin, 2008).

In the study area, no evidence of alluvial deposition during the late Pliocene and early Pleistocene was found. It is unlikely that the Cimarron River was continually incising during this period and it is concluded that early-Pleistocene alluvial fills were eroded and reworked by lateral stream migration during the mid to late Pleistocene.

During late MIS 5 through MIS 4, the Cimarron River was an aggrading high-energy braided stream. Paleoenvironmental data from the T-2 fill suggest a cool and likely wet environment at this time (ca. 77–58 ka). Paleoenvironmental data from eolian sediments, however, indicate that this period (ca. 84–54 ka) was characterized by multiple climatic shifts that resulted in episodic eolian deposition on the High Plains surface.

During MIS 3, the paleoenvironmental record from both alluvial (ca. 52–28 ka) and eolian (ca. 52–29 ka) deposits indicates a shift to warmer and drier climatic conditions. This shift resulted in slower rates of alluviation and the formation of a cumulic soil (soil $3_{T2}$) in the T-2 fill. Rates of eolian deposition on the uplands also slowed at this time, resulting in the formation a soil that represents the Gilman Canyon Formation pedocomplex.

Chronostratigraphic data indicate that the Cimarron River incised over 25 m after the abandonment of the T-2 surface and before aggradation of the T-1 fill that began ca. 28 ka. This significant amount of incision is unlikely to have been caused by climatic forcing alone and other forcing mechanisms were considered. In the Cimarron River valley, evidence exists for local base level control in the Meade and Ashland basins located ~50 km downstream of the study area. Local base level lowering, produced by the integration of drainages from formerly isolated dissolution-subsidence areas during the late Pleistocene (e.g., Frye and Schoff, 1942; Frye, 1950), likely resulted in significant headward valley deepening in the Cimarron River valley and caused the abandonment of the T-2 surface sometime between ca. 48–28 ka.

The Cimarron River deposited the bulk of the T-1 fill between ca. 28 and 13 ka. During this period, the $\delta^{13}C$ record and regional paleoenvironmental reconstructions suggest that climates were likely cooler with greater effective moisture than present. Around 13 ka, sedimentation rates declined, resulting in the formation of a cumulic soil (soil $5_{T1}$) in the T-1 fill. The $\delta^{13}C$ record suggests that climatic conditions during this time were warmer and perhaps drier in the study area. Effective moisture, however, must have been high enough to promote continued alluviation, albeit at a slower pace that favored cumulic soil formation.

Overall, this dissertation research provides important insights into Plio-Pleistocene landscape evolution in the Cimarron River valley of southwestern Kansas. In particular, the record of paleoenvironmental change and subsequent landscape response during MIS 5 and MIS 3 is an important contribution because so little is known about these periods in the Great Plains. This study highlights the significance of late-Pleistocene alluvial and eolian deposits as paleoenvironmental archives, and future investigation of these deposits will continue to enhance our understanding of paleoclimatic change and landscape evolution in the Great Plains.

## REFERENCES CITED


Aitken, M.J., 1998. An introduction to optical dating: the dating of Quaternary sediments by the use of photon-stimulated luminescence. Oxford University Press, Oxford. 278 pp.

Aleinikoff, J.N., Muhs, D.R., Bettis, E.A., Johnson, W.C., Fanning, C.M., Benton, R., 2008. Isotopic evidence for the diversity of late Quaternary loess in Nebraska: Glaciogenic and nonglaciogenic sources. Geological Society of America Bulletin 120, 1362–1377.

Antevs, E., 1935. The Occurrence of Flints and Extinct Animals in Pluvial Deposits near Clovis, New Mexico, Part II: Age of the Clovis Lake Clays. Proceedings of the Academy of Natural Sciences of Philadelphia, 304–312.

Baker, R.G., Bettis III, E.A., Mandel, R.D., Dorale, J.A., Fredlund, G.G., 2009. Mid-Wisconsinan environments on the eastern Great Plains. Quaternary Science Reviews 28(9), 873–889.

Balco, G., Rovey, C.W., 2008. An isochron method for cosmogenic-nuclide dating of buried soils and sediments. American Journal of Science, 308, 1083–1114.

Balco, G., Rovey, C.W., 2010. Absolute chronology for major Pleistocene advances of the Laurentide Ice Sheet. Geology, 38 (9), 795–798.

Bartlein, P.J., Anderson, K.H., Anderson, P.M., Edwards, M.E., Mock, C.J., Thompson, R.S., Webb. R.S., Webb, T., Whitlock, C., 1998. Paleoclimate simulations for North America over the past 21,000 years features of the simulated climate and comparisons with paleoenvironmental data. Quaternary Science Reviews 17, 549–585.

Bement, L.C., Carter, B.J., Varney, R.A., Cummings, L.S., Sudbury, J.B., 2007. Paleo-environmental reconstruction and bio-stratigraphy, Oklahoma Panhandle, USA. Quaternary International 169, 39–50.

Bettis III, E.A., Mandel, R.D., 2002. The effects of temporal and spatial patterns of Holocene erosion and alluviation on the archaeological record of the Central and Eastern Great Plains, U.S.A. Geoarchaeology: An International Journal 17, 141–154.

Bettis, E.A., Muhs, D.R., Roberts, H.M., Wintle, A.G., 2003. Last Glacial loess in the conterminous USA. Quaternary Science Reviews 22, 1907–1946.

Birkeland, P.W., 1999. Soils and Geomorphology, (3rd Edition). Oxford University Press, Oxford. 430 pp.

Blum, M., Pecha, M., 2014. Mid-Cretaceous to Paleocene North American drainage reorganization from detrital zircons. Geology 42, 607–610.

Blum, M.D., Törnqvist, T.E., 2000. Fluvial responses to climate and sea-level change: a review and look forward. Sedimentology 47, 2–48.

Boellstorff, J., 1978. Chronology of some late Cenozoic deposits from the central United States and the Ice Ages: Transactions of the Nebraska Academy of Science 6, 35–49.

Borchert, J.R., 1950. The climate of the central North American grassland. Annals of the Association of American Geographer 40, 1–30.

Boutton, T.W., 1991. Stable carbon isotope ratios of natural materials: II. Atmospheric, terrestrial, marine, and freshwater environments. Carbon isotope techniques 1, 173.

Boutton, T.W., 1996. Stable carbon isotope ratios of soil organic matter and their use as indicators of vegetation and climate change. In: Boutton, T.W., Yamasaki, S.I. (Eds.), Mass Spectrometry of Soils. Marcel Dekker, New York, pp. 47–82.

Bowring, S.A., Erwin, D.H., Jin, Y.G., Martin, M.W., Davidek, K., Wang, W.,1998. U/Pb zircon geochronology and tempo of the end-Permian mass extinction. Science 280(5366), 1039–1045.
Bull, W.B., 1991. Geomorphic response to climatic change. Oxford University Press, Oxford. 326 pp.
Catt, J.A., 1998. Report from working group on definitions used in paleopedology. Quaternary International 51, p 84.
Cerling, T.E., Quade, J., 1993. Stable carbon and oxygen isotopes in soil carbonate. In: Swart, P.K., Lohman, K.C., McKenzie, J., Savin, S., (Eds.), Climate change in continental isotopic records. Geophysical Monograph, 78. American Geophysical Union, Washington, pp. 217–231.
Cerling, T.E., Wang, Y., 1996. Stable carbon and oxygen isotopes in soil CO2 and soil carbonate: Theory, practice, and application to some prarie soils of upper Midwestern North America. In: Boutton, T.W., and Yamasaki, S., (Eds.), Mass spectrometry of soils. Marcel Dekker, New York, pp. 113–131.
Cerling, T.E., Quade, J., Wang, Y., Bowman, J.R., 1989. Carbon isotopes in soils and paleosols as ecology and paleoecology indicators. Nature 341, 138–139.
Chapin C.E., 2008. Interplay of oceanographic and paleoclimate events with tectonism during middle to late Miocene sedimentation across the southwestern USA. Geosphere 4, 976–991.
Cooperative Holocene Mapping Project (COHMAP), 1988. Climatic changes of the last 18,000 years: observations and model simulations. Science 24, 1043–1052.
Cordova, C.E., Johnson, W.C., Mandel, R.D., Palmer, M.W., 2011. Late Quaternary environmental change inferred from phytoliths and other soil-related proxies: case studies from the central and southern Great Plains, USA. Catena 85(2), 87–108.
Daniels, J.M., Knox, J.C., 2005. Alluvial stratigraphic evidence for channel incision during the Mediaeval Warm Period on the central Great Plains, USA. The Holocene 15, 736–747.
Dansgaard, W., et al., 1993. Evidence for general instability of past climate from a 250-kyr ice-core record. Nature 364(6434), 218–220.
Dickinson, W.R., Gehrels, G.E., 2009. Use of U–Pb ages of detrital zircons to infer maximum depositional ages of strata: a test against a Colorado Plateau Mesozoic database. Earth and Planetary Science Letters 288(1), 115–125.
Diffendal, R.F., 1982. Regional implications of the geology of the Ogallala Group (upper Tertiary) of southwestern Morrill County, Nebraska, and adjacent areas. Geological Society of America Bulletin 93, 964–976.
Dorale, J.A., Edwards, L.A., Ito, E., González, L.A., 1998. Climate and vegetation history of the mid continent from 75 to 25 ka: A speleothem record from Crevice Cave, Missouri, USA. Science 282, 1871–1874.
Eaton, G.P., 2008. Epeirogeny in the southern Rocky Mountains region: Evidence and origin. Geosphere 4, 764–784.
Farnham, T.M., Kraus, M.J., 2002. The stratigraphic and climatic significance of Paleogene alluvial paleosols in synorogenic strata of the Denver Basin, Colorado. Rocky Mountain Geology 37(2), 201–213.

Feng, Z.-D., Johnson, W.C., Lu, Y.-C., Ward III, P.A., 1994b. Climatic signals from loess-soil sequences in the Central Great Plains, USA. Palaeogeography, Palaeoclimatology, Palaeoecology 110, 345–358.
Fenneman, N.M.,1931. Physiography of Western United States. McGraw-Hill, New York. 534 pp.
Follmer, L.R., 1978. The Sangamon soil in its type area—A review. In: Mahaney, W.C. (Ed.), Quaternary Soils. Toronto, York University Press, 125–165.
Forman, S.L., Pierson, J., 2002. Late Pleistocene luminescence chronology of loess deposition in the Missouri and Mississippi river valleys, United States. Palaeogeography, Palaeoclimatology, Palaeoecology 186, 25–46
Forman, S.L., Oglesby, R., Markgraf, V., Stafford, T., 1995. Paleoclimatic significance of late Quaternary eolian deposition on the Piedmont and High Plains, central United States. Global and Planetary Change 11, 35–55.
Fox, D.L., Koch, P.L., 2003. Tertiary history of $C_4$ biomass in the Great Plains, USA. Geology 31(9), 809–812.
Fox, D.L., Honey, J.G., Martin, R.A., Peláez-Campomanes, P., 2012. Pedogenic carbonate stable isotope record of environmental change during the Neogene in the southern Great Plains, southwest Kansas, USA: Oxygen isotopes and paleoclimate during the evolution of C4-dominated grasslands. Geological Society of America Bulletin 124, 444–462.
Fredlund, G.G., 1995. Late Quaternary pollen record from Cheyenne Bottoms, Kansas. Quaternary Research 43, 67–79.
Fredlund, G.G., Jaumann, P.J., 1987. Late Quaternary palynological and paleobotanical records from the central Great Plains. In: Johnson, W.C. (Ed.), Quaternary Environments of Kansas, Kansas Geological Survey, Lawrence, pp. 167–178.
Fredlund, G.G., Tieszen, L.L., 1997. Phytolith and carbon isotope evidence for late Quaternary vegetation and climate change in the southern Black Hills, South Dakota. Quaternary Research 47, 206–217.
Frye, J.C., 1950. Origin of Kansas Great Plains depressions. Kansas Geological Survey Bulletin 86, Kansas Geological Survey, Lawrence.
Frye, J.C., Hibbard, C.W., 1941. Pliocene and Pleistocene stratigraphy and paleontology of the Meade basin, southwestern Kansas. Kansas Geological Survey Bulletin 38, Kansas Geological Survey, Lawrence.
Frye, J.C., Leonard, A.B., 1952. Pleistocene Geology of Kansas. Kansas Geological Survey Bulletin 99, Kansas Geological Survey, Lawrence, 230 pp.
Frye, J.C., Schoff, S.L., 1942. Deep-seated solution in the Meade Basin and vicinity, Kansas and Oklahoma. Transactions, American Geophysical Union 23, 35–39.
Frye, J.C., Swineford, A., Leonard, A.B., 1956. Stratigraphy of the Ogallala Formation (Neogene) of northern Kansas. Kansas Geological Survey Bulletin 118, Kansas Geological Survey, Lawrence, 92 pp.
Galbraith, R.F., Roberts, R.G., 2012. Statistical aspects of equivalent dose and error calculations and display in OSL dating: An overview and some recommendations. Quaternary Geochronology 11, 1–27.
Gardner, L.R., Diffendal, R.F., Williams, D.F., 1992. Stable isotope composition of calcareous paleosols and ground-water cements from the Ogallala Group (Neogene), western Nebraska. Rocky Mountain Geology 29(2), 97–109.

Geyh, M.A., Roeschmann, G., Wijmstra, T.A., Middeldorp, A.A., 1983. The unreliability of $^{14}C$ dates obtained from buried sandy Podzols. Radiocarbon 25, 409–416.
Guerin, G., Mercier, N., Adamiec, G., 2011. Dose-rate conversion factors: update. Ancient TL 29, 5–8.
Grimley, D.A., Follmer, L.R., Hughes, R.E., Solheid, P.A., 2003. Modern, Sangamon and Yarmouth soil development in loess of unglaciated southwestern Illinois. Quaternary Science Reviews 22, 225–244.
Gustavson, T.C., 1986. Geomorphic development of the Canadian River valley, Texas Panhandle: An example of regional salt dissolution and subsidence. Geological Society of America Bulletin 97, 459–472.
Gustavson, T.C., Winkler, D.A., 1988. Depositional facies of the Miocene-Pliocene Ogallala Formation, northwestern Texas and eastern New Mexico. Geology 16, 203–206.
Gutentag, E.D., 1963. Studies of the Pleistocene and Pliocene deposits in southwestern Kansas. Transactions of the Kansas Academy of Science 66, 606–621.
Halfen, A.F., Hasiotis, S.T., 2010. Neoichnological study of the traces and burrowing behaviors of the western harvester ant Pogonomyrmex occidentalis (Insecta: Hymenoptera: Formicidae): paleopedogenic and paleoecological implications. Palaios 25, 703–720.
Hall, S.A., 1990. Channel trenching and climatic change in the southern US Great Plains. Geology 18, 342–345.
Harden, J.W., 1982. A quantitative index of soil development from field descriptions: examples from a chronosequence in central California. Geoderma 28, 1–28.
Harlow, R.H., 2013. Depositional and paleoclimatic evolution of the Cenozoic High Plains succession from core: Haskell Co., Kansas. Thesis, University of Kansas, Lawrence.
Haynes Jr, C.V., Agogino, G.A., 1966. Prehistoric springs and geochronology of the Clovis site, New Mexico. American Antiquity 31, 812–821.
High Plains Aquifer Atlas, 2014. Change in saturated thickness, predevelopment to average 2012-2014, Kansas High Plains Aquifer. Kansas Geological Survey, Lawrence (http://www.kgs.ku.edu/HighPlains/HPA_Atlas/Water%20Levels /index.html# accessed Dec 2014).
High Plains Regional Climate Center, 2014. Period of record monthly climate summary for Sublette, Kansas (147922). University of Nebraska, Lincoln (http://www.hprcc.unl.edu/cgi-bin/cli_perl_lib/cliMAIN.pl?ks7922 accessed Nov 2014).
Hill, H.W., Flower, B.P., Quinn, T.M., Hollander, D.J., Guilderson, T.P., 2006. Laurentide Ice Sheet meltwater and abrupt climate change during the last glaciation. Paleoceanography 21(1), PA1006.
Holliday, V.T., 1995. Stratigraphy and paleoenvironments of late Quaternary valley fills on the Southern High Plains. Geological Society of America Memoir 186.
Holliday, V.T., 2000. Folsom drought and episodic drying on the Southern High Plains from 10,900–10,200 $^{14}C$ B.P. Quaternary Research 53, 1–12.
Holliday, V.T., Haynes Jr., C.V., Hofman, J.L., Meltzer, D.J., 1994. Geoarchaeology and geochronology of the Miami (Clovis) site, Southern High Plains of Texas. Quaternary Research 41, 234–244.

Holliday, V.T., Hovorka, S.D., Gustavson, T.C.,1996. Lithostratigraphy and geochronology of fills in small playa basins on the Southern High Plains. Geological Society of America Bulletin 108, 953–965.

Holliday, V.T., Meltzer, D.J., Mandel, R.D., 2011. Stratigraphy of the Younger Dryas chronozone and paleoenvironmental implications: central and southern Great Plains. Quaternary International 242, 520–533.

Huntley, D.J., Godfrey-Smith, D.I., Thewalt, M.L.W., 1985. Optical dating of sediments. Nature 313, 105–107.

Hu, Z.Z., Huang, B., 2009. Interferential impact of ENSO and PDO on dry and wet conditions in the US Great Plains. Journal of Climate 22, 6047–6065.

Jacobs, P.M., Knox, J.C., 1994. Provenance and pedology of a long-term Pleistocene depositional sequence in Wisconsin's Driftless Area. Geoderma 22, 49–68.

Jacobs, K.C., Fritz, S.C., Swinehart, J.B., 2007. Lacustrine evidence for moisture changes in the Nebraska Sand Hills during Marine Isotope Stage 3. Quaternary Research 67, 246–254.

Johnson, W.C., Martin, C.W., 1987. Holocene alluvial-stratigraphic studies from Kansas and adjoining states of the East-Central Plains. In: Johnson, W.C. (Ed.), Quaternary Environments of Kansas, Guidebook Series 5. Kansas Geological Survey, Lawrence, pp. 109–122.

Johnson, W.C., Willey, K.L., 2000. Isotopic and rock magnetic expression of environmental change at the Pleistocene–Holocene transition in the Central Great Plains. Quaternary International 67, 89–106.

Johnson, W.C., May, D.W., Valastro, S., 1998. Temporal and environmental resolution of a buried loessal pedostratigraphic unit in Kansas and Nebraska. Quaternary International 51, 48–49.

Johnson, W.C., Willey, K.L., Mason, J.A., May, D.W., 2007. Stratigraphy and environmental reconstruction at the middle Wisconsinan Gilman Canyon formation type locality, Buzzard's Roost, southwestern Nebraska, USA. Quaternary Research 67, 474–486.

Knox, J.C., 1983. Responses of river systems to Holocene climates. In: Wright Jr., H.E. (Ed.), Late Quaternary Environments of the United States–the Holocene. University of Minnesota Press, Minneapolis, pp. 26–41.

Kraus, M.J., 1999. Paleosols in clastic sedimentary rocks: their geologic applications. Earth-Science Reviews 47(1), 41–70.

Krull, E.S., Skjemstad, J.O., 2003. $\delta^{13}C$ and $\delta^{15}N$ profiles in $^{14}C$-dated oxisol and vertisols as a function of soil chemistry and mineralogy. Geoderma 112, 1–29.

Küchler, A.W., 1964. Potential natural vegetation of the conterminous United States. American Geographical Society Special Publication 36, 39 pp.

Kutzbach, J.E., 1987. Model simulations of the climatic patterns during the deglaciation of North America. In: Ruddiman, W.F., Wright Jr., H.E. (Eds.), North America and Adjacent Oceans during the Last Deglaciation, The Geology of North America, Vol. K-3. Geological Society of America, Boulder, Colorado, pp. 425–426.

Langbein, W.B., Schumm, S.A., 1958. Yield of sediment in relation to mean annual precipitation. Transactions, American Geophysical Union 39, 1076–1084.

Leighton, M.M., Willman, H.B., 1950. Loess formations of the Mississippi Valley. The Journal of Geology 58, 599–623.

Ludvigson, G.A., Sawin, R.S., Franseen, E.K., Watney, W.L., West, R.R., Smith, J.J., 2009. A review of the stratigraphy of the Ogallala Formation and revision of Neogene ("Tertiary") nomenclature in Kansas. Current Research in Earth Science: Kansas Geological Survey Bulletin 256, 1–9.
Maat, P.W., Johnson, W.C., 1996. Thermolumescence and new $^{14}C$ age estimates for late Quaternary loesses in southwestern Nebraska. Geomorphology 17, 115–128.
Mandel, R.D., 1994. Holocene landscape evolution in the Pawnee River Basin, Southwestern Kansas. Bulletin 236. Kansas Geological Survey, Lawrence. 117 pp.
Mandel, R.D., 2008. Buried Paleoindian-age landscapes in stream valleys of the Central Plains, USA. Geomorphology 101, 342–361.
Mandel, R.D., Bettis III, E.A., 1995. Late Quaternary landscape evolution and stratigraphy in Eastern Nebraska. In: Flowerday, C.A. (Ed.), Geologic Field Trips in Nebraska and Adjacent Parts of Kansas and South Dakota. Conservation and Survey Division, Institute of Agriculture and Natural Resources, University of Nebraska-Lincoln, Guidebook 10, pp. 77–90
Mandel, R.D., Bettis III, E.A., 2001. Late Quaternary landscape evolution in the South Fork Big Nemaha River Valley, Southeastern Nebraska and Northeastern Kansas. Guidebook No. 11, Conservation and Survey Division, University of Nebraska, Lincoln, 58 pp.
Mandel, R.D., Hofman, J.L., Holen, S.R., Blackmar, J.M., 2004. Buried Paleo-Indian landscapes and sites on the High Plains of northwestern Kansas. In Nelson, E.P. (Ed.), Field Trips in the Southern Rocky Mountains, USA. Field Guide 5. The Geological Society of America, Boulder, Colorado, 69–88.
Markewich, H.W., Wysocki, D.A., Pavich, M.J., Rutledge, E.M., 2011. Age, genesis, and paleoclimatic interpretation of the Sangamon/Loveland complex in the Lower Mississippi Valley, USA. Geological Society of America Bulletin 123, 21–39.
Mason, J.A., Jacobs, P.M., Hanson, P.R., Miao, X.D., Goble, R.J., 2003. Sources and paleoclimatic significance of Holocene Bignell Loess, Central Great Plains, USA. Quaternary Research 60, 330–339.
Mason, J.A., Joeckel, R.M., Bettis III, E.A., 2007. Middle to Late Pleistocene loess record in eastern Nebraska, USA, and implications for the unique nature of Oxygen Isotope Stage 2. Quaternary Science Reviews 26(5), 773–792.
Maupin, M.A., Barber, N.L., 2005. Estimated withdrawals from principal aquifers in the United States, 2000. U.S. Geological Survey Circular 1279, 46 pp.
Mayer, J.H., Burr, G.S., Holliday, V.T., 2008. Comparisons and interpretations of charcoal and organic matter radiocarbon ages from buried soils in north-central Colorado, USA. Radiocarbon 50, 331–346.
McCabe, G.J., Palecki, M.A., Betancourt, J.L., 2004. Pacific and Atlantic Ocean influences on multidecadal drought frequency in the United States. Proceedings of the National Academy of Sciences 101, 4136–4141.
McGuire, V.L., 2009. Water-level changes in the High Plains aquifer, predevelopment to 2007. U.S. Geological Survey Scientific Investigations Report 2009-5019, 9 pp.
McKay, E.D., 1986. Illinoian and older loesses and tills at the Maryville section. Quaternary records of southwestern Illinois and adjacent Missouri: Illinois State Geological Survey Guidebook 23, 21–30.

Merriam, D.F., 1963. The geologic history of Kansas. Kansas Geological Survey Bulletin 162, Kansas Geological Survey, Lawrence, 317 pp.
Merriam, D.F., Frye, J.C., 1954. Additional studies of the Cenozoic of western Kansas. Kansas Geological Survey Bulletin 109, pp. 49–64.
Mintz, J.S., Driese, S.G., Breecker, D.O., Ludvigson, G.A., 2011. Influence of changing hydrology on pedogenic calcite precipitation in Vertisols, Dance Bayou, Brazoria County, Texas, USA: implications for estimating paleoatmospheric $pCO_2$. Journal of Sedimentary Research 81(6), 394–400.
Muhs, D.R., Bettis III, E.A., 2003. Quaternary loess-paleosol sequences as examples of climate-driven sedimentary extremes. Geological Society of America Special Paper 370, 53–74.
Muhs, D.R., Aleinikoff, J.N., Stafford Jr., T.W., Kihl, R., Been, J., Mahan, S.A., Cowherd, S., 1999. Late Quaternary loess in northeastern Colorado: Part I–Age and paleoclimatic significance. Geological Society of America Bulletin 111, 1861–1875.
Muhs, D.R., Bettis, E A., Aleinikoff, J.N., McGeehin, J.P., Beann, J., Skipp, G., Benton, R., 2008. Origin and paleoclimatic significance of late Quaternary loess in Nebraska: Evidence from stratigraphy, chronology, sedimentology, and geochemistry. Geological Society of America Bulletin 120, 1378–1407.
Mullin, M.R.D., 2010. Stable isotope record of soil carbonates from the Eocene-Oligocene transition, Badlands National Park, South Dakota, USA. Dissertation, Ball State University, Muncie.
Murray, A.S., Wintle, A.G., 2000. Luminescence dating of quartz using an improved single-aliquot regenerative-dose protocol. Radiation Measurements 32, 57–73.
Nordt, L.C., Boutton, T.W., Hallmark, C.T., Waters, M.R., 1994. Late Quaternary vegetation and climate changes in central Texas based on the isotopic composition of organic carbon. Quaternary Research 41, 109–120.
Nordt, L.C., Boutton, T.W., Jacob, J.S., Mandel, R.D., 2002. $C_4$ plant productivity and climate-$CO_2$ variations in south-central Texas during the late quaternary. Quaternary Research 58, 182–188.
Obradovich, J.D., 2002. Geochronology of Laramide synorogenic strata in the Denver Basin, Colorado. Rocky Mountain Geology 37(2), 165–171.
Olson, C.G., Porter, D.A., 2002. Isotopic and geomorphic evidence for Holocene climate, southwestern Kansas. Quaternary International 87, 29–44.
Olson, C.G., Nettleton, W.D., Porter, D.A., Brasher, B.R., 1997. Middle Holocene aeolian activity on the High Plains of west-central Kansas. The Holocene 7 (3), 255–261.
Peel, M.C., Finlayson, B.L., McMahon, T.A., 2007. Updated world map of the Köppen-Geiger climate classification. Hydrology and earth system sciences discussions 4(2), 439–473.
Perkins, M.E., Nash, W.P., Brown, F.H., Fleck, R.J., 1995. Fallout tuffs of Trapper Creek, Idaho—a record of Miocene explosive volcanism in the Snake River Plain volcanic province. Geological Society of America Bulletin 107(12), 1484–1506.
Perkins M.E., Nash B.P., 2002. Explosive silicic volcanism of the Yellowstone hotspot: The ash fall tuff record. Geological Society of America Bulletin 114, 367–381.

Porter, D.A., 1997. Soil genesis and landscape evolution within the Cimarron Bend area, southwest Kansas. Dissertation, Department of Agronomy, Kansas State University, Manhattan. UMI Dissertation Services No. 9817174, Ann Arbor, MI.
Prescott, J. R., Hutton, J.T., 1994. Cosmic ray contributions to dose rates for luminescence and ESR dating. Radiation Measurements 23, 497–500.
Raynolds, R.G., 2002. Upper Cretaceous and Tertiary stratigraphy of the Denver basin, Colorado. Rocky Mountain Geology 37(2), 111–134.
Reed, E.C., Dreeszen, V. H., 1965. Revision of the classification of the Pleistocene deposits of Nebraska: Nebraska Geological Survey Bulletin 23, 65 p.
Reid, M.R., Coath, C.D., 2000. In situ U-Pb ages of zircons from the Bishop Tuff: No evidence for long crystal residence times. Geology 28(5), 443–446.
Rittenour, T. M., Goble, R.J., Blum, M.D., 2005. Development of an OSL chronology for Late Pleistocene channel belts in the lower Mississippi valley, USA. Quaternary Science Reviews 24, 2539–2554.
Rittenour, T.M., Blum, M.D., Goble, R.J., 2007. Fluvial evolution of the lower Mississippi River valley during the last 100-kyr glacial cycle: Response to glaciation and sea-level change. Geological Society of America Bulletin 119, 586–608.
Rittenour, T. M., 2008. Luminescence dating of fluvial deposits: applications to geomorphic, palaeoseismic and archaeological research. Boreas 37, 613–635.
Reimer, P.J., Bard, E., Bayliss, A., Beck, J.W., Blackwell, P.G., Bronk Ramsey, C., Buck, C.E., Cheng, H., Edwards, R.L., Friedrich, M., Grootes, P.M., Guilderson, T.P., Haflidason, H., Hajdas, I., Hatte, C., Heaton, T.J., Hogg, A.G., Hughen, K.A., Kaiser, K.F., Kromer, B., Manning, S.W., Niu, M., Reimer, R.W., Richards, D.A., Scott, E.M., Southon, J.R., Turney, C.S.M., van der Plicht, J., 2013. IntCal13 and MARINE13 radiocarbon age calibration curves 0-50000 years cal BP. Radiocarbon 55(4), 1869–1887.
Rodbell, D. T., Forman, S. L., Pierson, J., & Lynn, W. C. (1997). Stratigraphy and chronology of Mississippi Valley loess in western Tennessee. Geological Society of America Bulletin 109, 1134–1148.
Rousseau, D-D., Kukla, G., 1994. Late Pleistocene climate record in the Eustis loess section, Nebraska, based on land snail assemblages and magnetic susceptibility. Quaternary Research 42, 176–187.
Rutter, N.W., Velichko, A.A., Dlussky, K.G., Morozova, T.D., Little, E.C., Nechaev, V.P., Evans, M.E., 2006. New insights on the loess/paleosol Quaternary stratigraphy from key sections in the US Midwest. Catena 67(1), 15–34.
Ruhe, R.V., 1974. Sangamon paleosols and Quaternary environments in Midwestern U.S. In: Mahaney, W.C., (Ed.), Quaternary Environments: Proceedings of a symposium. Geographical Monographs. Toronto, York University Press, 153–167.
Schoeneberger, P.J., Wysocki, D.A., Benham, E.C., Broderson, W.D., 2012. Field book for describing and sampling soils, Version 3. Natural Resources Conservation Service, National Soil Survey Center, Lincoln, NE.
Schumm, S.A., 1977. The Fluvial System. John Wiley, New York.
Schumm, S.A., 1993. River response to base level change: implications for sequence stratigraphy. The Journal of Geology, 279–294.
Seni S.J., 1980. Sand-body geometry and depositional systems, Ogallala Formation, Texas. Texas Bureau of Economic Geology Report of Investigations 105, 36 pp.

Serefiddin, F., Schwarcz, H.P., Ford, D.C., Baldwin, S., 2004. Late Pleistocene paleoclimate in the Black Hills of South Dakota from isotope records in speleothems. Palaeogeography, Palaeoclimatology, Palaeoecology 203, 1–17.
Simpkins, W.W., 1995. Isotopic composition of precipitation in central Iowa. Journal of Hydrology 172, 185–207.
Sionneau, T., Bout-Roumazeilles, V., Meunier, G., Kissel, C., Flower, B.P., Bory, A., Tribovillard, N., 2013. Atmospheric re-organization during Marine Isotope Stage 3 over the North American continent: sedimentological and mineralogical evidence from the Gulf of Mexico. Quaternary Science Reviews 81, 62–73.
Smith, H.T.U., 1940. Geologic studies in southwestern Kansas. Kansas Geological Survey Bulletin 34, Kansas Geological Survey, Lawrence.
Smith, J.J., Ludvigson, G.A. Harlow, H. Platt, B., 2014. Ogallala-High Plains Aquifer Special Study Phase III: Lithologic Calibration of Practical Saturated Thickness in the Ogallala-High Plains Aquifer. Kansas Geological Survey, Open-file Report 2014-2, 9 pp.
Soil Survey Staff, 1982. Procedure for collecting soil samples and methods of analysis for soil survey. Soil Survey Investigations Report 1. USDA-SCS, Washington, DC.
Soil Survey Staff, 1993. Soil survey manual. Soil Conservation Service. U.S. Department of Agriculture Handbook 18.
Souders, V.L., Kuzila, M.S., 1990. A report on the geology and radiocarbon ages of four superimposed horizons at a site in the Republican River valley, Franklin County Nebraska. Proceedings of the Nebraska Academy of Sciences 65.
Swineford, A., Leonard, A.B., Frye, J.C., 1958. Petrology of the Pliocene pisolitic limestone in the Great Plains. Kansas Geological Survey Bulletin 130, Kansas Geological Survey, Lawrence.
Terri, J.A., Stowe, L.G., 1976. Climatic patterns and the distribution of C4 grasses in North America. Oecologia 23, 1–12.
Tripsanas, E.K., Bryant, W.R., Slowey, N.C., Bouma, A.H., Karageorgis, A.P., Berti, D., 2007. Sedimentological history of Bryant Canyon area, northwest Gulf of Mexico, during the last 135 kyr (Marine Isotope Stages 1–6): a proxy record of Mississippi River discharge. Palaeogeography, Palaeoclimatology, Palaeoecology, 246, 137–161.
Tucker, G.E., Arnold, L., Bras, R.L., Flores, H., Istanbulluoglu, E., Sólyom, P., 2006. Headwater channel dynamics in semiarid rangelands, Colorado high plains, USA. Geological Society of America Bulletin 118, 959–974.
VanLooy, J.A., Martin, C.W., 2005. Channel and vegetation change on the Cimarron River, southwestern Kansas, 1953–2001. Annals of the Association of american Geographers 95, 727–739.
Van Meerbeeck, C.J., Renssen, H., Roche, D.M., 2009. How did Marine Isotope Stage 3 and Last Glacial Maximum climates differ? Perspectives from equilibrium simulations. Climate of the Past 5, 33–51.
Voelker, A.H., 2002. Global distribution of centennial-scale records for Marine Isotope Stage (MIS) 3: a database. Quaternary Science Reviews 21(10), 1185–1212.
Wallinga, J., 2002. Optically stimulated luminescence dating of fluvial deposits: a review. Boreas 31(4), 303–322.

Wang, H., Lundstrom, C.C., Zhang, Z., Grimley, D.A., Balsam, W.L., 2009. A Mid–Late Quaternary loess–paleosol record in Simmons Farm in southern Illinois, USA. Quaternary Science Reviews 28(1), 93–106.
Wells, P.V., Stewart, J.D., 1987. Cordilleran-boreal taiga and fauna on the Central Great Plains of North America, 14,000–18,000 years ago. American Midland Naturalist 118, 94–106.
William, H.B., Frye, J.C., 1970. Pleistocene stratigraphy of Illinois. Illinois State Geological Survey Bulletin 94, 204 pp.
Wynn, J.G., 2007. Carbon isotope fractionation during decomposition of organic matter in soils and paleosols: implications for paleoecological interpretations of paleosols. Palaeogeography, Palaeoclimatology, Palaeoecology 251(3), 437–448.

# APPENDIX A

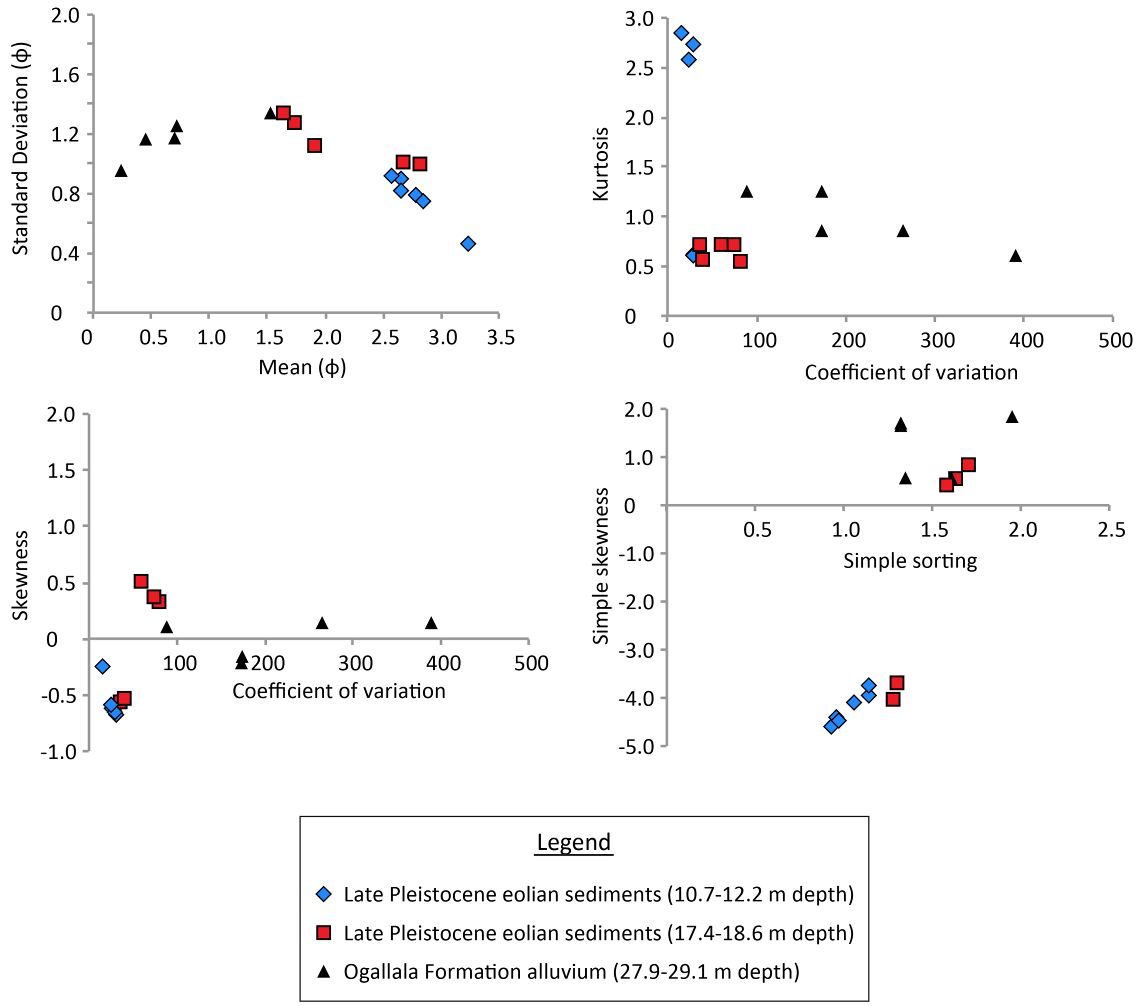


Ro-Tap sieve analyses of sediments from the CMC1 core.

APPENDIX B

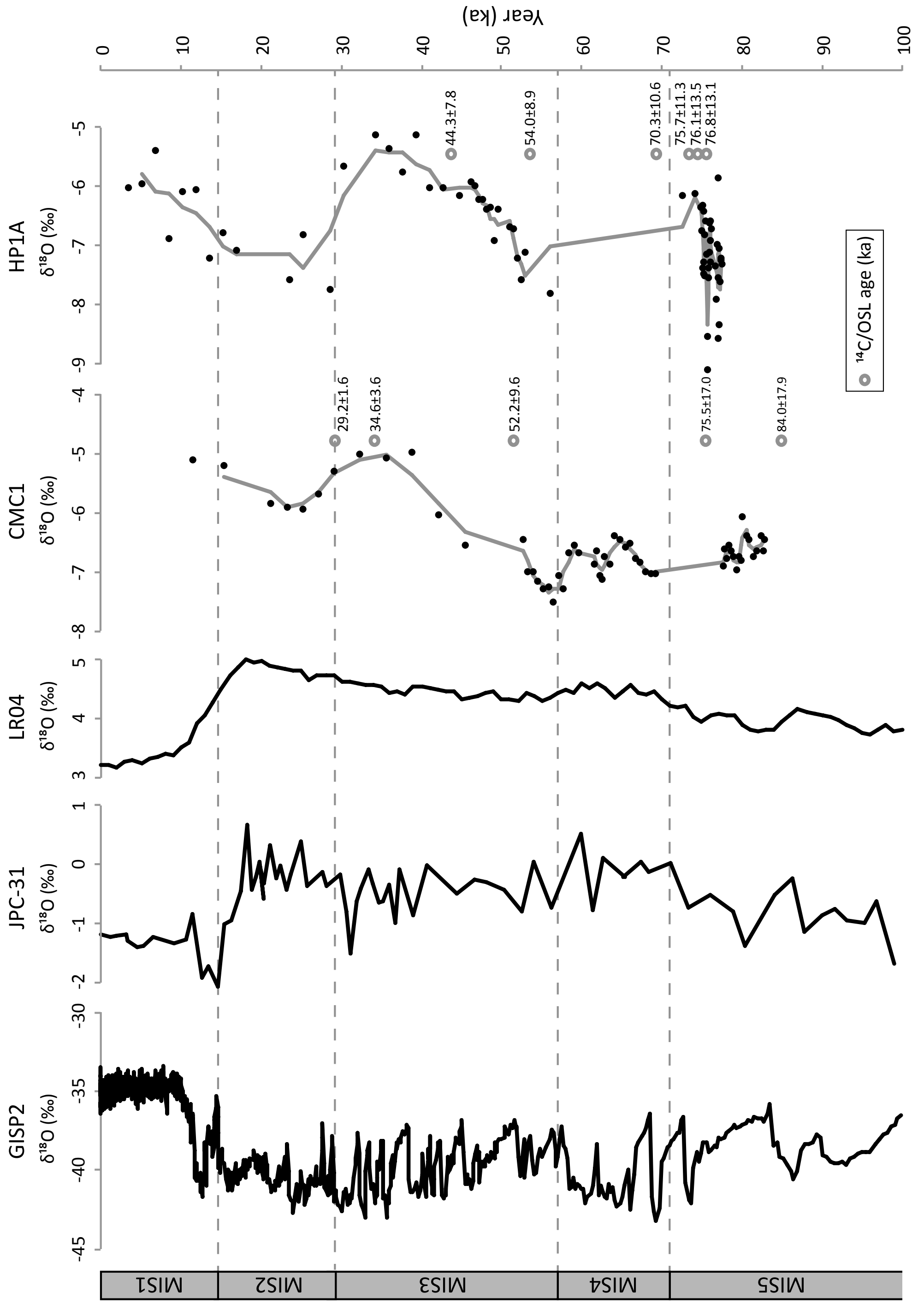


Comparative plots of $\delta^{18}O$ records: GISP2 – Greenland ice core (ftp://ftp.ncdc.noaa.gov/pub/data/paleo/icecore/greenland/summit/gisp2/isotopes/d18o1yr.txt); JPC-31 – Gulf of Mexico sediment core (Tripsanas et al., 2007); LR04 – stack of 57 globally distributed benthic $\delta^{18}O$ records (Lisiecki and Raymo, 2005); CMC1 and HP1A – Pedogenic carbonates from the High Plains of southwestern Kansas (this study; see chapter 3). Age-depth model for CMC1 and HP1A cores assumes linear sedimentation rate between dated intervals.

# APPENDIX C

# PALEOENVIRONMENTAL RECONSTRUCTIONS AND WATER RESOURCES MANAGEMENT IN WESTERN KANSAS

## 1. Introduction

This dissertation research was conducted under the auspices of an NSF Integrative Graduate Education and Research Traineeship (IGERT) Program at the University of Kansas. Part of this program requires an assessment of the policy implications of the dissertation findings. In order to fulfill this requirement, the following discussion highlights the utility of paleoenvironmental reconstructions for assessing drought variability and the implications for water resources management in western Kansas.

Environmentally and economically, drought is one of the most costly natural disasters in North America. Droughts impact both surface and groundwater resources and often result in reductions in water supply and crop failure, particularly in agriculturally sensitive areas such as the High Plains. This region is becoming increasingly vulnerable to drought due to a variety of factors, including the increased cultivation of marginal lands and the increased use of groundwater resources from the High Plains aquifer.

Drought conditions in the United States cost on average \$6–8 billion every year, but have ranged as high as \$39 billion during the three-year drought of 1987–1989 (Riebsame et al., 1991). In Kansas alone, the recent 2011 drought resulted in losses in excess of \$1.7 billion (Kansas Department of Agriculture, 2011). The earlier 1930s and 1950s droughts, however, remain the benchmarks for the 20$^{th}$ century in terms of duration, severity, and spatial extent. Various paleoclimatic proxy records, however, indicate that the major 20th-century droughts are not the two most intense or enduring droughts to hit Kansas. Paleoclimatic proxy records, therefore, allow one to assess a more complete range of drought variability by utilizing data that span longer periods of time than the instrumental record of the last century.

**2. Paleoenvironmental reconstructions**

Droughts of unusually long duration compared to those observed in the instrumental record are often termed "megadroughts" (e.g., Stahl et al., 2007). Many of the past megadroughts documented in Holocene paleoclimate records occur during two periods known as the Medieval Warm Period (MWP) and the Altithermal. The MWP lasted from ca. 900–1300 AD (1050–650 yr B.P.) and was characterized by significant climatic variability compared to the modern period (e.g., Seager et al., 2007). In North America, paleoclimate studies during this period record a series of severe droughts across the west (e.g., Cook et al., 2004), extending eastward into the central Great Plains (e.g., Woodhouse and Overpeck, 1998). In Kansas, megadroughts appear to be most prevalent from 850–1500 AD (Layzell, 2012). Dune records from the Central Plains show significant sand dune activation due to increasing aridity and reductions in vegetation cover between 950 and 1350 AD (e.g., Arbogast, 1996; Lepper and Scott, 2005; Hanson et al., 2010; Halfen et al., 2011). Support for the occurrence of protracted drought during the MWP can also be gleaned from the archaeological record, which highlights the destabilizing effects of past severe droughts on a variety of pre-historic populations, including the Anasazi, Fremont, and Mississippian peoples (e.g., Benson et al., 2007;

Cobb and Butler, 2002; Cook et al., 2007). Overall, multiple lines of evidence indicate that the arid conditions in North America during the MWP were remarkably more severe than the benchmark droughts for the $20^{th}$ century (i.e., the 1930s and 1950s droughts).

The Altithermal was a period of warm, dry conditions that prevailed across the western United States during the mid-Holocene. Paleoenvironmental reconstructions from the Great Plains during this period indicate an increase in $C_4$ vegetation, suggesting warmer conditions, with grassland ecosystems dominating by ca. 6 ka (e.g., Nordt et al., 1994; Cordova et al., 2010). Stratigraphic, geomorphic, and pedologic data indicate that the Altithermal was characterized by landscape instability in the Central and High Plains (e.g., Mandel, 1995). Studies have shown that sand dune activation and loess deposition (Bignell Loess) occurred throughout the High Plains from ca. 9–5 ka in response to arid conditions (e.g., Holiday, 1989; Olson, 1997; Forman et al., 2001; Mason et al., 2003, 2004). Also, extensive evaporation and reduction of playa lakes was documented on the Southern High Plains during this period (e.g., Holliday et al., 1996). Corroboration of protracted drought during the Altithermal from the archaeological record is less evident than during the MWP in part due to geomorphic processes that removed or deeply buried sites of this age (e.g., Mandel, 1995). Nevertheless, there is some evidence for adaptive strategies of hunter-gatherer populations to severe aridity during this period (e.g., Meltzer, 1999). Overall, multiple lines of evidence indicate that arid conditions in North America during the Altithermal were significantly more protracted than periods of aridity during the late Holocene.

This dissertation provides paleoenvironmental data that indicate prolonged periods of aridity during the late Pleistocene in southwestern Kansas. In particular, the alluvial record suggests that arid conditions prevailed between ca. 48–28 ka and ca. 13–12.5 ka in the Cimarron River valley. These findings are supported by regional paleoenvironmental reconstructions that indicate drying of wetlands and lakes (e.g., Fredlund, 1995; Jacobs et al., 2007) and increases in $C_4$ vegetation (e.g., Serefidden et al., 2004; Cordova et al., 2010) during these time periods. Although late-Pleistocene paleoenvironmental records do not have the same resolution as those from the late Holocene, they do provide a more complete picture of drought variability in the Central and High Plains. Such records can therefore be used to test and refine climate model simulations and thereby enhance our understanding of how the climate system operates and how it has varied in the past (e.g., Bartlein et al., 1998).

### 3. Policy and Management Implications

Arid conditions have a significant impact on surface and groundwater resources. Water systems are commonly designed to handle the "drought of record," identified as the most severe hydrological event from the instrumental record. For the state of Kansas, the 1950s drought (1952-1957) remains the planning benchmark and is used to calculate reservoir yield through droughts with a 2% chance of occurrence in any one year. However, the evidence presented herein indicates that drought variability in the 20$^{th}$ century is just a subset of the full range of variability that one should expect under naturally occurring climatic conditions for the High Plains. In fact, various paleoclimatic reconstructions indicate that droughts of greater severity and longer duration have occurred in the past. Such severe drought conditions are of great concern because modern-day agricultural and water systems may not have the resilience to survive droughts beyond the “worst case scenario” droughts of the past 100 years (Cook et al., 2007).

In terms of water resource management, paleoclimatic data have important implications. For example, reservoirs in Kansas are typically designed with conservation pools to specific meet water demand during drought conditions similar to the worst on record. However, would these designs be adequate under megadrought conditions? Additionally, management of withdrawals from the High Plains aquifer aims to accommodate high demand during drought while sustaining or extending the usable lifetime of the resource. Groundwater usage of the High Plains aquifer, however, has escalated since the 1950s and it is questionable whether a balance between demand and sustainability can be met under periods of severe, protracted drought such as those seen in paleoenvironmental records. Given these challenges, it would be wise to adopt a probabilistic approach to drought planning that incorporates the full range of drought variability as indicated in the paleoclimatic record. Continued investigations into paleoclimatic change and drought variability will provide a clearer understanding of the forcing mechanisms behind past periods of aridity and enable scientists and policymakers to better plan for the sustainability of water resources in the High Plains of western Kansas.

## References


Arbogast, A.F., 1996. Stratigraphic evidence for late-Holocene aeolian sand mobilization and soil formation in south-central Kansas, USA. Journal of Arid Environments 34, 403–414.

Bartlein, P.J., Anderson, K.H., Anderson, P.M., Edwards, M.E., Mock, C.J., Thompson, R.S., Webb. R.S., Webb, T., Whitlock, C., 1998. Paleoclimate simulations for North America over the past 21,000 years features of the simulated climate and comparisons with paleoenvironmental data. Quaternary Science Reviews 17, 549–585.

Benson, L.V., Berry, M.S., Jolie, E.A., Spangler, J.D., Stahle, D.W., Hattori, E.M., 2007. Possible impacts of early-11th-, middle-12th-, and late-13th-century droughts on western native Americans and the Mississippian Cahokians. Quaternary Science Reviews 26, 336–350.

Cobb, C.R., Butler, B.M., 2002. The vacant quarter revisited: late Mississippian abandonment of the Lower Ohio Valley. American Antiquity 67, 625–641.

Cook, E.R., Woodhouse, C., Eakin, C.M., Meko, D.M., Stahle, D.W., 2004. Long-term aridity changes in the western United States. Science 306, 1015–1018.

Cook, E.R., Seager, R., Cane, M.A., Stahle, D.W., 2007. North American drought: reconstructions, causes and consequences. Earth Science Reviews 81, 93–134.

Cordova, C.E., Johnson, W.C., Mandel, R.D., Palmer, M.W., 2011. Late Quaternary environmental change inferred from phytoliths and other soil-related proxies: case studies from the central and southern Great Plains, USA. Catena 85(2), 87–108.

Forman, S.L., Oglesby, R., Webb, R.S., 2001. Temporal and spatial patterns of Holocene dune activity on the Great Plains of North America: megadroughts and climate links. Global and Planetary Change 29(1), 1–29.

Fredlund, G.G., 1995. Late Quaternary pollen record from Cheyenne Bottoms, Kansas. Quaternary Research 43, 67–79.

Halfen, A.F., Johnson, W.C., Hanson, P.R., Woodburn, T.L., Young, A.R., Ludvigson, G.A., 2012. Activation history of the Hutchinson dunes in east-central Kansas, USA during the past 2200 years. Aeolian Research 5, 9-20.

Hanson, P.R., Arbogast, A.F., Johnson, W.C., Joeckel, R.M., Young, A.R., 2010. Megadroughts and late Holocene dune activation at the eastern margin of the Great Plains, north-central Kansas, USA. Aeolian Research 1, 101–110.

Holliday, V.T., 1989. Middle Holocene drought on the southern High Plains. Quaternary Research 31, 74–82.

Holliday, V.T., Hovorka, S.D., Gustavson, T.C., 1996. Lithostratigraphy and geochronology of fills in small playa basins on the Southern High Plains, United States. Geological Society of America Bulletin 108(8), 953–965.

Jacobs, K.C., Fritz, S.C., Swinehart, J.B., 2007. Lacustrine evidence for moisture changes in the Nebraska Sand Hills during Marine Isotope Stage 3. Quaternary Research 67, 246–254.

Kansas Department of Agriculture, 2011: http://www.ksda.gov/news/id/405

Layzell, A.L., 2012. A thousand years of drought and climatic variability in Kansas: Implications for water resources management. Kansas Geological Survey Open File Report 2012-18.
Lepper, K., Scott, G.F., 2005. Late Holocene aeolian activity in the Cimarron River Valley of west-central Oklahoma. Geomorphology 70, 42–52.
Mandel, R., 1995. Geomorphic controls of the Archaic record in the central Plains of the United States. In: Bettis, E.A. (Ed.), Archaeological Geology of the Archaic Period in North America. Geological Society of America Special Paper 297, Boulder, CO, pp. 37– 66.
Mason, J.A., Jacobs, P.M., Hanson, P.R., Miao, X.D., Goble, R.J., 2003. Sources and paleoclimatic significance of Holocene Bignell Loess, Central Great Plains, USA. Quaternary Research 60, 330–339.
Mason, J.A., Swinehart, J B., Goble, R.J., Loope, D.B., 2004. Late-Holocene dune activity linked to hydrological drought, Nebraska Sand Hills, USA. The Holocene 14(2), 209–217.
Meltzer, D.J., 1999. Human responses to middle Holocene (Altithermal) climates on the North American Great Plains. Quaternary Research *52*(3), 404–416.
Nordt, L.C., Boutton, T.W., Hallmark, C.T., Waters, M.R., 1994. Late Quaternary vegetation and climate changes in central Texas based on the isotopic composition of organic carbon. Quaternary Research 41(1), 109–120.
Olson, C.G., Nettleton, W.D., Porter, D.A., Brasher, B.R., 1997. Middle Holocene aeolian activity on the High Plains of west-central Kansas. The Holocene 7 (3), 255–261.
Riebsame, W.E., Changnon, S.A., Karl, T.R., 1991. Drought and natural resources management in the United States: impacts and implications of the 1987-89 drought. Westview Press: Boulder, 174 pp.
Seager, R., Graham, N., Herweijer, C., Gordon, A. L., Kushnir, Y., Cook, E., 2007. Blueprints for Medieval hydroclimate. Quaternary Science Reviews 26(19), 2322–2336.
Serefiddin, F., Schwarcz, H.P., Ford, D.C., Baldwin, S., 2004. Late Pleistocene paleoclimate in the Black Hills of South Dakota from isotope records in speleothems. Palaeogeography, Palaeoclimatology, Palaeoecology 203, 1–17.
Stahle, D.W., Fye, F.K., Cook, E.R., Griffin, R.D., 2007. Tree-ring reconstructed megadroughts over North American since A.D. 1300. Climate Change 83, 133–149.
Woodhouse, C.A., Overpeck, J.A., 1998. 2000 Years of Drought Variability in the Central United States. Bulletin of the American Meteorological Society 79, 2643–2714.